Neuroanatomical changes in patients with loss of visual function

Prins, Doety

NEUROANATOMICAL CHANGES IN PATIENTS WITH LOSS OF VISUAL FUNCTION

Doety Prins

The research described in this thesis was suported by the MD/PhD programme of the Junior Scientific Masterclass, and by a research grant from Stichting Nederlands Oogheelkundig Onderzoek (SNOO).

Publication of this thesis was financially supported by the Graduate School for Behavioral and Cognitive Neurosciences, the University of Groningen, and the Professor Mulder Stichting.

Layout: Douwe Oppewal, www.oppewal.nl
Printing: Netzodruk
ISBN printed version: 978-90-367-9330-8
ISBN digital version: 978-90-367-9329-2

rijksuniversiteit groningen

Neuroanatomical changes in patients with loss of visual function

Proefschrift

ter verkrijging van de graad van doctor aan de
Rijksuniversiteit Groningen
op gezag van de
rector magnificus prof. dr. E. Sterken
en volgens besluit van het College voor Promoties

De openbare verdediging zal plaatsvinden op

woensdag 23 november 2016 om 12:45 uur

door

Doety Prins

geboren op 24 oktober 1986
te Sneek

Promotores
Prof. dr. F.W. Cornelissen
Prof. dr. J.M.M. Hooymans
Prof. dr. N.M. Jansonius

Beoordelingscommissie
Prof. dr. P. van Dijk
Prof. dr. A.V. van den Berg
Prof. dr. T. van Laar

Contents

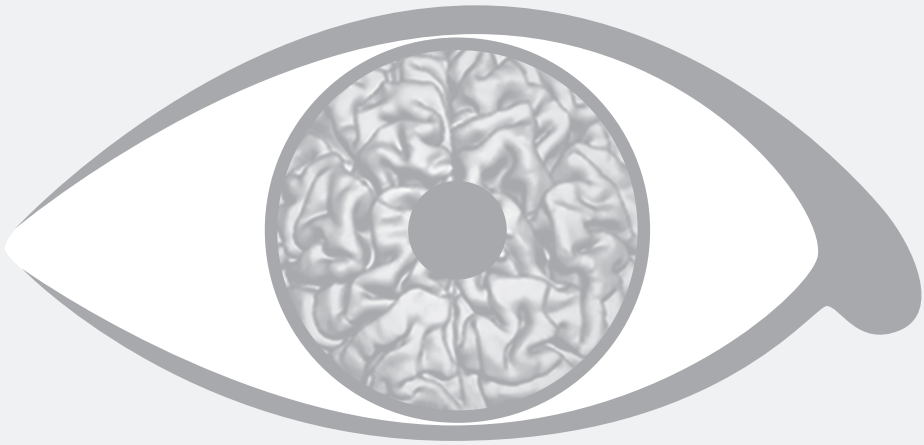

Introduction of the thesis

Introduction of the thesis

Vision is one of the most important senses for human beings. The eye gives us a detailed perception of the world around us. We use it continuously in our daily activities. Loss of visual function can therefore cause a substantial decrease in quality of life. Light emitted by a light source or reflected by a surface enters the eye through the cornea, which refracts the light through the pupil to the lens, which in turns refracts the light through the vitreous body, to project it onto the retina. The light projected onto the retina is converted into electrical signals by the photoreceptors and further processed in the various layers of the retina. From the retina, electrical pulses pass on to the optic nerve, which transports the signal further along the visual pathways. At the optic chiasm, the optic nerves split. The nerve fibres from the right half of the retina of both eyes, which contain information from the left visual field, continue on to the right hemisphere of the brain, whereas the fibres from the left half of the retina of both eyes continue on to the left hemisphere. From the chiasm, the visual information is transferred through the optic tract to the lateral geniculate bodies, from which the optic radiations transport the signal to the visual cortex, in which the input is processed resulting in us perceiving a certain object.

Association between ocular pathology and neuroanatomical changes

In the last decade, numerous studies have found an association between eye diseases and changes in the neuroanatomical properties of the visual pathways. This has most often been studied in eye diseases that cause a loss of visual input as a consequence of visual field defects, such as macular degeneration and glaucoma. Why are these findings important? And are the outcomes of these studies clinically relevant for patients suffering from these eye diseases?

A topic of high interest in ophthalmology is the treatment of blindness through vision restoration. Over the past two decades, developments in the fields of genetics, stem-cell therapy and retinal prosthesis have accelerated, such that treatment of blindness may become a reality in the relatively near future for at least some types of ocular pathology. In the context of these developments, it is important to gain knowledge about the chances of success of such vision restoration treatments, and to determine which factors affect their success. One of these factors might be the remaining capability of the visual pathways and the central visual system to guide the visual information from the eye towards the visual cortex and process it appropriately. Without a properly functioning central visual system, one cannot accurately perceive the visual information, even though the visual input might still be intact or might have been restored. Therefore, it is important to investigate what happens in the central visual system in eye diseases that can cause – partial – blindness. Furthermore, such research can provide more insight in the pathophysiology of the investigated eye disease. This, in turn, can give directions to

future research on the treatment of the eye disease (e.g. moving from treatment of the eye alone towards treatment of both the eye and brain).

There are several factors that can explain the association between ocular pathology and neuroanatomical changes:

- Functional deprivation: the ocular pathology may reduce the activity in the visual pathways – for example as a result of overlapping visual field defects in both eyes – which, in turn, may lead to neuroanatomical changes;
- Anterograde transsynaptic degeneration. This process might cause neuroanatomical changes by "passing on" the pregeniculate degeneration of axons from the eye towards postgeniculate neurons and even to the visual cortex.
- Ocular pathology, such as glaucoma and macular degeneration, could be part of a more generalized neurodegenerative disorder that affects the brain as well as the eye.

Aim of the thesis

The aim of my thesis was to discover which of the above described mechanisms can explain the association between ocular pathology and neuroanatomical changes in general. To achieve this aim, I addressed a number of sub-questions:

- *Is macular degeneration associated with neuroanatomical alterations? (Chapter 2 and 3)*

Juvenile macular degeneration (JMD) and age-related macular degeneration (AMD) are degenerative retinal diseases that cause central visual field defects. The retinotopic organisation of the visual cortex, i.e. the projection of the visual field onto the visual cortex is well known. Specifically, the centre of the visual field is located in the occipital pole. Therefore, in macular degeneration, the expected locations of neuroanatomical changes that would result from functional deprivation or transsynaptic degeneration are also in the occipital pole. Degeneration beyond these expected locations would suggest an influence of more general neurodegenerative processes.

- *Is monocular blindness associated with neuroanatomical alterations? (Chapter 4)*

Monocular blindness due to, for example, a trauma, in the absence of a degenerative ocular disease, constitutes a unique model in which the loss of visual input is well-defined and in which stereopsis is lost. All other visual functions are still supported by input from the contralateral eye. Moreover, as there is no further pathology, we can exclude that general neurodegenerative processes affect the visual pathways and brain. The presence of neuroanatomical changes in monocular blindness can therefore provide insight in whether these are caused by functional deprivation or transsynaptic degeneration.

- *Is primary open-angle glaucoma with a monocular visual field defect associated with neuroanatomical alterations? (Chapter 5)*

Primary open-angle glaucoma (POAG) with a monocular visual field defect combines the consequences of suffering from a degenerative ocular disease with partial loss of visual input from one eye. In this specific group, functional deprivation is not expected to play a role as visual functions are still fully supported by the intact visual input from the contralateral eye and stereopsis is mostly preserved. The presence of neuroanatomical changes might therefore reveal whether these are caused by transsynaptic degeneration or by more general neurodegenerative processes affecting the visual pathways and brain.

Outline of the thesis

Chapter 1 introduces the topic of this thesis in depth. It contains a review of the currently existing literature on this topic. It gives an overview of the findings of structural brain MRI-studies in patients with compromised visual acuity and/or a visual field defect, due to glaucoma, AMD, hereditary retinal dystrophies, albinism or amblyopia. This chapter also addresses the question of the causality of the structural changes in the brain in patients suffering from one of the aforementioned diseases.

Chapter 2 describes an international multi-centre VBM-study in AMD and JMD patients, addressing the question whether these pathologies are associated with volumetric alterations of the visual pathways.

Chapter 3 is a follow-up on the study described in chapter 2, which additionally uses SBM-analysis to study cortical thickness, surface area and mean curvature in AMD and JMD patients.

Chapter 4 addresses the question whether monocular blindness affects neuroanatomical properties of the visual pathways. The neuroanatomical properties were defined by grey and white matter volume, cortical thickness, surface area and mean curvature.

In **Chapter 5,** I assess the neuroanatomical properties of the visual pathways of POAG patients with a monocular visual field defect. I compared these patients to age-matched healthy controls and age-matched monocularly blind controls.

Chapter 6 integrates the results of the experimental chapters of this thesis into a broader general discussion of structural brain MRI-studies in ocular pathology. I discuss the outcomes of these studies and present the most parsimonious theory that can explain the association between ocular pathology and neuroanatomical changes in general. Furthermore, I discuss the clinical relevance of these brain MRI-studies in eye diseases in the context of future vision restorative therapies and suggest directions for future research in the field.

Structural brain magnetic resonance imaging (MRI) analysis

The research questions of this thesis were addressed using structural MRI of the brain. In structural MRI, one can measure neuroanatomical properties of a subject's brain, such as grey and white matter volume, surface area, cortical thickness and mean curvature. To determine whether these neuroanatomical properties statistically differ one has to compare these between various groups of subjects – for example a group of patients and a group of healthy controls. There are several techniques that can be used to extract and compare the neuroanatomical properties from the structural MRI images. The volumes of the grey and white matter can be determined using voxel-based morphometry (VBM). Cortical thickness, gyrification pattern and surface area of the cortex can be determined using surface-based morphometry (SBM).

Voxel-based morphometry (VBM)

VBM is a method that compares structural MR-images in a voxel-by-voxel manner. A voxel is the 3D equivalent of a pixel, and can have different dimensions. In this thesis, the size of a voxel is 1 mm x 1 mm x 1 mm. VBM overlays a grid of these voxels over the brain, and thus divides the brain into tiny cubes. After separating the brain structures in the image from all non-brain tissue, the brain is segmented into grey matter, white matter and cerebrospinal fluid. The likelihood that the tissue represented by a voxel belongs to one of these tissue classes is determined by assessing the intensity of a voxel. This results in the three tissue segments. Next, the segments of the individual brains are registered to an average template brain to make them approximately equal in size. Subsequently, a comparison of the grey and white matter volumes can be performed between patients and controls. This can be done for the entire brain (whole brain analysis) or be limited to specific regions of interest (ROI) analysis.

Surface-based morphometry (SBM)

SBM is a technique that determines several neuroanatomical properties based on estimating the grey/white matter boundary and the grey/pial boundary. SBM can use these estimates to measure the thickness of the cortex, the gyrification pattern and the surface area of the cortex. SBM first removes the non-brain tissue, performs intensity normalisation and segments the brain into grey and white matter. It registers all the individual cortices to a sphere and inflates them for visualization purposes. After these steps, comparison of the neuroanatomical properties can be performed for the whole brain or in particular ROIs. SBM is limited to analysing properties of the cortex only.

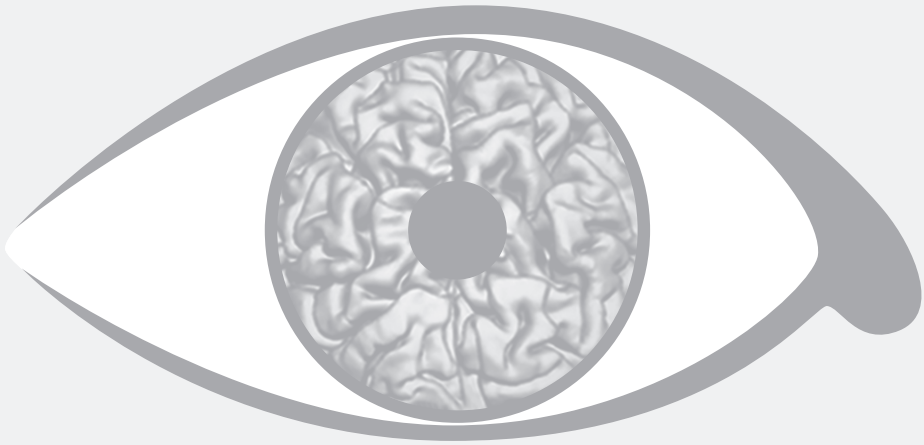

CHAPTER 1

General introduction of the topic and a review of the literature

Based on: Doety Prins, Sandra Hanekamp & Frans W. Cornelissen. Structural brain MRI studies in eye diseases: are they clinically relevant? A review of current findings.

Acta Ophthalmologica 2016; 94(2): 113-21.

1.1 Introduction

Recently, numerous magnetic resonance imaging (MRI) studies have shown that eye diseases are associated with brain changes, in particular in the visual pathways (an overview of what I mean by the general term "brain changes" is given in Box 1.1).(Barnes et al. 2010, Boucard et al. 2009, Bridge et al. 2012, Hernowo et al. 2011, Hernowo et al. 2014, Plank et al. 2011, Xiao et al. 2007, Xie et al. 2007) These brain changes have primarily been shown in eye diseases that reduce visual acuity or are associated with the occurrence of retinal defects, such as glaucoma, age-related macular degeneration (AMD) and hereditary retinal dystrophies.

Box 1.1: Concepts of neurodegeneration and plasticity

Neurodegeneration
In general, neurodegeneration can be explained as progressive loss of neuronal structure, function, and cell death. Neurodegenerative diseases each have their own characteristic profile of regional neuronal cell death. Also referred to as neuronal degeneration or transsynaptic degeneration. (Przedborski et al. 2003)

Neuroplasticity
Neuroplasticity indicates changes in the organization of the brain as a result of development, learning, memory, experience or recovery from brain injury. It can occur on different levels, ranging from changes in synapses and neural pathways (*synaptic plasticity*) due to learning, to major changes in the cortical representation of the body in response to bodily injury (*cortical remapping*). (Liepert et al. 2000, Pascual-Leone et al. 2005)

Regenerative brain plasticity
This term is used to describe that neuroplasticity occurred despite of previously observed neurodegeneration.

Cortical structural changes
This paper uses the term cortical structural changes when grey or white matter changes (e.g. increase or decrease) are observed using neuroimaging without making an assumption of the cause. Also described in this paper as brain changes.

Retinotopic-specific neuronal degeneration
Neurodegeneration caused by decreased visual input. In the occurrence of a visual field defect, the corresponding part of the retinotopic organized visual cortex no longer receives input. The absence of stimulation can result in cell death.

This phenomenon is an example of anterograde transsynaptic degeneration. (Boucard et al. 2009)

Anterograde transsynaptic degeneration
Neurodegeneration caused by a loss of input or after injury. Breakdown of presynaptic neurons at the primary injury site spreads towards connected postsynaptic neurons (e.g. distal axon terminal), causing the death of these cells. Also described in literature as anterograde degeneration. (Nauta and Ebbesson 1970)

Retrograde transsynaptic degeneration
Retrograde transsynaptic degeneration is the degeneration is the opposite direction of anterograde degeneration. It occurs when an axon from the point of damage, which spreads back towards the proximal cell body (e.g. presynaptic neurons). It occurs when target tissues no longer receive trophic support. (Nauta and Ebbesson 1970)

The potential role of MRI studies in ophthalmology is increasing due to current advances in ophthalmic therapeutic strategies, such as the development of retinal implants and neuroprotective agents. The success of these therapies may require that the central visual system is still capable of transmitting and processing the retinal signals. Therefore, it is becoming increasingly important to establish the integrity of the visual pathways and brain and their ability to transmit and process potentially restored input. Furthermore, parallel developments in brain imaging and analysis techniques make it more and more feasible that brain imaging could perhaps be used as a diagnostic tool or to evaluate the response to neuroprotective agents.

I reviewed the current literature on structural brain changes in humans associated with the eye diseases albinism, amblyopia, hereditary retinal dystrophies, AMD, and glaucoma. For each eye disease, I focused on two main questions. First, what have structural studies found thus far, and second, what is the potential clinical relevance of these findings? In the discussion of this thesis I will generalize these findings and give directions for future research.

Although numerous animal and functional MRI (fMRI) studies have also been performed, I limited the scope of this literature review to the results obtained in humans with structural imaging and analysis techniques such as voxel- and surface based morphometry (VBM/SBM) and diffusion tensor imaging (DTI) (see Box 1.2). (For reviews focusing on fMRI, I refer to *Wandell and Smirnakis (2009)* and *Haak et al. (2014)*.

Box 1.2: Structural brain imaging techniques

The first approaches to identify brain changes in ocular diseases have been carried out by using conventional magnetic resonance (MR) imaging. Brain regions are delineated and measured based on reliable anatomical landmarks.
Voxel-based morphometry (VBM) comprises a location-by-location statistical comparison of the local tissue concentration of grey matter volume, white matter volume or cerebrospinal fluid between different groups of subjects. Therefore, VBM can quantify the magnitude of structural differences between patients and healthy controls. (Ashburner and Friston 2000, Ashburner and Friston 2001, Bookstein 2001, Good et al. 2001)
Diffusion tensor imaging (DTI) visualizes the axonal architecture of white matter fibres based on the diffusion of water molecules in each voxel along axons. The diffusion of water molecules is described by anisotropy and related to axonal integrity. Several parameters can be derived which describe the anisotropy in each voxel. Fractional anisotropy quantifies the underlying fibre tract orientation (measure of shape) and is assumed to be sensitive in a broad spectrum of pathological conditions. Other parameters are mean diffusivity, which quantifies the diffusion-freedom that water molecules have in a voxel (a volume element analogous to a pixel); radial diffusivity (a measure of diffusion orthogonal to axon) is thought to be modulated by myelin in the white matter and axial diffusivity (a measure of diffusion parallel to axon), which is more specific to axonal degeneration. (Alexander et al. 2007; Basser et al. 2000, Jones et al. 1999a, Jones et al. 1999b)

1.2 Methods

Search protocol
The data base search was updated last on December 2014. The searched databases are: EMBASE, PubMed, and Web of Science.

Search terms
For each eye disease a specific search string was used. The part of the search string that corresponds to structural neuroimaging was equal for all eye diseases. An example of the search string for glaucoma is given below. Search strings for each eye disease can be found in Supplement 1.

Example of search string for glaucoma
glaucoma[Title] AND (diffusion tensor imaging [Title] OR magnetic resonance

imaging[Title] OR grey matter [Title] OR gray matter [Title] OR white matter [Title] OR Morphometric analyses [Title]) AND humans[Filter] NOT ("review"[Publication Type] OR "review literature as topic"[MeSH Terms] OR "review"[All Fields])

Inclusion criteria studies

All articles were screened and selected for inclusion according to several criteria. Inclusion was based on the following criteria:

- *Methodology*: use of structural neuroimaging (e.g. DTI, VBM, or conventional MRI examination) and use of human population
- *Research question*: investigation of brain changes
- *Type of eye disease*: albinism, amblyopia, hereditary retinal dystrophies, AMD, and glaucoma

1.3 Results

1.3.1 Albinism

Pathology

Albinism refers to a heterogeneous group of genetically determined disorders that are characterized by hypopigmentation in the skin, hair, and eyes. Ocular features in albinism are reduced visual acuity and nystagmus, which are related to the degree of ocular pigmentation; hypoplasia of the fovea; hypopigmentation of the fundus; translucency of the iris; strabismus; high refractive errors; and red deviation in colour vision. (Kinnear et al. 1988)

What has been found?

A conventional MRI study revealed structural abnormalities in albino patients: the diameters of the optic nerves and optic tracts and the width of the chiasm were smaller, and the shape of the chiasm was different (Schmitz et al. 2003).

In more recent VBM studies, more subtle changes in the brain have been shown. *Von dem Hagen et al*. found a regionally specific decrease in grey matter volume at the occipital poles in albinism. The location of the decrease in grey matter corresponds to the cortical representation of the central visual field. This reduction was possibly a direct result of decreased ganglion cell numbers in the central retina in albinism (von dem Hagen et al. 2005). Moreover, the calcarine fissure was shorter and the mean surface area of the calcarine fissure was smaller in albinism than in healthy controls (Neveu et al. 2008). More recently, *Bridge et al.* (2012) reported increased grey matter volume in the calcarine sulcus in albinism, which was related to increased cortical thickness. They also found decreased grey matter volume in the posterior ventral occipital cortex.

These results suggest that albinism is associated with pregeniculate and postgeniculate changes.

What is the potential clinical relevance of the findings?
It is unclear if the reported brain abnormalities in albinism are congenital, or if they are secondary to the ocular symptoms in albinism. The hypoplasia of the fovea, the subsequently reduced visual acuity, and the nystagmus can all cause abnormal input. This abnormal input could be a plausible explanation for the observed alterations the brain.

No curative therapy for albinism is currently available. Therapy is aimed at treatment of the symptoms of albinism, such as the prevention of possible development of amblyopia, appropriate refraction and protection against sun. Therefore, at present, the findings of brain abnormalities do not have implications for the treatment of albinism, but they do provide us more insight in the disorder itself.

1.3.2 Amblyopia

Pathology
Amblyopia is a reduction of best-corrected central visual acuity by misuse of disuse during the critical period of visual development. It has no exact identifiable organic cause, although it is thought to originate in the central nervous system. Disuse or misuse mostly occurs because of deprivation, unequal refractive errors, or strabismus and is classified accordingly. The decrease in vision develops in the first decade of life and does not decline thereafter. It occurs most often unilaterally, but it can also appear bilaterally.

What has been found?
Using VBM, decreased grey matter density in the visual cortex has been found in children with amblyopia, compared to children with normal sight (Xiao et al. 2007, Xie et al. 2007). In a study of children and adults with anisometropic or strabismic amblyopia, decreased grey matter volume was found in the visual cortex in both age groups, although this volumetric reduction was more widespread in children than in adults (Mendola et al. 2005). Moreover, *Barnes et al.* (2010) found decreased grey matter concentration in the LGN in adult patients with strabismic amblyopia Lv et al. (2008) found no difference in mean global cortical thickness and the mean regional thickness of the primary and secondary visual cortex (V1 and V2) in amblyopic subjects, compared to healthy controls. However, in the unilateral amblyopic subjects, a difference between the two hemispheres was shown More recently, grey and white matter changes were observed in a group of unilaterally amblyopic children. These changes contained both increases and decreases in the visual cortex and around the calcarine areas. The volumetric loss

occurred in cortices related to spatial vision(Li et al. 2013a). In summary, this indicates that amblyopia is linked to changes in the pregeniculate and geniculate part of the visual pathways.

What is the potential clinical relevance of the findings?
From these studies we may conclude that both the grey and white matter of the visual pathways are involved in amblyopia. This has mostly been shown in the visual cortex. The reduced visual acuity probably causes a lack of information transported through the visual pathways to the visual cortex. It is unknown whether regeneration of the visual cortex is possible. However, the fact that occlusion therapy in amblyopia is often successful in children indicates that the visual pathways are still capable of receiving input from the affected side in childhood, but not necessarily in adults.

1.3.3 Hereditary retinal dystrophies

Pathology
Hereditary retinal dystrophies are a collective name for Medelian genetic eye diseases such as Juvenile macular degeneration (e.g. Stargardt's disease and Best's vitelliform retinal dystrophy (Best's disease)), cone-rod dystrophy, central areolar choroidal dystrophy and retinitis pigmentosa. They start early in life and lead to dysfunction and cell death of various retinal cell types. Non-progressive forms of this disease often result in reduced visual acuity and visual field defects. Forms in which cell death predominates mostly lead to permanent vision loss. In many of these diseases, there is progressive appearance of pigmentary deposits in the retina as a result of changes in the retinal pigment epithelium, often accompanied by the death of the retinal photoreceptors (PRs).

What has been found?
When analysed with VBM, patients with a binocular central visual field defect due to hereditary retinal dystrophies showed a reduction of grey matter volume around the calcarine sulcus in both hemispheres, particularly on the posterior part of the calcarine sulcus.(Plank et al. 2011) This suggests that neuronal degeneration is retinotopically related to the location of the visual field defect.

In an earlier DTI study in (only) 6 patients with acquired blindness, of which 5 patients were blind due to retinitis pigmentosa, no significant difference in the fractional anisotropy of the visual fibre tracts was found in blind patients compared to the healthy control subjects. (Schoth et al. 2006) Hernowo et al (2014) observed white matter changes in JMD patients in the optic radiations and visual cortex. Taken together, these results show that in hereditary retinal dystrophies post-geniculate changes are observed.

What is the potential clinical relevance of the findings?
The various eye conditions that are described in hereditary retinal dystrophies are usually considered to be exclusively eye diseases. The finding of degeneration in the post-geniculate part of the visual pathways in these patients can have extensive consequences for the treatment with artificial retinal implants or stem-cell-derived retinal implants. Such implants have been used experimentally in humans with retinitis pigmentosa, thus far with rather variable results.(Stingl et al. 2010) Brain involvement in hereditary retinal dystrophies could be an explanation for these results, because the central visual system in these patients should still be capable of transmitting and processing visual signals for these therapies to be successful. Degeneration of the pathways and cortex could interfere with this. Hence, a retinal implant might be more effective when implanting it at an earlier stage of the disease, ideally at the time when degeneration of the visual pathways has not yet occurred

1.3.4 Age-related macular degeneration

Pathology
In AMD, the retinal metabolism is obstructed by the accumulation of drusen in the macular area. This in turn induces degeneration of the macula, which causes a central visual field defect.(Arden 2006, Gehrs et al. 2006, Holz et al. 2004, Zarbin 2004) AMD is the most prevalent cause of visual impairment in the European adult population. (Augood et al. 2006)

What has been found?
By using VBM, *Boucard et al.* (2009) found an association between visual field defects caused by long-standing glaucoma and AMD, and reductions in grey matter density in the occipital cortex. In AMD patients, the main reduction was found near the occipital pole (primarily in the left hemisphere), particularly around the posterior part of the calcarine sulcus. *Hernowo et al.* (2014) confirmed such grey matter changes in the visual cortex and additionally found white matter reductions in the optic radiations and visual cortex. Interestingly, a white matter decrease in the frontal lobe was found. Collectively, this means that besides post-geniculate changes, frontal changes are observed as well.

What is the potential clinical relevance of the findings?
Degeneration in the post-geniculate part of the visual pathways of patients with AMD could be explained by decreased input from the visual field towards the visual cortex. However, *Hernowo et al.* (2014) found white matter volumetric reduction in the frontal lobe of AMD patients, which was proposed to be the neural correlate of a previously described association between AMD and mild cognitive impairment (MCI) or AD.(Hernowo et al. 2014, Ikram et al. 2012, Klaver et al. 1999, Woo et al. 2012)

Several studies have revealed that AMD and AD share multiple clinical and pathological features. This supports the notion that AMD could be the manifestation of a more general neurodegenerative disease, of which the visual pathway degeneration may be the primary manifestation. Contrarily, it seems that these two diseases have a different genetic background (Proitsi et al. 2012). Further, in a recent AMD cohort of 65.984 people concluded that the chance of developing AD after AMD is no different from that expected by chance (Keenan et al. 2014). For the treatment of AMD, the distinction between eye disease and neurodegenerative disease is highly relevant. Studies on treatments that aim to restore visual function in AMD patients have been performed, such as macular translocation (Eckardt and Eckardt 2002) and retinal pigment epithelium transplantation (Van Zeeburg et al. 2012). These studies showed varying results in improvement of visual function. However, if AMD turns out to be a neurodegenerative disease, then the neurodegenerative component might be responsible for the sometimes poor effects of such treatments. So far, studies on treatment of AMD have mainly been focused on ocular treatment only.

1.3.5 Glaucoma

Pathology

Primary open angle glaucoma (POAG) is a common neurodegenerative disease of retinal ganglion cells (RGCs) characterized by axon degeneration of the optic nerve, causing progressive loss of peripheral visual fields and ultimately blindness. The exact pathophysiology of POAG is not yet fully understood (Chang and Goldberg 2012, Fechtner and Weinreb 1994, Nickells 1996). Although RGC and optic nerve damage is often associated with the presence of elevated intraocular pressure (IOP), glaucoma with normal levels of IOP – normal tension glaucoma – is commonly diagnosed as well.

What has been found?

There have been a number of structural MRI studies investigating brain changes in glaucoma. By conventional examination of MR images, earlier studies found that patients with glaucoma had a lower optic chiasm height (Iwata et al. 1997, Kashiwagi et al. 2004) and smaller optic nerve diameter (Kashiwagi et al. 2004). More recently, MRI studies have confirmed degeneration of the lateral geniculate nucleus (LGN).(Gupta et al. 2009, Zhang et al. 2012, Zikou et al. 2012)

Using VBM, *Boucard et al.* (2009) found reduced grey matter density in glaucoma patients in the region of the calcarine sulcus. In agreement with the more peripheral location of visual field defects in glaucoma, this reduction was more pronounced in the anterior than in the posterior region. Together with their results in AMD, this suggests that long-term cortical deprivation – due to retinal lesions acquired later in life – is associated with retinotopic-specific neuronal degeneration of the visual cortex.

A follow-up study by *Hernowo et al.* (2011) indicated decreased volume along the full length of the visual pathway in glaucoma in both grey and white matter. More recently, studies examining grey matter volume in glaucoma patients have reported both increases as well as decreases of grey matter in various areas of the brain.(Chen et al. 2013, Li et al. 2012, Williams et al. 2013) Inconsistent findings with respect to grey matter volume changes may be explained by differences in glaucoma stages of the patients included in these various studies.

Brain involvement in glaucoma has also been observed using diffusion MR imaging, also referred to as DTI. Previous studies using DTI have reported white matter abnormalities in different parts of the visual pathway, such as the optic nerve, optic tract, chiasm, optic radiation and occipital lobe.(Chang et al. 2013, Chen et al. 2013, Dai et al. 2012, Doerfler et al. 2012, El-Rafei et al. 2013, Garaci et al. 2009, Liu et al. 2012, Murai et al. 2013, Wang et al. 2013, Zhang et al. 2012) *Zikou et al* (2012)demonstrated white matter changes in brain structures that play a role in visuospatial processing. In support of this, the robustness of white matter changes in glaucoma is recently confirmed by a meta-analyse of existing DTI studies by revealing changes in the optic nerve, optic radiation, and optic tract changes compared to controls. Together with age, glaucoma severity was found to be an important factor correlated with the extend of the damage. (Li et al. 2014)

In summary, although the specific results still vary, the common finding in all these VBM and DTI studies is that the pregeniculate, geniculate, and post-geniculate structures are affected in glaucoma, at least in later stages of the disease. In addition, some studies reveal changes in other parts of the brain as well.

What is the potential clinical relevance of the findings?

To consider the clinical relevance of these findings, it is important to know whether glaucoma should be considered as solely an eye disease, or as a neurodegenerative brain disease. Although I cannot yet conclude whether brain changes occurred before, simultaneously, or after the development of the eye disease, the most plausible explanation seems to be that glaucomatous changes in the eye cause the brain changes, since thus far no differences in grey matter volume have been found in early stage POAG.(Li et al. 2012) However, this may be a consequence of a lack of power in studies performed thus far. Moreover, several studies have found correlations between changes in visual pathway structures and glaucoma severity (Chen et al. 2013, Dai et al. 2012, Garaci et al. 2009, Michelson et al. 2013, Wang et al. 2013), which supports the notion that brain changes are caused by the eye disease itself. On the contrary, some researchers suggest an association between Alzheimer's disease (AD) and glaucoma. Glaucoma and AD share several characteristics: they are both neurodegenerative, chronic, progressive, age-related and cause irreversible neuronal cell loss. This may indicate that glaucoma and AD are connected through the same underlying pathologic mechanism.(Ghiso et

al. 2013, Inoue et al. 2013, Janssen et al. 2013, Sivak 2013) However, this notion is still being questioned after the publication of conflicting epidemiologic reports. Some epidemiologic studies find an increased prevalence of glaucoma in AD (Bayer et al. 2002, Tamura et al. 2006), while other studies do not.(Kessing et al. 2007, Ou et al. 2012) In support of the hypothesis that glaucoma may be part of a neurodegenerative disease, some studies examined trans-lamina cribrosa pressure difference (TLCPD), which is calculated as the intraocular pressure (IOP) minus the cerebrospinal fluid pressure (CSFP). These studies suggest that TLCPD has a better association with glaucoma presence than IOP (Jonas et al. 2014, Wang et al. 2013, Wostyn et al. 2013, Zhang et al. 2014). This could be an indication that glaucoma should be seen as part of a neurological disorder.

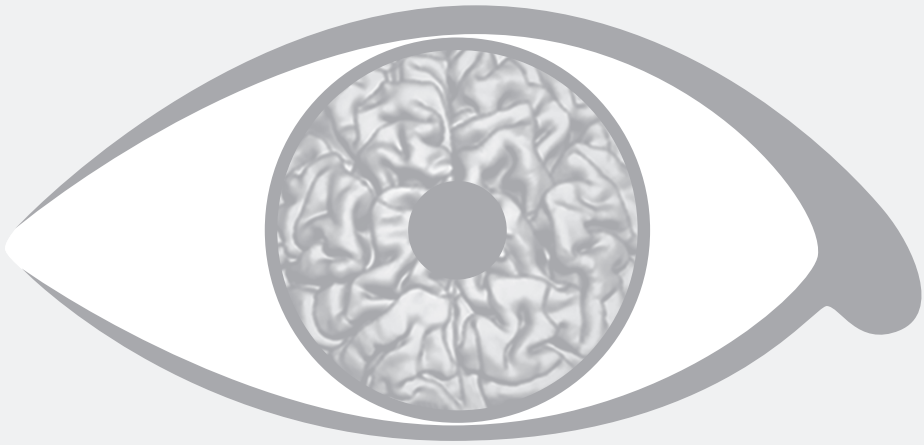

CHAPTER 2

Morphometric analyses of the visual pathways in macular degeneration

Doety Prins*, Aditya T. Hernowo*, Heidi A. Baseler, Tina Plank, Andre Gouws, Johanna M.M. Hooymans, Antony B. Morland, Mark W. Greenlee and Frans W. Cornelissen.

Published in: Cortex 2014; 56: 99-110.

* The first and second author contributed equally to this work

Abstract

Introduction. Macular degeneration (MD) causes central visual field loss. When field defects occur in both eyes and overlap, parts of the visual pathways are no longer stimulated. Previous reports have shown that this affects the grey matter of the primary visual cortex, but possible effects on the preceding visual pathway structures have not been fully established.
Methods. In this multicentre study, we used high-resolution anatomical magnetic resonance imaging and voxel-based morphometry to investigate the visual pathway structures up to the primary visual cortex of patients with age-related macular degeneration (AMD) and juvenile macular degeneration (JMD).
Results. Compared to age-matched healthy controls, in patients with JMD we found volumetric reductions in the optic nerves, the chiasm, the lateral geniculate bodies, the optic radiations and the visual cortex. In patients with AMD we found volumetric reductions in the lateral geniculate bodies, the optic radiations and the visual cortex. An unexpected finding was that AMD, but not JMD, was associated with a reduction in frontal white matter volume.
Conclusion. MD is associated with degeneration of structures along the visual pathways. A reduction in frontal white matter volume only present in the AMD patients may constitute a neural correlate of previously reported association between AMD and mild cognitive impairment.

2.1 Introduction

Macular degeneration (MD) is a class of eye diseases that causes visual field defects that are located in or near the central visual field (central scotoma). According to the World Health Organization, in 2002, age-related macular degeneration (AMD) and the juvenile-type macular degeneration (JMD) were the causes of blindness and low-vision in 8.7% of the 160 million cases worldwide (Resnikoff et al., 2004). In recent reports, AMD prevalence ranged from approximately 3 - 12% (Cheung et al., 2012; Finger et al., 2011; Jenchitr et al., 2011; Jonasson et al., 2011; Klein et al., 2011; Nangia et al., 2011; Ngai et al., 2011; Spanish Eyes Epidemiological study group, 2011; Stein et al., 2011; Yoon et al., 2011), while the prevalence of JMD was 0.03% (Pi et al., 2012). In Europe, the retinal pathologies underlying AMD and JMD are listed in the top five of causes of visual loss in both children and adults (Kocur and Resnikoff, 2002). In the European adult population, AMD is the most common cause of visual impairment (Augood et al., 2006).

Visual field loss in both AMD and JMD is primarily due to a loss of photoreceptors. Despite this, and the similarity in the resulting visual field defects, AMD and JMD do not share a common disease mechanism. The various macular pathologies underlying JMD may start early in childhood and are mostly inherited. They include diseases such as Stargardt's disease, Best's vitelliform retinal dystrophy (Best's disease), cone-rod dystrophy, and central areolar choroidal dystrophy. In AMD, the accumulation of sub-macular deposit called drusen compromises retinal metabolism and leads to the degeneration of the macula with or without neovascularization (Arden, 2006; Gehrs et al., 2006; Holz et al., 2004; Zarbin, 2004).

An absence of afferent or efferent stimulation may result in structural brain changes, and this has been reported in many conditions (Johansson, 2004; Merzenich et al., 1984). In cases where the central visual field defects in MD overlap in the two eyes, this results in a reduced stimulation of part of the visual pathways and visual cortex (Baseler et al., 2011; Masuda et al., 2008). This, in turn, could result in changes to the structure of the visual cortex (Boucard et al., 2009). Indeed, various retinal and optic nerve conditions have been found to be associated with cortical thinning or cortical grey matter loss (Alcauter et al., 2011; Boucard et al., 2009; Kitajima et al., 1997; Plank et al., 2011), and with volumetric reduction of the more proximal visual pathway structures such as the optic nerves (Hernowo et al., 2011). This raises the question whether MD might also affect the structural integrity of the visual pathways. This question is relevant, as a positive answer might implicate a need for modifications of the clinical management of MD. The question is also relevant in the light of the conflicting reports on the presence of functional occipital reorganization following retinal lesions (Baker et al., 2005, 2008; Dilks et al., 2009; Masuda et al., 2008; Schumacher et al., 2008; Smirnakis et al., 2005; Sunness et al., 2004). Here, we investigate whether MD affects the structural integrity of the visual pathways

by comparing their structural MRI morphometry in patients with MD and healthy controls.

2.2 Methods

2.2.1 Subjects

Participants of this study were recruited in Groningen (the Netherlands), York and London (United Kingdom) and Regensburg (Germany). This study conformed to the tenets of the Declaration of Helsinki and was approved by the respective medical review board of each centre participating in the study, and national regulatory ethics bodies, where necessary. The inclusion criteria required that subjects must be free from neurological or psychiatric disorders, and in the case of the patients present with central visual field defect attributed to bilateral macular degeneration. All participants gave their written informed consent before participation. The participants with macular degeneration were classified into two groups: patients with JMD and patients with AMD. In total, 114 subjects participated in this study: 25 with AMD, 34 with JMD, and the remaining 55 were healthy controls. However, one patient with AMD decided to quit the study, leaving in total 113 subjects included in the analyses.
The control subjects had a mean age of 49.6 years (range 13 to 83 years), and 46% of them were males. Of these controls, 22 subjects were age-matched (mean age 68, range 61-83 years) to the AMD group. The other 33 subjects (mean age 37.4, range 13 - 60 years) were age-matched to the JMD group. The characteristics of the affected participants are described in Table 2.1. In Table 2.2, the number of participants scanned at each location, and mean age of the separate groups are shown.
In the remainder of the paper, we therefore consider four groups: 1) AMD patients, 2) JMD patients, 3) the group of healthy older control subjects (HCO), age-matched to the AMD patients, and 4) the group of healthy young controls (HCY), age-matched to the JMD patients.

2.2.2 Magnetic resonance image acquisition

Since the datasets were from three different study centres, the magnetic resonance (MR)-acquisition parameters varied to some extent. However, all of the acquisitions were of 1 mm x 1 mm x 1 mm resolution. MR imaging was performed on three different scanners. Groningen datasets were acquired on a 3.0 Tesla Philips Intera (Eindhoven, The Netherlands) at the MRI Centrum, University Medical Center Groningen. A three-dimensional structural image was acquired on each subject using a sequence T1W/3D/TFE-2, 8^{o} flip angle, repetition time 8.70 ms, matrix size 256 x 256, field of view 230 x 160 x 180, yielding 160 slices. The York dataset was acquired using 8-channel, phase- array head coils on a Siemens Trio 3 Tesla at the Combined Universities Brain Imaging Center (Royal Holloway University of London). Multi-average, whole-head T1-weighted anatomical volumes were acquired for each

Characteristics	Values	
	AMD	JMD
Number of subjects	24	34
Age, mean (range), years	75.2 (52 - 91)	40.2 (12 - 66)
Female, sex, %	42	38
Visual acuity in logMAR, mean (range)		
OD	.96 (1.60 - .50)	1.12 (3.00 - .30)
OS	.88 (1.80 - .10)	1.16 (3.00 - .66)
Scotoma diameter, mean (range), degree	14 (4 - 25)	20 (3 - 65)

Table 2.1. Baseline patient characteristics. Characteristics of the two patient groups (AMD and JMD) were age, sex proportion (in percentage), visual acuity for one or both eyes (expressed in logMAR), and scotoma diameter (expressed in degree). AMD – age-related macular degeneration; JMD – juvenile type macular degeneration; logMAR – logarithm of minimum angle of resolution; OD - right eye (oculus dexter); OS - left eye (oculus sinister).

	AMD	HCO	JMD	HCY	Total
Groningen					
number of subjects	8	7	0	3	18
Age, mean (range), years	73.3 (52 – 83)	67.6 (61 – 83)		56.7 (56 – 58)	
York					
number of subjects	8	5	8	7	28
Age, mean (range), years	81.1 (71 – 91)	68.4 (61 – 78)	33.1 (20 – 50)	27.1 (19 – 38)	
Regensburg					
number of subjects	8	10	26	23	67
Age, mean (range), years	71.3 (54 – 83)	68.1 (61 – 83)	42.4 (12 – 66)	38.0 (13 – 60)	
Disease duration, mean, years	7.6 (1 – 21)		15.9 (2 – 42)		
Total number of subjects	24	22	34	33	113

Abbreviations: JMD - juvenile macular degeneration; HCY - healthy controls young (age-matched to JMD); AMD - age-related macular degeneration; HCO - healthy controls old (age-matched to AMD).

Table 2.2. Distribution of the four subject groups to the three different scanner locations. The table shows the number of subjects, mean age and, if available, mean duration of the disease in the specific subject group scanned at each location.

participant. Sequences used were MDEFT 16º flip angle, repetition time 7.90 ms, matrix size 256 x 256, field of view 176 x 256 x 256, yielding 176 sagittal slices. The Regensburg dataset was acquired on a 3.0 Tesla Allegra Scanner (Siemens, Erlangen, Germany). One hundred and sixty slices covering the whole brain, field of view = 256 x 256 mm, were obtained from each subject, using the Alzheimer's Disease Neuroimaging Initiative (ADNI; Jack et al., 2008) sequence (TR = 8.79 ms, TE = 2.6 ms, flip angle 9°).

2.2.3 Data preprocessing

Bias correction and noise reduction
The images were converted from their native formats into analyse (NIFTI) format. We performed bias correction (implemented in the SPM8 segmentation tool) and noise reduction using SUSAN (Smallest Univalue Segment Assimilating Nucleus) (Smith and Brady, 1997) prior to the next steps. SUSAN is a part of FSL (FMRIB Software Library, http://www.fmrib.ox.ac.uk/fsl).

Rigid body registration
We performed rigid body registration on the brains to a common template using SPM8's tool for co-registration. In this step, the brains are reoriented into the common template space using six linear transformation parameters: 3 translations and 3 rotations. All transformations are performed within a 3-dimensional coordinate system, with x, y, and z as its axes. This rendered the images to have uniform dimensions and to be in approximate alignment to each other.

Segmentation, registration, and modulation
We used SPM8's DARTEL (Diffeomorphic Anatomical Registration through Exponentiated Lie Algebra) suite of tools (Ashburner, 2007; Klein et al., 2009). DARTEL tools enabled us to create modulated grey and white matter images that were registered to a common reference image specifically representing our sample. The study-specific approach we used here enabled a more accurate inter-subject registration of brain images with improved localization and sensitivity of the voxel-based morphometry (VBM).
The process began with SPM8's segmentation, which segmented the co-registered T_1-weighted images, except for lateral geniculate body extraction. For the latter structure, we used FAST (FMRIB's Automated Segmentation Tool) and fed the output into the DARTEL pipeline. After all the brains were segmented, a reference –or template– image was generated. The first step in generating this reference image was averaging the images of all brains. Following this, the individual brains were deformed and registered as closely as possible to this reference image. Next, using the registered brain images, a new average reference image was created to which the individual brain images were again registered. After 6 of these averaging and registration cycles, the final reference image was generated. The final reference image was then used as

the template to which the native segmentations of the individual brains in the study were registered and modulated.

2.2.4 Data analysis

We performed two types of analyses: (1) a whole brain voxel-wise analysis; and (2) a region-of-interest (ROI)-based analysis. In the first type of analysis we did a whole brain analysis to examine whether there were volumetric differences in general in AMD and JMD patients. In the second type of analysis, we used masks to single out the visual pathways from the brain and analyze data specifically in those regions.

Voxel-wise analysis

The process from the segmentation to the voxel-wise statistical analyses is known as VBM, and is implemented in the SPM8 software package (Wellcome Department of Imaging Neuroscience, London, UK; http://www.fil.ion.ucl.ac.uk/spm) (Ashburner and Friston, 2000). VBM statistically assesses local changes in grey and/or white matter volume between groups of anatomical scans, and makes it possible to spatially detect any deviation in the visual pathways. Comparisons using ANCOVA were done separately for the AMD group to their specific group of age-matched controls, and for the JMD to their specific group of age-matched controls. Age was entered as a covariate in the analysis. Threshold-free cluster enhancement (TFCE) methods (Smith and Nichols, 2009) were applied to minimize the need for large scale smoothing or for predefining a significant cluster size.

To control for a scanning site effect, we included scanner location as a covariate in the voxel-wise analyses.

Differences in volumes between patients and healthy control subjects are shown in the figures for voxels with an associated $p<.01$ for the whole brain analysis, and $p<.05$ for the masked voxel-wise analysis (uncorrected for multiple comparisons). Only clusters with a minimum of 10 voxels are displayed.

ROI definition

In the ROI-based analysis, we used masks to extract ROI volumes from the modulated normalized brain segments. We used masks for the pregeniculate structures, the lateral geniculate bodies, the geniculo-calcarine radiations, the occipital pole, and the intracalcarine and supracalcarine cortices. The masks that we used to extract the volume of the pregeniculate structures and the lateral geniculate bodies were created manually, as the boundaries of those structures can be clearly defined visually. These visually defined masks were created on the average of all the images. The mask for the geniculo-calcarine radiations was taken from the Jülich histological atlas (Burgel et al., 1999, 2006), whereas the mask that covered the occipital pole, intra- and supracalcarine cortices were taken from the Harvard Center for Morphometric Analysis (Desikan et al., 2006; Frazier et al., 2005; Goldstein et al., 2007; Makris et al., 2006).

We defined five regions-of-interest (ROIs) along the visual pathway: pregeniculate structures (PGCL), which include the optic nerve, the chiasm and the optic tract, lateral geniculate bodies (LGB), geniculocalcarine radiations (GCR), also known as optic radiations, the occipital pole (OCP) and the calcarine region (CCR), which contains the intracalcarine and supracalcarine cortices. These ROIs mark the separate volumes

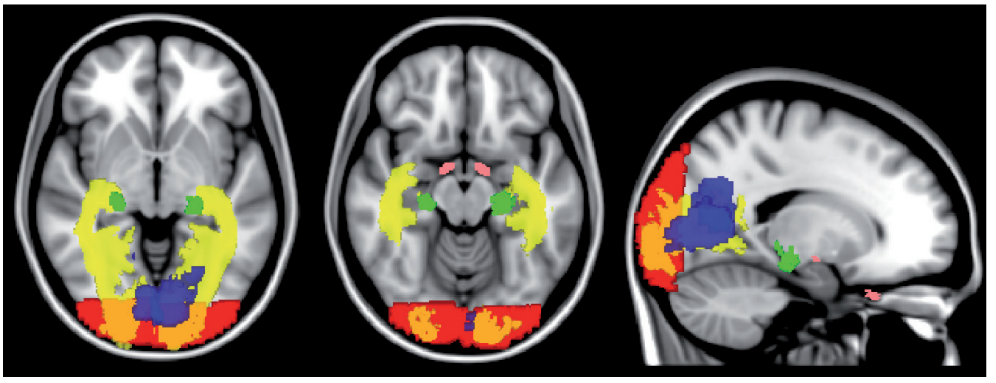

Figure 2.1. Location of the regions of interest located along the visual pathways.
Colour codes for the different regions of interest: Pink – Pregeniculate structures (PGCL); Green – Lateral geniculate bodies (LGB); Yellow – Geniculocalcarine radiations (GCR); Red – occipital pole (OCP); Blue – Calcarine region (CCR).

along the visual pathway we were interested in. Figure 2.1 shows the locations of the masks used to define the ROIs on a template brain.

Statistical analysis of the ROI data

Prior to the statistical analysis, we verified that the extracted values of the ROIs were normally distributed with the Kolmogorov-Smirnov test. Using repeated measures ANOVA, we analyzed the significance of the differences in volume of the entire visual pathway between the patient groups and their respective age-matched control groups. In this analysis, group was entered as a between-subject variable and ROI as a within-subject variable. Age and scanner location were added as a covariate. The significance of the differences in volume of the separate ROIs were analyzed with t-tests.

We visualized these differences within the defined ROIs using a masked voxel-wise analysis.

2.3. Results

2.3.1 Whole brain voxel-wise analysis

We performed a whole brain voxel-wise analyses to examine whether there were differences in the grey and the white matter in MD in the visual pathways, but also in regions outside of the visual pathways. Figure 2.2 shows results for this analysis. The upper row of images shows the results for the JMD group, while the lower row of images is for the AMD group, compared to their respective age-matched healthy controls.

In both the JMD and the AMD groups, we found reductions of grey (green and yellow color coded, respectively) and white (red and blue color coded, respectively) matter located in the visual cortex and the optic radiations. The reductions, in particular in the white matter, appear more pronounced in the AMD group than for the JMD group.

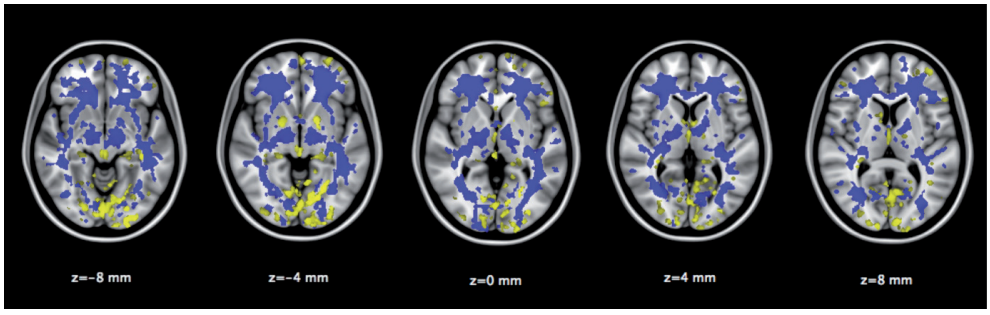

Figure 2.2. Volumetric reductions in juvenile (JMD) and age-related (AMD) macular degeneration
The transversal slices on the upper row highlight the areas where the JMD group shows significantly lower volume compared to the age-matched controls (p<.01, uncorrected). Green shows the involvement of grey matter, and red shows the involvement of white matter.
The transversal slices on the lower row highlight the areas where the AMD group shows significantly lower volume compared to the age-matched controls (p<.01, uncorrected). Yellow shows the involvement of grey matter, blue shows the involvement of white matter.
Talairach position of the slices is given by their "z" value.

In the AMD group, we also find marked differences outside of the visual pathways. These were mainly located in white matter in the frontal lobe, as shown in Figure 2.2, compared to the age-matched healthy controls (shown here at p<.01, uncorrected). These unexpected frontal white matter differences remained present also after applying a more stringent family-wise error correction (p<.01, corrected), as shown in figure S1 of the supplementary information.

We did not find any increases in grey or white matter in the whole brain voxel-wise analyses for either type of MD.

2.3.2 ROI-based analysis

In both the patients and the controls groups, the distribution of the volumes of the ROIs did not deviate from normality. Table 2.3 shows, for the five ROIs, the mean volume and the relative differences of the ROI volume for the patient groups relative to their age-matched controls. Next, we tested whether there were volumetric differences in the defined ROIs along the visual pathway between patients and controls.

	ROI μ ± σμ				
	PGCL (mm^3)	**LGB (mm^3)**	**GCR (cm^3)**	**OCP (cm^3)**	**CCR (cm^3)**
AMD	401.58 ± 21.94	86.67 ± 3.17	9.51 ± .23	5.72 ± .12	6.66 ± .20
HCO	459.41 ± 24.75	91.77 ± 3.02	11.29 ± .17	6.64 ± .12	8.09 ± .29
JMD	382.62 ± 13.44	95.94 ± 3.48	10.78 ± .18	6.35 ± .11	7.91 ± .16
HCY	419.06 ± 12.64	109.76 ± 3.49	11.68 ± .19	6.95 ± .15	8.58 ± .23
	Relative difference to the controls (%)				
AMD	-12.6	-5.6	-15.8	-13.9	-17.7
JMD	-8.7	-12.6	-7.7	-8.6	-7.8

Table 2.3. ROI morphometry. Morphometric values in term of area or volume were extracted from ROIs situated along the visual pathway. ROI - regions of interest; μ - mean; σμ - standard errors of mean; AMD - age-related macular degeneration; HCO - healthy controls old (age-matched to AMD); JMD - juvenile macular degeneration; HCY - healthy controls young (age-matched to JMD); PGCL - pregeniculate structures; LGB - lateral geniculate bodies; GCR - geniculocalcarine radiation; OCP - occipital poles; CCR – calcarine region.

Figure 2.3 shows the mean volumes of each ROI for all four groups: the AMD patients, the JMD patients, the older healthy controls and the younger healthy controls.
Figure 2.4 shows the distribution of the ROI volume as a function of age for the various ROIs. The regression lines show the effect of age for the two control groups combined. In PGCL and GCR, there is no significant correlation between ROI volume and age in the healthy controls. In the other ROIs – LGB, OCP and CCR – volume reduces with age. The Pearson correlation coefficients are respectively -.310, -.223 and -.252, in the LGB and CCR these correlation are significant ($p<.05$). We therefore included age as a covariate in our subsequent analyses.
In general, for all ROIs, the volume is lower in the AMD patients than in the age-matched control group ($F(1, 42) = 20.415$, $p<.001$). The same is true for the volume of the ROIs in the JMD compared to the age-matched control group ($F(1, 63) = 26.170$,

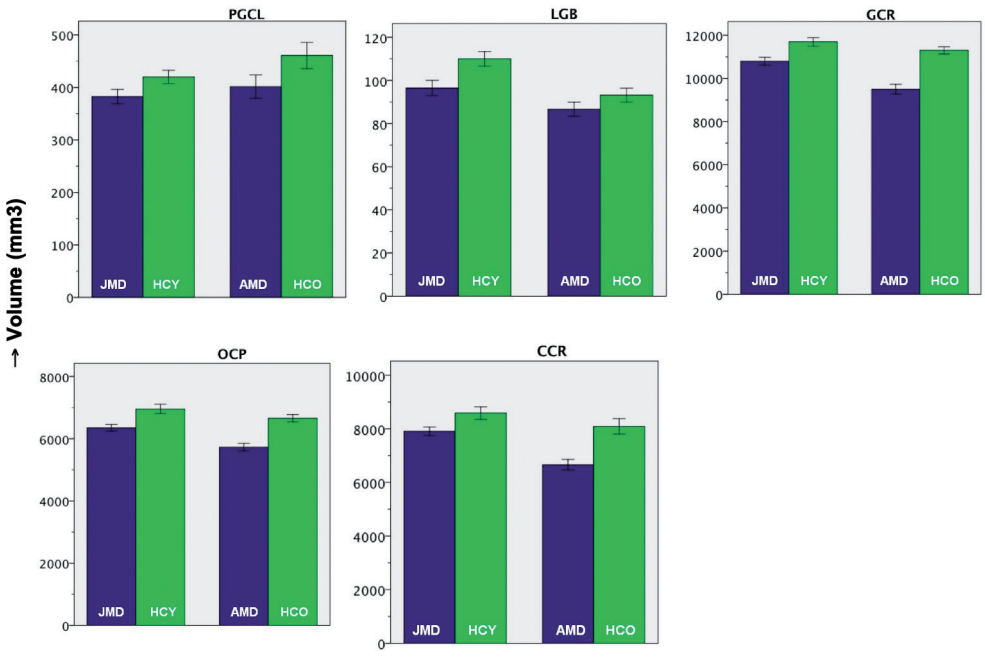

Figure 2.3. Mean volume of five ROIs located along the visual pathways. ROI – region of interest; JMD – patients with juvenile macular degeneration; HCY - healthy controls young (age-matched to JMD); AMD – patients with age-related macular degeneration; HCO – healthy controls old (age-matched to AMD);
ROI abbreviations: PGCL – pregeniculate structures; LGB – lateral geniculate bodies; GCR - geniculocalcarine radiation; OCP - occipital poles; CCR – calcarine region.
The bars show the mean value of the ROI-volume in the particular group. The error bars show +/- 1 standard error of the mean.

p<.001). T-tests showed that for the AMD vs. HCO groups the differences were significant in the GCR, OCP and CCR ROIs, and for the JMD vs. HCY the differences were significant in the LGB, GCR and OCP ROIs (all p<0.01). Table 2.4 shows all statistical values for the comparisons of ROI volumes between patients and controls.

In the subgroup of patients from Regensburg, data on duration of the macular degeneration at the time of scanning, was available. This subgroup from Regensburg contained 34 patients in total, of which 26 were JMD patients and 8 were AMD patients. In this group, we did not find a significant correlation between ROI volume and disease duration in AMD or in JMD.

2.3.3 ROI-masked voxel-wise visualization

To visualize the distribution of the volumetric differences in the ROIs, voxel-wise statistical comparisons were done on the ROI brain regions of the visual pathway of AMD and JMD patients. Figure 2.5 shows a comparison between AMD patients and

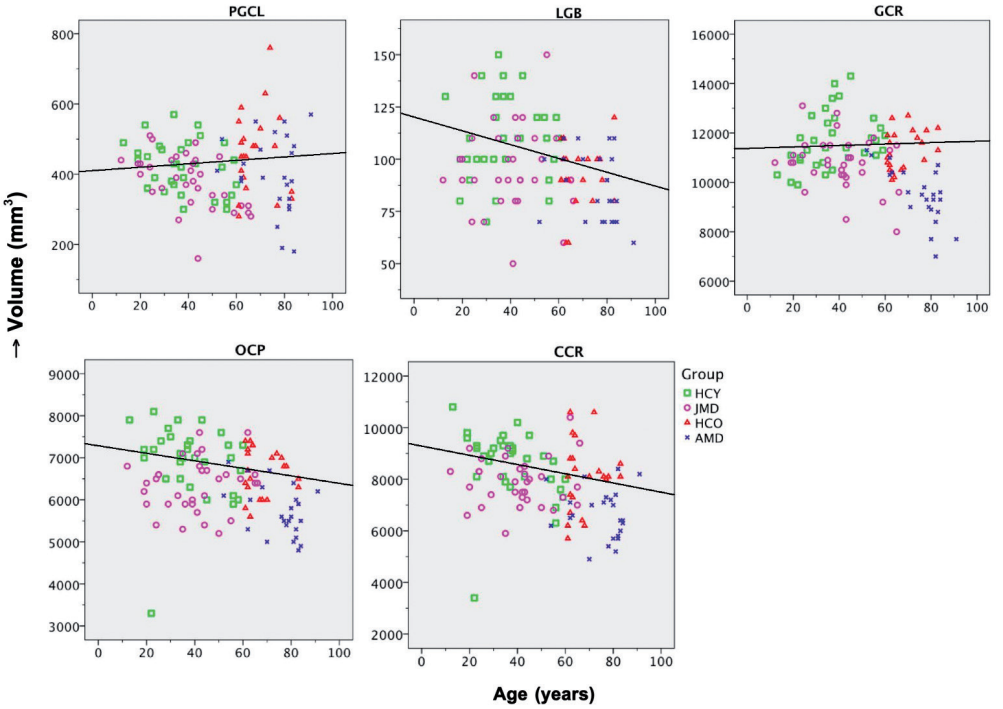

Figure 2.4. ROI volume as a function of age.
ROI – region of interest; HCY - healthy controls young (age-matched to the JMD-patients); JMD – patients with juvenile macular degeneration; HCO - healthy controls old (age-matched to the AMD-patients); AMD - patients with age-related macular degeneration.
ROI abbreviations: PGCL – pregeniculate structures; LGB – lateral geniculate bodies; GCR - geniculocalcarine radiation; OCP - occipital poles; CCR – calcarine region.

Comparison		Regions of Interest				
		PGCL	LGB	GCR	OCP	CCR
AMD – HCO	t-value (df = 44)	1.783	1.421	6.310	5.458	4.153
	p-value	.082	.162	<.001	<.001	<.001
JMD – HCY	t-value (df = 65)	2.018	2.759	3.381	3.301	2.408
	p-value	.048	.008	.001	.002	.019

Abbreviations: JMD - juvenile macular degeneration; HCY - healthy controls young (age-matched to JMD); AMD - age-related macular degeneration; HCO - healthy controls old (age-matched to AMD); PGCL - pregeniculate structures; LGB - lateral geniculate bodies; GCR - geniculocalcarine radiation; OCP - occipital poles; CCR – calcarine region.

Table 2.4. Statistics for comparison of ROI volumes between patients and controls. The upper part shows the statistical values for the comparison of the AMD group to the HCO group, whereas the lower part shows the statistical values for the comparison of the JMD group to the HCY group (t-values, degrees of freedom and p-values are given).

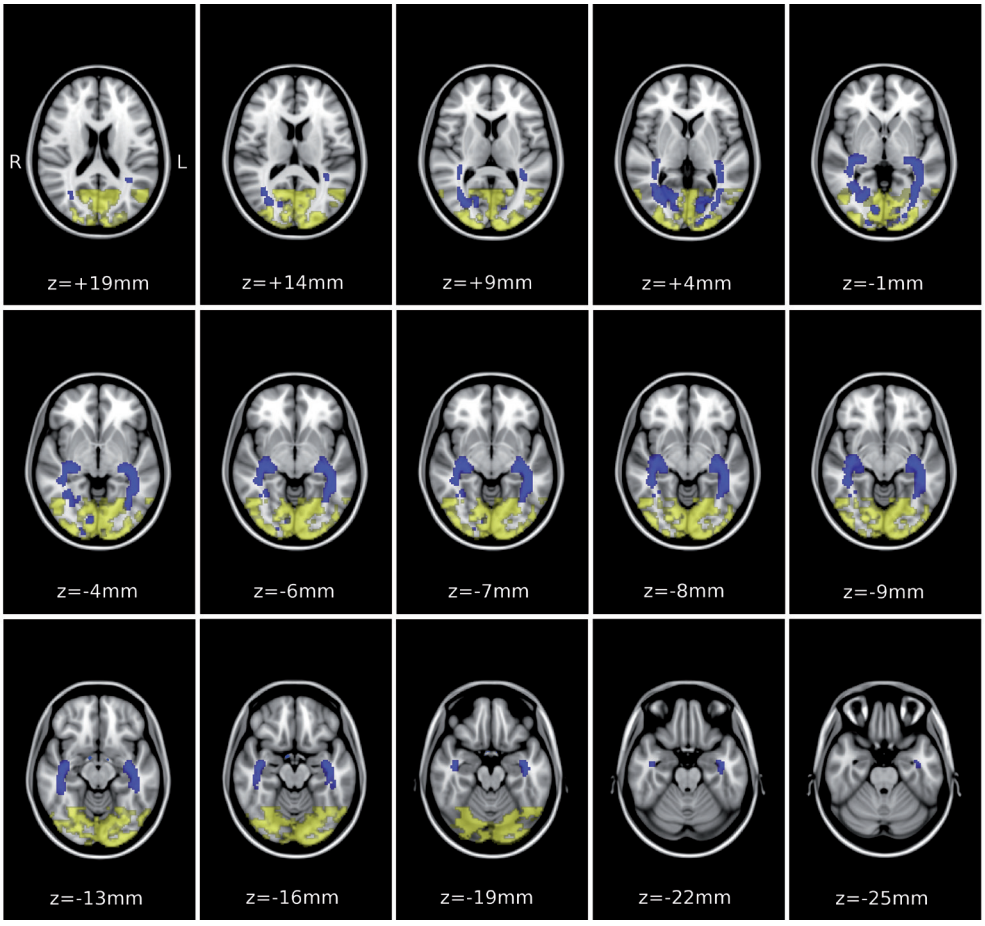

Figure 2.5. Volumetric reductions in the masked visual pathway ROIs in age-related macular degeneration (AMD). The transversal slices of the template brain highlight the areas where the AMD group shows significantly lower volume compared to the age-matched controls ($p<.05$, uncorrected), within the defined ROI masks along the visual pathway. Involvement of the grey matter (yellow) can be seen in the visual cortex, whereas white matter involvement (blue) can be seen in the optic tract and in the regions corresponding to the geniculocalcarine radiation. The Talairach position of the slices is given by the "z" value.

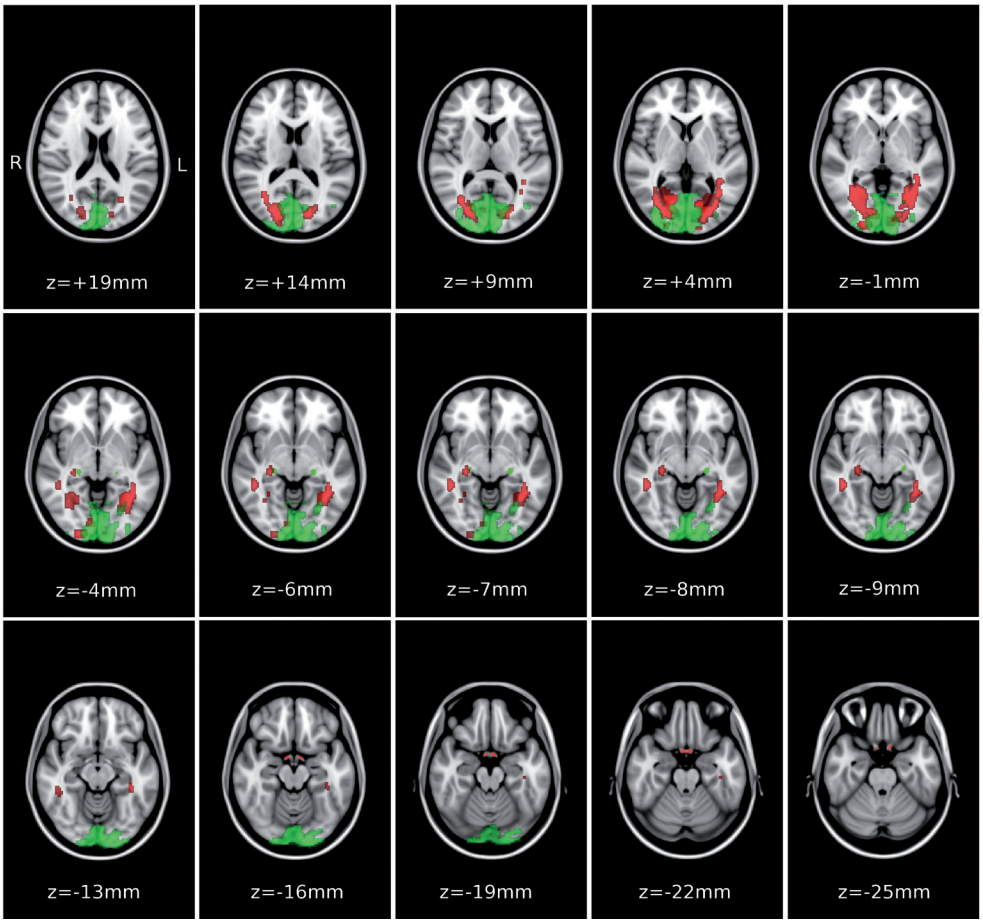

Figure 2.6. Volumetric reductions in the masked visual pathway ROIs in juvenile macular degeneration (JMD). The transversal slices of the template brain highlight the areas where the JMD group shows significantly lower volume compared to the age-matched controls ($p<.05$, uncorrected), within the defined ROI masks along the visual pathway. Involvement of the grey matter (green) can be seen in the visual cortex and at the position of the lateral geniculate bodies, whereas white matter involvement (red) can be seen in the pregeniculate structures and in regions corresponding to the geniculo-calcarine radiation. The Talairach position of the slices is given by the value "*z*".

---

age-matched controls, whereas Figure 2.6 shows the comparison for the JMD patients and age-matched controls. For this visualization, a rather liberal threshold of $p<.05$ (uncorrected) was used, to indicate the extent of the changes within the ROIs.
In both types of MD, the volumetric reductions identified by our ROI analysis are dispersed throughout all of the retrobulbar afferent visual pathway structures.

2.4 Discussion

MD is known as one of the primary causes of blindness and its retinal pathology has been studied extensively. Only in recent years, however, the involvement of the cerebral cortex in this pathology has become a topic of study (Baker et al., 2005, 2008; Boucard et al., 2009; Clarke, 1994; Liu et al., 2010; Masuda et al., 2008; Nguyen et al., 2003). Our previous findings of grey matter loss in the visual cortex in AMD and glaucoma (Boucard et al., 2009), as well as in JMD (Plank et al., 2011), and a reduced volume of the visual pathways in glaucoma (Hernowo et al., 2011) prompted us to study the question whether the (pre-cortical) visual pathway in MD might also be affected. Here, we found that in MD there was indeed volumetric loss of the visual pathway structures. Moreover, in the whole brain voxel-wise analysis we found a volumetric reduction in the frontal lobe in AMD patients, mainly in the white matter, While previous studies have shown that in MD the brain is functionally and structurally affected (Baseler et al., 2011; Boucard et al., 2009; Plank et al., 2011), to our knowledge, this is the first one to report on the extensiveness of the structural changes.

What may have caused this volumetric loss of the pathway structures in MD? A similar loss has previously been reported in glaucoma (Hernowo et al., 2011). In glaucoma, it is rather intuitive that the retrobulbar visual pathway may be involved in its pathology as there is a loss of retinal ganglion cells (RGCs) and their axons form the optic nerve. However, in MD, the primary loss of vision is due to damage of the photoreceptors (Margalit and Sadda, 2003), which are first-order neurons. This degeneration does not necessarily have to be transferred across the retinal layers to the bipolar (second-order neuron) and RGC (third-order neuron) layers and their projecting axons. This argument would hold even more for the geniculate and post-geniculate structures. However, studies indicate that a loss of RGCs may also be associated with the loss of photoreceptors in both wet AMD (Medeiros and Curcio, 2001) as well as in the later stages of dry AMD (geographic atrophy) (Clarke, 1994; Kim et al., 2002). This indicates that RGCs can be affected by the adverse effect of photoreceptor degeneration and provides a possible mechanism that can explain the volumetric reduction of the visual pathway and cortex in patients with MD.

Our ROI-based analysis, in which we investigate the volume of the separately defined structures of the visual pathways, indicated changes in both AMD and JMD, when compared to the age-matched controls (Figure 2.3, and Table 2.3). We also plotted ROI volume against age to verify the presence of a correlation with age. Indeed, in the healthy controls we found a negative correlation of age and volume to be present in the LGB, OCP and CCR (Figure 2.4). To account for such age effects, age was included as a co-variate in the ROI- and voxel-wise analyses..

In JMD, we found volumetric differences along the full extent of the visual pathways. In AMD we found volumetric differences in the optic radiations and the visual cortex.

Moreover, we could confirm the previous findings of a reduction in grey matter in the early visual cortex of AMD (Boucard et al., 2009), and JMD (Plank et al., 2011) patients. In JMD we found a lower volume in PGCL and LGB compared to healthy controls, while in AMD we did not find such volumetric differences. This difference in results between JMD and AMD group can have various possible explanations. First, in the JMD group, the mean visual acuity was worse than in AMD group and also the scotoma diameter was on average larger in JMD group than in AMD group (Table 2.1), It could also be caused by the lower number of AMD patients (24), compared to JMD patients (34). Finally, it could be associated with the notion that the volume of the PGCL appears to be larger in the older control group than in the younger control group, as shown in Table 2.3. This apparent increase in pre-geniculate volume with age might be a factor in the difference in results between AMD and JMD, although the difference in PGCL volume between HCO and HCY is not significant.

In both AMD and JMD groups, the volume of the optic radiations is reduced markedly. The effect in the optic radiations actually appears to be larger than the effect in the anterior visual pathways. A possible reason for this could be that besides feedforward projections from the LGB to the visual cortex, corticogeniculate neurons provide input from the visual cortex back to the LGB (Briggs and Usrey, 2011). Such feedback pathways have not been found between the LGB and the retina. Therefore, the optic radiations could be affected more than the anterior visual pathways. Besides that, the size of the GCR ROI is much larger than the PGCL, which implies that there might be more overlap in effects between the subjects in the GCR ROI than in the PGCL ROI. Even though the visual cortex is one of the regions of cerebral cortex that is least affected by age (Raz et al., 2005) the age effects in the control groups suggest that it is necessary to account for age in the analyses. Duration of the disease could possibly also have an effect on the degree of changes in the visual pathways. In this study there was data available on disease duration only for the participants from Regensburg. In this subgroup, we did not find a significant correlation between disease duration and ROI volume. Nevertheless, we suggest that future studies should still consider taking the duration of disease into account. JMD starts earlier in life and thus, at a particular age of the subject, the disease period is usually longer, and thus hypothetically JMD will have had a larger chance than AMD to affect the retrobulbar visual pathway.

Unexpectedly, in the whole brain voxel-wise analysis, we also found a lower volume in white matter in the frontal lobe, specifically in the AMD participants. As far as we know, no relationship between AMD and frontal lobe volume has been described. This finding could be associated with a possible link between AMD and mild cognitive impairment and Alzheimer's disease, which has been suggested earlier, based on a number of epidemiological studies (Kamran Ikram et al., 2012; Klaver et al., 1999; Pham et al., 2006; Woo et al., 2012). It should be noted, however, that smoking is an important co-factor in this correlation (Klaver et al., 1999). Unfortunately, we did not

have information about smoking habits on our patients. Nevertheless, a common pathogenic mechanism for AMD and Alzheimer's disease has been described (Ohno-Matsui, 2011). It is less plausible that reduced frontal lobe volume could be due to a decreased activity of AMD participants as a consequence of their visual impairment. If so, we would expect to find a similar effect in the JMD participants, which was not the case. We suggest that a follow-up study is required to confirm the presence of an association between AMD and frontal lobe grey and white matter density.
Our study design was cross-sectional, therefore we can not determine which happened first, the volumetric reduction in the brain, or the degeneration of the macula. Macular degeneration has been managed clinically as an ocular pathology. However, the structural changes, mainly in the lateral geniculate bodies and the visual cortex, may alert clinicians to the possibility that brain-related mechanism are involved in the disease. A neuroprotective approach to preserve the photoreceptors and retinal pigment epithelium by the administration of ciliary neurotrophic factors (Biarnes et al., 2011) or anti-inflammatory (Forrester et al., 2010) drugs might be worthwhile to consider as a first step. Our findings suggest that any retinal neuroprothesis (Zrenner, 2002) should be implanted as early as possible to avoid long-term, and perhaps irreversible, reductions in grey matter of the visual pathway. A better comprehension of the pathology underlying the various macular degeneration types and diagnostic approach are of utmost importance to allow the quantification of treatment outcome. We believe that neuroimaging and retinal imaging (Keane and Sadda, 2010), as well as their quantification methods (Ashburner and Friston, 2000; Boucard et al., 2009; Göbel et al., 2011; Menke et al., 2011), could – over time – become clinically viable options to evaluate the progress of the disease and the treatment outcome.

In summary, in both age-related and juvenile MD the volume of the visual pathway is significantly reduced. The extent of involvement was different for the two types of disease, with JMD showing the most widespread involvement of the visual pathway. This implies that it could be useful to also investigate the chronology of the visual pathway changes in macular degeneration. Moreover, we found an indication that the white matter volume in the frontal lobe is reduced in AMD. This could be the neural correlate of the proposed link between AMD and mild cognitive impairment and Alzheimer's disease.

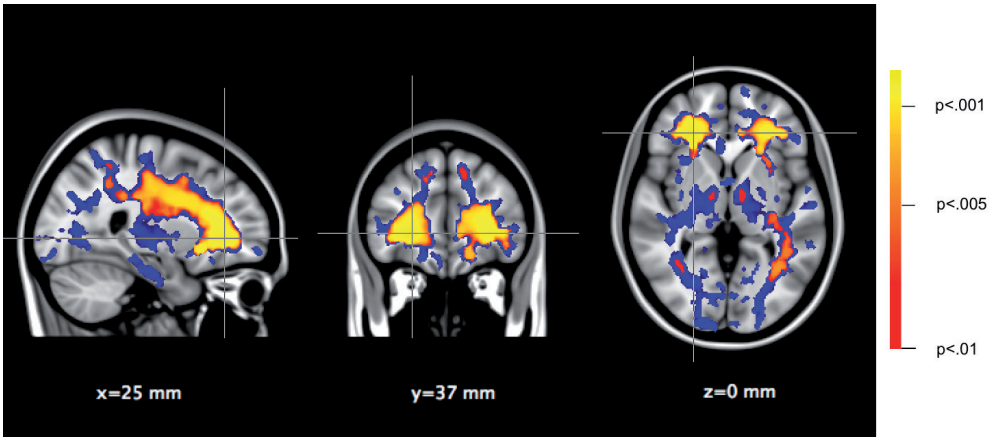

Figure S1. Volumetric reductions in white matter in age-related macular degeneration (AMD). The sagittal, coronal and transversal slices show the areas where the AMD group shows significantly lower volume of white matter compared to the age-matched controls. The blue area shows the uncorrected results (p<.01), the same threshold as used in Figure 2.2 of the main paper. Red-yellow shows the involvement of white matter after applying a family-wise error correction and again thresholding at p<.01.
Talairach position of the slices is given by their "x", "y" and "z" value.

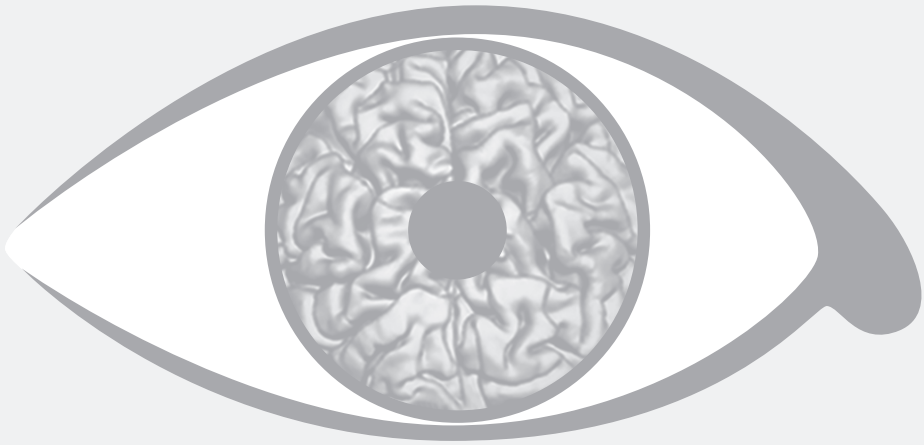

CHAPTER 3

Surface-based analyses of anatomical properties of the visual cortex in macular degeneration

Doety Prins, Tina Plank, Heidi A. Baseler, André D. Gouws, Anton Beer, Antony B. Morland, Mark W. Greenlee, Frans W. Cornelissen

Published in: PLoS One 2016; 11(1):e0146684

Abstract

Introduction. Macular degeneration (MD) can cause a central visual field defect. In a previous study, we found volumetric reductions along the entire visual pathways of MD patients, possibly indicating degeneration of inactive neuronal tissue. This may have important implications. In particular, new therapeutic strategies to restore retinal function rely on intact visual pathways and cortex to reestablish visual function. Here we reanalyze the data of our previous study using surface-based morphometry (SBM) rather than voxel-based morphometry (VBM). This can help determine the robustness of the findings and will lead to a better understanding of the nature of neuroanatomical changes associated with MD.

Methods. The metrics of interest were acquired by performing SBM analysis on T1-weighted MRI data acquired from 113 subjects: patients with juvenile MD (JMD; n = 34), patients with age-related MD (AMD; n = 24) and healthy age-matched controls (HC; n = 55).

R**esults.** Relative to age-matched controls, JMD patients showed a thinner cortex, a smaller cortical surface area and a lower grey matter volume in V1 and V2, while AMD patients showed thinning of the cortex in V2. Neither patient group showed a significant difference in mean curvature of the visual cortex.

Discussion. The thinner cortex, smaller surface area and lower grey matter volume in the visual cortex of JMD patients are consistent with our previous results showing a volumetric reduction in their visual cortex. Finding comparable results using two rather different analysis techniques suggests the presence of marked cortical degeneration in the JMD patients. In the AMD patients, we found a thinner cortex in V2 but not in V1. In contrast to our previous VBM analysis, SBM revealed no volumetric reductions of the visual cortex. This suggests that the cortical changes in AMD patients are relatively subtle, as they apparently can be missed by one of the methods.

3.1 Introduction

Macular degeneration (MD) is a group of retinal diseases which can cause a central visual field defect, due to damage in the macular region. In a previous neuro-imaging study, voxel-based morphometry (VBM) analysis showed volumetric changes in the visual cortex of MD patients with binocular central visual field defects, compared to healthy controls.(Hernowo et al. 2014) The goal of the current study was to further characterize these volumetric changes in the same group of MD patients using surface- rather than voxel-based metrics of brain morphology. Surface-based morphometry (SBM) can provide additional information about the brain structure such as cortical thickness, curvature and surface area.(Hutton et al. 2009) Hence, analyses using SBM may provide further insight into the nature of the neuroanatomical changes previously found in MD patients. This is important, as such structural changes might limit future treatments of MD that aim to restore visual function, such as retinal implants, stem-cell treatment and retinal pigment epithelium transplantation.(Zrenner 2002, Van Zeeburg et al. 2012)

MD can be divided into age-related macular degeneration (AMD) and juvenile macular degeneration (JMD). In AMD, the macula degenerates by the accumulation of drusen in the macular area, which in turn interferes with the retinal metabolism. The degeneration of the macula can cause a central visual field defect.(Arden 2006, Gehrs et al. 2006, Holz et al. 2004) Worldwide, AMD is the third most prevalent cause of blindness (8.7%).(Resnikoff et al. 2004) However, in diverse parts of the world, the prevalence of AMD as a cause of visual impairment or blindness varies.(Congdon et al. 2004, Rahmani et al. 1996, Munoz et al. 2000, Klaver et al. 1998, VanNewkirk et al. 2001) JMD is a group of diverse eye diseases, which includes Stargardt's disease, Best's vitelliform retinal dystrophy (Best's disease), cone-rod dystrophy, and central areolar choroidal dystrophy. These diseases start in the early decades of life and are mostly hereditary. The different pathological mechanisms of these diseases all lead to the loss of photoreceptors, and therefore cause a central visual field defect.

If the visual field defect in MD occurs in both eyes and overlaps – which is common – the activity in specific parts along the visual pathways is reduced, potentially causing functional deprivation. This deprivation may be responsible for the structural changes in the visual pathways. Alternatively, changes may be caused by anterograde transsynaptic degeneration, in which damage of the retinal ganglion cells transmits to related neurons, resulting in axonal damage of the visual pathways.

In both AMD and JMD patients, previous studies have found a reduction of the grey matter volume near the occipital pole in the posterior part of the calcarine sulcus.(Plank et al. 2011, Boucard et al. 2009) This indicates that MD is associated with retinotopic-specific neuronal degeneration of the visual cortex, as the central visual field is projected at the occipital pole. In addition to a decreased grey matter volume, a recent study from our group also showed a decreased white matter volume along the visual pathways in

both AMD and JMD patients. Additionally, in AMD, a decreased white matter volume was found outside the visual pathways, particularly in the frontal lobe.(Hernowo et al. 2014)

The goal of the current study was to further characterize the previously reported volumetric changes in the visual cortex in MD patients. To do so, we applied SBM to the same group of AMD and JMD patients in which we previously applied VBM and demonstrated changes in grey and white matter volume.(Hernowo et al. 2014) Using the surface-based analysis package Freesurfer, we investigated whether these volumetric differences are also reflected in changes in the cortical thickness, mean curvature or cortical surface area of the MD patients compared to age-matched controls. Moreover, we also reassessed grey matter volume using this surface-based approach. Recently, SBM showed a decreased gyrification in albinism in the same areas where VBM had indicated a decreased grey matter volume.(Bridge et al. 2012) Therefore, we hypothesized to find a decreased gyrification in addition to a reduced volume in the visual cortex of MD patients as well.

3.2 Methods

3.2.1 Ethics statement

This study conformed to the principles of the Declaration of Helsinki, and was approved by the respective medical review board of each centre participating in the study: the Medical Ethical committee of the University Medical Center Groningen in Groningen; the York Neuroimaging Centre Ethics committee and the local National Health Service Ethics committee in York; the Royal Holloway Ethics committee of the University of London and the local National Health Service ethics committee in London; and the Ethical committee of the University of Regensburg in Regensburg. All participants gave written informed consent before participating in the study. Written informed consent from the children enrolled in the study were obtained from both the child and from the respective parent.

3.2.2 Subjects

For this study, we included 113 subjects, which comprises the same group of subjects that was included in the study of Hernowo et al..(Hernowo et al. 2014) These subjects were recruited in Groningen (the Netherlands), York and London (United Kingdom) and Regensburg (Germany). Patients were included in this study when they suffered from a binocular visual field defect due to MD. Healthy control subjects had a good visual acuity in both eyes, and were free from visual field defects. All subjects were free from neurological or psychiatric disorders.

Here, we will briefly specify the subjects characteristics. For the more complete

description of our subjects, we refer to Hernowo et al..(Hernowo et al. 2014) We included 34 JMD patients, 24 AMD patients and 55 healthy control subjects. The patients were assigned to either the JMD or the AMD group based on their clinical diagnosis. We split the group of healthy controls into 33 controls for the JMD patients and 22 controls for the AMD patients, based on their age. This makes four subject groups for the analyses: 1) JMD patients, 2) young healthy controls (HCY), age-matched to the JMD patients, 3) AMD patients, and 4) old healthy controls (HCO), age-matched to the AMD patients. JMD patients had a mean age of 40.2 years (range 12 – 66 years), the HCY subjects had a mean age of 37.4 years (range 13 – 60 years). AMD patients had a mean age of 75.2 years (52 – 91 years), the HCO subjects had a mean age of 68 years(61 – 83 years). Table 3.1 shows the mean scotoma diameter for the AMD and JMD patients and the mean disease duration for the AMD and JMD patients from Regensburg.

Characteristics	Values	
	AMD	JMD
Number of subjects	24	34
Scotoma diameter, mean (range), degree	14 (4 - 25)	20 (3 - 65)
Subjects from Regensburg		
Number of subjects	8	26
Disease duration, mean (range), years	7.6 (1 - 21)	15.9 (2 – 42)

Table 3.1. Patient characteristics. Scotoma diameter in degrees of visual angle; mean duration of the disease in the subjects from Regensburg. JMD - juvenile macular degeneration; AMD - age-related macular degeneration.

3.2.3 Data acquisition

Magnetic resonance images (MRI) were acquired using three different scanners in three centers. However, all acquisitions were of 1 mm x 1 mm x 1 mm resolution. Information on the MRI acquisition has also been described in the previous publication of Hernowo et al..[1]

Groningen: the dataset was obtained using an 8-channel phased-array SENSE head coil on a 3.0 Tesla Philips Intera (Eindhoven, The Netherlands) at the Neuroimaging Center, University of Groningen, University Medical Center Groningen. Three-dimensional structural images were acquired using a sequence T1W/3D/TFE-2, 8° flip angle, repetition time (TR) 8.70 ms, echo time (TE) 4.4 ms, matrix size 256 x 256, field of view 230 x 160 x 180, yielding 160 slices.

York: the dataset was obtained using an 8-channel, phased-array head coil on a

Siemens Trio 3 Tesla at the Combined Universities Brain Imaging Center, Royal Holloway University of London. Multi-average, whole head T1-weighted anatomical images were acquired using an MDEFT sequence with 16° flip angle, TR 7.90 ms, TE 2.5 ms, matrix size 256 x 256, field of view 176 x 256 x 256, yielding 176 sagittal slices.

Regensburg: the dataset was obtained using a multicoil phased-array head coil on a 3.0 Tesla Allegra Scanner (Siemens, Erlangen, Germany). Whole brain T1-weighted images were obtained using a 3D-MPRAGE sequence, matrix size 256 x 256, field of view of 256 x 256 x 160, yielding 160 slices, using the Alzheimer's Disease Neuroimaging Initiative (ADNI) sequence (TR = 8.79 ms, TE = 2.6 ms, flip angle 9°).(Jack et al. 2008)

3.2.4 Surface-based morphometry

SBM analyses of cortical thickness, mean curvature, surface area and grey matter volume were performed using the Freesurfer image analysis suite (version 5.3.0, available at: http://surfer.nmr.mgh.harvard.edu/). The processing includes removal of non-brain tissue,(Ségonne et al. 2004) automated Talairach transformation, intensity normalization,(Sled et al. 1998) tessellation of the grey/white and grey/cerebrospinal fluid boundaries and automatic correction of topologic inaccuracies,(Fischl et al. 2001, Ségonne et al. 2007) surface deformation and inflation,(Dale et al. 1999, Fisch et al. 1999a) registration to a spherical atlas(Fisch et al. 1999b) and automatic parcellation of the cortex surface based on gyral and sulcal structures.(Desikan et al. 2006, Fischl et al. 2004) The reconstruction process resulted in of a variety of surface-based data, such as cortical thickness, mean curvature, surface area measurement and grey matter volume.

3.2.5 Data analysis

We performed both whole brain and region-of-interest (ROI) -based analyses. In the whole brain analyses, we analyzed the cortical thickness and the mean curvature. We studied differences in cortical thickness and mean curvature, and differences in the correlation between age and cortical thickness and the correlation between age and mean curvature between patients and their age-matched controls. To correct for any sources of variance exclusively related to age or scanner location, we added age and scanner location at which the subject was scanned as covariates to this analysis. To correct for multiple comparisons, we applied a false-discovery rate (FDR) value of 0.05.

Cortical thickness was calculated as the shortest distance between the grey/white boundary and the grey/cerebrospinal fluid boundary at each vertex across the cortex in millimeters (mm). Mean curvature was calculated as the mean of the minimum and maximum bending of the surface in each vertex in mm-1. Surface area was measured by calculating the surface area size of each triangle, in which the surface was divided by connecting the vertices, in mm2. The surface area of a single triangle depends on the number of vertices the cortex was divided into, which in turn depends on the size of the brain. Since it is not yet clear whether this would reflect the actual surface area

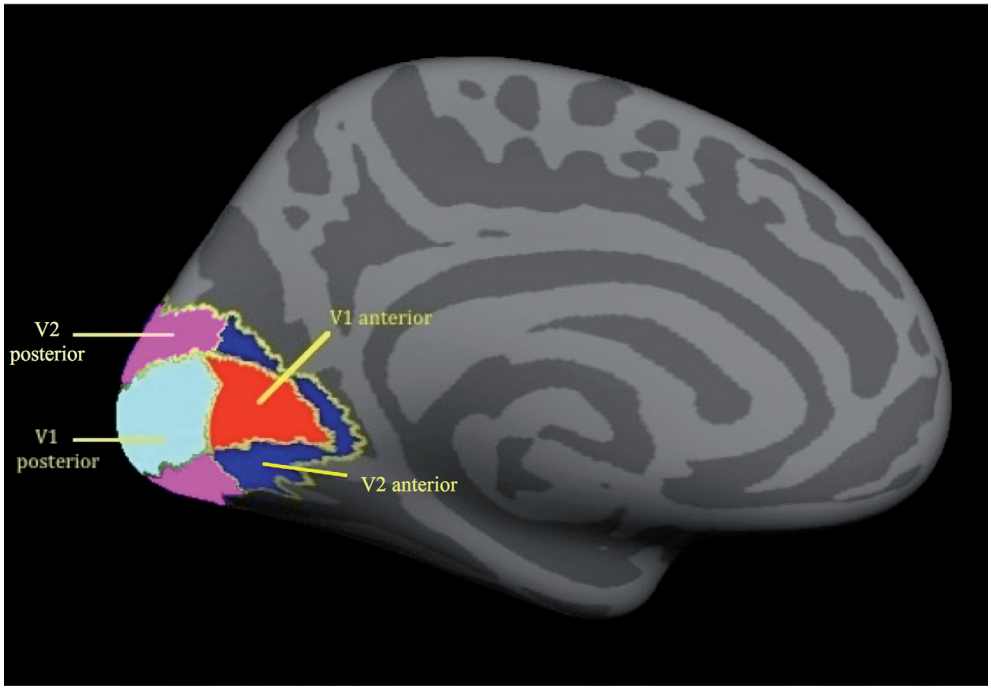

Figure 3.1. ROIs in the visual cortex. ROIs are depicted on the left hemisphere.
Red – V1 anterior; Cyan – V1 posterior; Dark blue – V2 anterior; Magenta – V2 posterior.
ROI – region of interest.

in whole brain analysis, we decided not to perform whole brain analysis on surface area. Grey matter volume was calculated as the product of the surface area and cortical thickness in mm3, therefore we did also not perform a whole brain analyses on grey matter volume.

For the ROI-analyses we examined the surface area and grey matter volume, as well as the cortical thickness and mean curvature. We defined our ROIs using the Freesurfer labels for the areas V1 and V2. Moreover, we consecutively divided both V1 and V2 in an anterior and a posterior part. We chose to analyze the anterior and posterior parts of V1 and V2 separately because all patients had a central visual field defect. Since the central visual field is retinotopically represented in the occipital pole, we expected the anterior and posterior parts of V1 and V2 not to be equally affected. Therefore, an analysis of the entire V1 and V2 might not present sufficient details on the actual structural changes in our patient groups. Figure 3.1 depicts the defined ROIs on the left hemisphere of the average brain; the actual analyses were done on the ROIs in both hemispheres combined. For each ROI, data on cortical thickness, mean curvature, surface area and grey matter volume were extracted using Freesurfer. Differences between patients and controls in the specific ROIs were examined using MANCOVA. The dependent variables were

cortical thickness, mean curvature, surface area and grey matter, and the subject groups were entered as a fixed factor. Also in this analysis, age and scanner location were added as covariates.

Specifically in patients from Regensburg, data on disease duration was available. In this subgroup of patients, we analyzed whether there was a correlation between disease duration and cortical thickness, mean curvature, surface area and grey matter for each ROI. We tested this using the Pearson correlation test. Statistical tests were performed in the IBM SPSS Statistics software package, version 20.

3.3 Results

3.3.1 ROI-based analysis

Within the V1 anterior, V1 posterior, V1 anterior and V2 posterior ROIs, we performed analyses of the cortical thickness, mean curvature, surface area and grey matter volume. Figure 3.2 shows the mean values of the anatomical features for all four groups: the JMD patients, the younger healthy controls, the AMD patients and the older healthy controls. Table 3.2 presents more details on these values and highlights which features differed significantly between patients and controls in the individual ROIs.

In JMD patients, we found a thinner cortex in V1 posterior and V2 posterior, a smaller surface area in V1 anterior, V1 posterior and V2 posterior and a lower grey matter volume in V1 posterior, V2 anterior and V2 posterior compared to age-matched healthy controls ($p<0.05$). No differences were found in mean curvature measurements.

In AMD patients, we found a thinner cortex in V2 anterior and V2 posterior compared to age-matched healthy controls ($p<0.05$). We did not find differences in mean curvature, surface area size and grey matter volume.

Furthermore, we tested whether disease duration was correlated with cortical thickness, mean curvature, surface area or grey matter volume in the defined ROIs. Since data on disease duration was only available from patients from Regensburg, we performed these analyses only in these subgroups. In both JMD and AMD patients we found no significant correlation between disease duration and any of the parameters in the ROIs.

3.3.2 Whole brain analysis

We performed SBM analyses of the cortical thickness and mean curvature in the whole brain in the JMD and in the AMD group, both compared to their age-matched healthy control group. Compared to the healthy controls, we found no significant difference (applying an FDR value of 0.05) neither for the JMD nor for the AMD patient group. Furthermore, we analyzed the correlation between age and cortical thickness and the correlation between age and mean curvature in the whole brain in the JMD and the AMD group, compared to their age-matched control group. Also in this analysis, we

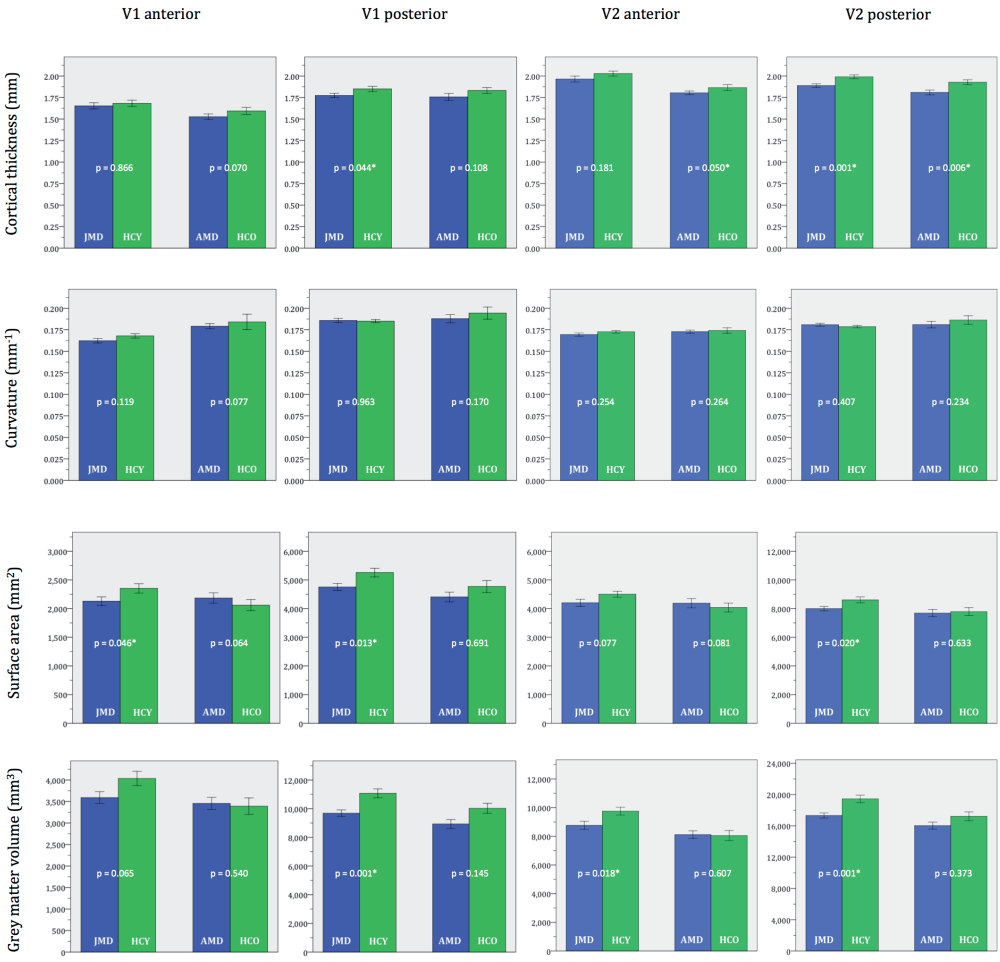

Figure 3.2. ROI morphometric values. Average cortical thickness, mean curvature, surface area and grey matter volume in the ROIs V1 anterior, V1 posterior, V2 anterior and V2 posterior. The bars show the mean value of the specific metric of the ROI in the particular group. The error bars show ±1 standard errors of the mean. p-values are given.
ROI - region of interest; JMD - juvenile macular degeneration; HCY - healthy controls young (age-matched to JMD); AMD - age-related macular degeneration; HCO - healthy controls old (age-matched to AMD).
* Significant difference between the patients group and the respective age-matched control group ($p < 0.05$).

found no significant differences (applying an FDR value of 0.05) for either the JMD or the AMD patients.

ROI μ ± σμ			JMD	HCY	f-value (df=1.63)	p-value	AMD	HCO	f-value (df=1.42)	p-value
	Average cortical thickness (mm)	V1 anterior	1.653 ± 0.036	1.682 ± 0.037	0.029	0.866	1.527 ± 0.033	1.594 ± 0.042	3.447	0.070
		V1 posterior	1.775 ± 0.024	1.851 ± 0.031	4.227	0.044 *	1.756 ± 0.041	1.832 ± 0.034	2.700	0.108
		V2 anterior	1.965 ± 0.035	2.029 ± 0.029	1.834	0.181	1.804 ± 0.022	1.865 ± 0.035	4.078	0.050 *
		V2 posterior	1.888 ± 0.021	1.991 ± 0.023	11.400	0.001 *	1.809 ± 0.028	1.929 ± 0.028	8.351	0.006 *
	Mean Curvature (mm-1)	V1 anterior	0.162 ± 0.003	0.168 ± 0.003	2.500	0.119	0.179 ± 0.003	0.184 ± 0.009	3.297	0.077
		V1 posterior	0.186 ± 0.002	0.185 ± 0.002	0.002	0.963	0.188 ± 0.005	0.194 ± 0.007	1.947	0.170
		V2 anterior	0.170 ± 0.002	0.173 ± 0.002	1.323	0.254	0.173 ± 0.002	0.174 ± 0.003	1.282	0.264
		V2 posterior	0.181 ± 0.002	0.179 ± 0.001	0.696	0.407	0.181 ± 0.004	0.186 ± 0.005	1.495	0.234
	Surface area (mm2)	V1 anterior	2130.29 ± 74.94	2352.67 ± 81.51	4.145	0.046 *	2185.38 ± 90.65	2060.50 ± 95.69	3.607	0.064
		V1 posterior	4753.91 ± 123.91	5256.55 ± 149.70	6.598	0.013 *	4408.08 ± 169.35	4770.41 ± 212.15	0.160	0.691
		V2 anterior	4203.88 ± 124.91	4502.91 ± 104.34	3.225	0.077	4189.17 ± 162.17	4037.82 ± 153.63	3.190	0.081
		V2 posterior	7998.18 ± 151.94	8613.58 ± 204.26	5.718	0.020 *	7688.42 ± 252.08	7795.09 ± 273.75	0.231	0.633
	Grey matter volume (mm3)	V1 anterior	3590.97± 138.45	4035.21 ± 166.09	3.516	0.065	3455.33 ± 140.77	3391.14 ± 192.45	0.381	0.540
		V1 posterior	9682.56 ± 229.84	11068.33 ± 311.69	11.898	0.001 *	8931.46 ± 312.43	10024.64 ± 347.80	2.205	0.145
		V2 anterior	8764.59 ± 280.49	9750.70 ± 272.10	5.890	0.018 *	8117.08 ± 266.15	8053.18 ± 349.58	0.269	0.607
		V2 posterior	17325.68 ± 331.33	19448.18 ± 485.69	12.028	0.001 *	16031.33 ± 446.11	17215.18 ± 564.76	0.811	0.373

Table 3.2. ROI morphometric values. Average cortical thickness, mean curvature, surface area and grey matter volume were extracted from the ROIs V1 anterior, V1 posterior, V2 anterior and V2 posterior (f-values, degrees of freedom and p-values are given).

ROI - region of interest; μ - mean; σμ - standard error of the mean; df – degrees of freedom; JMD - juvenile macular degeneration; HCY - healthy controls young (age-matched to JMD); AMD - age-related macular degeneration; HCO - healthy controls old (age-matched to AMD).

* Significant difference between the patients group and the respective age-matched control group ($p < 0.05$).

3.4 Discussion

To our knowledge, this is the first study that reports the results of a SBM analysis of the visual cortex of MD patients. The association of MD – a common cause of blindness world-wide – with structural changes in the brain has only recently become clear. (Hernowo 2014, Plank et al. 2011,Boucard et al. 2009, Baseler et al. 2011, Liu et al. 2010, Szlyk and Little 2009, Dilks et al. 2009, Baker et al. 2008, Masuda et al. 2008) Previous studies have reported volumetric reductions of grey and white matter along the entire visual pathways of MD patients.(Hernowo et al. 2014, Plank et al. 2011, Boucard et al. 2009) Here, we used a surface-based approach to examine several additional anatomical features of the visual cortex in MD, such as cortical thickness, mean curvature and surface area. This SBM analysis further characterizes the previously reported volumetric changes in the visual cortex of MD patients.

3.4.1 ROI-based analysis confirms the presence of structural changes in JMD patients

In the JMD patients, compared to age-matched controls, we found a smaller cortical thickness in V1 posterior and V2 posterior, a smaller surface area in V1 anterior, V1 posterior and V2 posterior, and lower grey matter volume in V1 posterior, V2 anterior and V2 posterior. We found no differences in mean curvature.

The majority of the changes were found in the posterior region of the visual cortex, where central vision is represented. This is in agreement with the notion that the central visual field defects may cause – through a loss of activity in the visual pathways – the structural changes. However, the surface area was also reduced in V1 anterior and the grey matter volume was also reduced in V2 anterior. In V2 anterior, the cortical thickness and the surface area were also lower in the JMD patients than in the healthy controls, but these findings did not reach significance ($p=0.181$ for cortical thickness; $p=0.077$ for surface area). These thinner cortex and smaller surface area, albeit not significant, can together explain the significant changes in grey matter volume in V2 anterior. This suggests that not all structural changes have a direct bearing on retinotopic-specific deprivation. Possibly, spontaneous oscillatory spike bursts of the retinal ganglion cells could partly explain these results. Such spontaneous activity has been reported in retinal degeneration mice and rats.(Pu et al. 2006, Stasheff 2008, Ye and Goo 2007)

Furthermore, MD patients have to rely on their peripheral visual field for their daily tasks. This means that the peripheral visual field has a different function in MD patients than healthy controls. However, previous fMRI studies have shown conflicting results on whether functional changes in the visual cortex appear in MD patients.(Baseler et al. 2011, Masuda et al. 2008, Sunness et al. 2004, Baker et al. 2005, Schumacher et al. 2008, Wandell and Smirnakis 2009) Nevertheless, even if functional changes do not appear in MD, the changed usage of the peripheral visual field might form an additional explanation for the anatomical changes in the anterior V1 and V2. Together, these findings in the ROI analyses show that our previously reported volumetric reductions of grey matter in the visual cortex of JMD patients are associated with a thinner cortex and a smaller surface area, but not with alterations in the mean cortical curvature.

3.4.2 Partial confirmation of reduced cortical thickness in AMD patients

In AMD patients, compared to age-matched controls, only cortical thickness in V2 anterior and V2 posterior was reduced. In contrast, in our previous VBM study, in the AMD patients, we found more widespread volumetric reductions of the grey matter in cortical regions including primary visual cortex. The fact that changes in cortical thickness were found in both V2 anterior and V2 posterior suggests that these may not have a direct bearing on a retinotopic-specific deprivation. However, also in AMD the previously suggested possibility of spontaneous activity of the retinal ganglion cells and the different function of the peripheral visual field might influence these anatomical changes.(Baseler et al. 2011, Masuda et al. 2008, Pu et al. 2006, Stasheff 2008, Ye and Goo 2007, Sunness et al. 2004, Baker et al. 2005, Schumacher et al. 2008, Wandell and Smirnakis 2009) Additionally, the observed neuroanatomical changes in MD might not only be explained by functional deprivation due to the visual field defect, but also to associated neurodegenerative processes. Specifically, a previously described association between AMD and Alzheimer's disease might play a role in the neuroanatomical changes.(Ikram et al. 2012, Klaver et al. 1999, Pham et al. 2006, Woo et al. 2012)

3.4.3 More widespread structural degeneration in the visual cortex of JMD compared to AMD patients

In the JMD patients we found more widespread cortical thinning, reduction of surface area and volume than in the AMD patients. This could be explained by the fact that – on average – the JMD patients in our study had larger visual field defects and a poorer visual acuity than the AMD patients. As a result, visual deprivation will have been more severe in the JMD patients too. If cortical structural degeneration is related to visual deprivation, AMD patients would be expected to show less extensive reductions than the JMD patients, as indeed we find here. Additionally, due to the ageing of their brains, also the healthy older subjects might show more variability in cortical structure, which can make it more difficult to demonstrate disease-related changes in AMD patients.

3.4.4 No evidence for a changed cortical gyrification pattern in MD patients

Based on *Bridge et al.*,(Bridge et al. 2012) who reported a decreased gyrification in albinism in an area where VBM showed decreased grey matter volume, we expected to find a similar decrease in gyrification also in our group of MD patients in the occipital pole – the area where previously grey matter volumetric reductions were found. However, in our patients, mean curvature is the only measurement that did not show any differences in either of the patient groups, compared to their age-matched healthy controls. This suggests that the cause of cortical degeneration in MD and albinism may be rather different in nature, which may be related to the fact that albinism is a congenital disease, whereas MD develops later in life.

3.4.5 Whole-brain analysis reveals no structural changes outside of visual cortex

To explore the further presence of anatomical changes, we also performed an exploratory whole brain SBM analysis. We were keen on performing these analyses, because morphological differences might also be present outside of the visual cortex. Specifically, our previous VBM analysis had indicated the presence of white matter volumetric reductions in the frontal lobe in the AMD patients.(Hernowo et al. 2014) However, compared to their respective age-matched controls, in neither the JMD nor the AMD patients we found differences in cortical thickness or in mean curvature. As mentioned above, such differences were revealed in the ROI-based SBM analyses in V1 and V2, and they were also more evident in the JMD patients than in the AMD patients. These differences between the results of whole-brain and ROI-analysis can be explained by the fact that the threshold for finding differences in whole-brain analysis was higher than in ROI analysis. The higher threshold in whole brain analysis was due to the correction for multiple comparisons, which is necessary when analysing such amounts of data points. In ROI-analysis it is not necessary to apply correction, since the amount of comparisons is much lower and the specific ROIs were selected based on the likelihood of finding differences based on previous studies

3.4.6 Comparison of SBM- and VBM-analyses

The surface-based approach that we used here indicates a number of structural changes that are consistent between our present SBM and our previous VBM study, particularly in the JMD patients. However, not all SBM results corroborate the VBM results. Part of the difference may be due to the use of different methodology. SBM applies a different method for segmenting the brain, and also for the calculation of the grey matter volume than VBM. Therefore, the border between grey matter and white matter and the cerebrospinal fluid is defined differently in each method. Consequently, the grey matter volume measurements can also be different. On the one hand, finding changes using such different approaches establishes their robustness. On the other hand, if one of the techniques is more sensitive than the other, subtle cortical changes could simply be missed by one of the methods. SBM might give a more accurate

representation of structural differences because it takes the highly folded nature of the cortex into account, which is not the case in VBM analysis. This could also explain some of the discrepancies between the results of our two studies. Likewise, previous studies in a variety of neurological and ophthalmological disorders also applied both types of analyses, and also found some differences in their results in surface-based analyses compared to voxel-wise analysis. SBM does not always find changes in cortical features in areas where VBM found differences in grey matter volume.[16,44–47]lesions are rare in neuromyelitis optica (NMO The opposite occurs as well: in some studies SBM revealed changes in cortical features in areas where VBM did not uncover volumetric differences. (Bridge et al. 2012, Whitwell et al. 2013, Lyoo et al. 2006) A limitation of SBM is that at present it is only able to uncover changes in grey matter.

3.4.7 Limitations

In our present study, the ROI definitions of V1 and V2 were not based on a retinotopic examination in the individual subjects, but on average brain templates, included in Freesurfer. In the individual subjects, this may cause a deviation of the borders of these ROIs from their actual ones, which may have affected our results in the ROI-analysis.

In this study, we combined structural MRI data from three different centers. The different MRI-scanners and setting at each location could potentially have an effect on analyses of the cortical properties. However, there are two reasons that we can exclude such effects. First, we avoid systematic influences of differences in scanner properties by including scanner location as a covariate in all of our analyses. Second, both patients and controls were scanned in all three scanners. An important advantage of combining the data is the large groups of patients and controls that are obtained in this way, which increases study power and allows drawing more robust conclusions.

From the analyses in the JMD patients, we can conclude that in the diseases that we investigated, the presence of a central visual field defect at a young age of onset, is associated with neuro-anatomical changes. However, it is not possible to determine whether such neuro-anatomical changes occur in the separate diseases from the present analyses. We included diseases of different entity in the JMD group for several reasons. First, patients with the different diseases included in the JMD group form small groups separately, from which we would not be able to draw strong conclusions. Second, although the etiology of the separate diseases is different, they have in common the development of a central visual field defect and the age of onset in the first decades of life. Therefore, we are able to draw robust conclusion from these analyses about the association between a central visual field defect which develops in the first decades of life and changes in the brain.

3.4.8 Future research

A strength of the present study is that we re-examined the same group of subjects with SBM as *Hernowo et al.*(Hernowo et al. 2014) did with VBM. Ther{Bibliography}efore, we were able to compare the outcomes of these two methods, determine the robustness of the structural brain changes in MD, and unravel more details regarding the nature of the previously found volumetric changes. It would be interesting to use both of these methods in the future in a new group of patients, preferably in a longitudinal study. With such a study design it would be possible to track changes in specific anatomical features in individual patients over time, and more precisely determine the relationship between disease progression and severity of the degeneration. In turn, this could guide future research into therapies for MD, which might have to expand their focus from exclusive ocular treatment to combining eye treatment with treatment of neurodegeneration.

With 3T MRI images and the current methods of segmentation of the brain it is possible to examine differences in neuroanatomical properties. However, it is not possible to specify whether changes in the cortex are supragranular, granular or infragranular, which would be particularly interesting for a better understanding of the pathogenesis of the brain changes. In the future, it might be possible to perform such analyses of the cortical layers, with 7T and super-high resolution (9T) MRI scanning. However, it will take some years before these techniques can be applied in large groups of patients, as we did in the present study.

3.4.9 Summary

In summary, using SBM, we found changes in several anatomical properties in the visual cortex of both JMD and AMD patients, compared to healthy age-matched controls. JMD patients showed a thinner cortex, smaller surface area and lower grey matter volume in V1 and V2. AMD patients showed a thinner cortex in V2 only. These different findings in JMD and AMD patients may be related to the larger visual field defect and poorer visual acuity in JMD patients compared to AMD patients. Adding to our previous VBM study in the same group of subjects, these results confirm the cortical degeneration in MD patients and indicate that the chance for successful therapeutic restoration of functional vision reduces with disease progression.

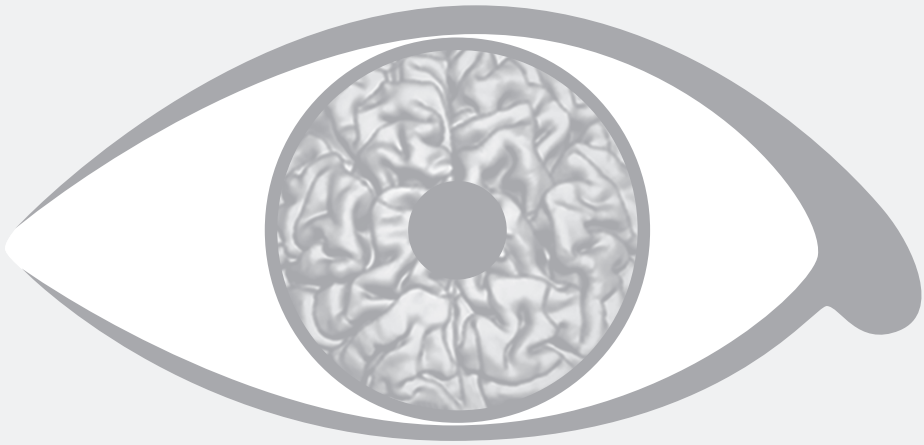

CHAPTER 4

Loss of binocular vision in monocularly blind patients causes selective degeneration of the superior lateral occipital cortices

Doety Prins, Nomdo M. Jansonius, Frans W. Cornelissen

Submitted

Abstract

Introduction. Chronic ocular pathology, such as glaucoma and macular degeneration, is associated with neuroanatomical changes in the visual pathways. It is a challenge to determine the mechanism responsible for these changes. This could be functional deprivation or transsynaptic degeneration. Acquired monocular blindness provides a unique opportunity to establish which mechanism underlies neuroanatomical changes in ocular pathology in general, since the loss of input is well defined, and it causes selective functional deprivation due to the loss of stereopsis.
Methods. High-resolution T1-weighted MR-images were obtained in 15 monocularly blind patients and 18 healthy controls. We used voxel- and surface-based morphometry to compare grey and white matter volume, cortical thickness, mean curvature, and surface area between these groups.
Results The grey matter volume in the bilateral superior lateral occipital cortices was decreased in the monocular blind patients. We found no volumetric differences in their early visual cortex.
Discussion. The volumetric decrease in the superior lateral occipital cortices is consistent with specific functional deprivation, as the superior lateral occipital cortices play an important role in depth perception. Moreover, in the absence of differences in the early visual cortex, the decrease is inconsistent with transsynaptic degeneration propagating from the degenerated retinal axons.

4.1 Introduction

Treatment of blindness is the ultimate challenge in ophthalmology; it has motivated the development of various vision restoration therapies, including retinal implants, stem-cell derived retinal pigment epithelium, and gene-therapy.(da Cruz et al. 2013, MacLaren et al. 2014, Stingl et al. 2010, Van Zeeburg et al. 2012) The potential success of such future treatments will depend to a great extent on the capacity of the brain to guide and process the new input following vision restoration. Previous studies found evidence for neuroanatomical changes in patients with various eye diseases, such as glaucoma, macular degeneration, and amblyopia.(Barnes et al. 2010, Boucard et al. 2009, Hernowo et al. 2011, Hernowo et al. 2014, Mendola et al. 2005, Plank et al. 2011, Prins, Hanekamp and Cornelissen 2016, Xiao et al. 2007, Xie et al. 2007) Due to such changes, the brain may no longer be able to optimally process new input from a retinal implant. As for a truly successful treatment it needs to be able to do so, it is important to precisely understand the mechanism underlying the association between prolonged partial blindness and neuroanatomical changes.

Three mechanisms may explain the association between loss of visual input and neuroanatomical changes. First, in functional deprivation a permanent loss of visual input leads to decreased activity in the visual pathways, which – in turn – leads to neuroanatomical degeneration. Second, in transsynaptic degeneration, the degenerating axons originating from the eye provoke degeneration of more posterior parts of the visual pathways. Distinguishing between the contributions of these two mechanisms has been problematic as neural and functional visual losses are usually highly correlated and difficult to characterize precisely. Third, there are indications that degenerative eye diseases, such as macular degeneration and glaucoma, are associated with general neurodegenerative diseases.(Cumurcu et al. 2013, Ghiso et al. n.d., Janssen et al. 2013, Sivak 2013, Tamura et al. 2006, Wostyn, Audenaert and De Deyn 2010) As such, the neuroanatomical changes might not exclusively be caused by functional deprivation or transsynaptic degeneration, but could be due to the general neurodegenerative character of the disease.

Studying patients with previously healthy eyes who became monocularly blind – due to for example an eye trauma – provides a unique opportunity to disentangle the possible causes of the association between altered visual function and neuroanatomical changes. Unlike in chronic ocular pathology, in this group the reduction of visual input is well defined. Moreover, monocular blindness causes a loss of binocular vision and stereopsis, resulting in a highly selective functional deprivation. Finally, there is no association with neurodegenerative diseases. If we can determine whether and where neuroanatomical changes occur in monocularly blind patients, we would gain more insight into the etiology of neuroanatomical changes associated with visual loss in general. As such, monocularly blind patients can also serve as a reference group for studies in patients with various eye diseases.

In contrast to bilateral blindness – which has been studied extensively (Jiang et al. 2009, Leporé et al. 2010, Li et al. 2013, Noppeney et al. 2005, Pan et al. 2007, Park et al. 2007, Park et al. 2009, Ptito et al. 2008, Schoth et al. 2006, Shimony et al. 2006, Shu et al. 2009, Wang et al. 2013, Zhang et al. 2012) – systematic research into neuroanatomical changes associated with monocular blindness is scarce.(Beatty et al. 1982, Levin et al. 2010). Since shape perception and motion processing are affected in monocularly blind patients, plasticity of the visual system has been suggested.(Steeves, González and Steinbach 2008)

The aim of our study was to determine whether and how monocular blindness affects the neuroanatomical properties of the visual pathways. Such neuroanatomical properties were defined by grey and white matter volume, cortical thickness, surface area, and mean curvature. In our study, we used voxel-based morphometry (VBM) and surface-based morphometry (SBM) to compare the abovementioned neuroanatomical properties between monocularly blind patients without a chronic or degenerative ocular disease and age-matched healthy controls. Using region of interest (ROI) analysis, we specifically assessed the visual pathways.

4.2 Materials and methods

4.2.1 Ethics statement

The Medical Ethical committee of the University Medical Center Groningen approved this study. The study conformed to the tenets of the Declaration of Helsinki. All subjects gave their written informed consent before participating in the study.

4.2.2 Subjects

We included 33 subjects in this study: 15 monocularly blind patients and 18 healthy age-matched controls. The inclusion criteria for the monocularly blind patients were the following. They had to be unilaterally light-perception negative for at least five years, due to a trauma (n = 11, in 11 patients the eye was removed) or after surgery for a tumor (n = 4, in 3 patients the eye was removed). The contralateral eye had to have a good visual acuity (0.8 or better) and an intact visual field. Healthy age-matched controls had to have a good visual acuity and intact visual field in both eyes. None of the subjects had previously been diagnosed with neurological disorders, psychiatric disorders, or any degenerative ocular disease.

The monocularly blind patients had a mean age of 63 years (range 54 – 72 years); 47% of them were males. The healthy controls had a mean age of 62 years (range 53 – 75 years); 61% of them were males. In the group of monocularly blind patients, seven patients were blind in their right eye, and eight were blind in their left eye.

4.2.3 Data acquisition

MR images of all subjects were obtained on a 3.0 Tesla MRI scanner (Philips Intera, Eindhoven, the Netherlands) at the Neuroimaging Center of the University Medical Center Groningen. Whole brain T1-weighted images with a voxel dimension of 1 x 1 x 1 mm were acquired using a sequence of T1W/3D/FFE, 30° flip angle, repetition time 25 ms, matrix size 256 x 256, and field of view 256 x 160 x 204, yielding 160 slices.

The visual acuity was measured with a Snellen chart with optimal correction for the viewing distance. The visual field was tested with frequency doubling technology (FDT; C20-1 screening mode).

4.2.4 Data analysis

We analyzed the anatomical properties of the visual pathways using VBM and SBM. VBM was used to study the volumes of the grey and white matter; SBM was used to study the cortical thickness, gyrification pattern, and surface area.

VBM analysis

We performed VBM analysis of the grey matter and white matter volume using the FMRIB Software Library (FSL) analysis tools (version 5.0.6, available at: http://www.fmrib.ox.ac.uk/fsl).(Jenkinson et al. 2012, Woolrich et al. 2009) First, we applied nonlinear noise reduction using Smallest Univalue Segment Assimilating Nucleus (SUSAN). Second, we segmented the brain from non-brain tissue, using the Brain Extraction Tool (BET). (Smith 2002) Subsequently, we performed bias field correction and segmented the brain into grey matter, white matter and cerebrospinal fluid with the FMRIB Automated Segmentation Tool (FAST) from the Oxford Centre for Functional Magnetic Resonance Imaging of the Brain .(Zhang, Brady and Smith 2001) We registered all the images to the template of the Montreal Neurological Institute (MNI template) with the FMRIB Linear Image Registration Tool (FLIRT) and the FMRIB Non-linear Image Registration Tool (FNIRT), and applied the registration to the grey and white matter segments.(Jenkinson et al. 2002, Jenkinson and Smith 2001) Using the FSL 'randomise' analysis tool, we performed nonparametric permutation tests on our data.(Winkler et al. 2014)

SBM analysis

We performed SBM analysis of cortical thickness, mean curvature, surface area, and grey matter volume using Freesurfer (version 5.3.0, available at: http://surfer.nmr.mgh.harvard.edu/). We digitally removed the non-brain tissue (Ségonne et al. 2004), and performed automated Talairach transformation and intensity normalization.(Sled, Zijdenbos and Evans 1998) Subsequently, tessellation of the grey/white and grey/cerebrospinal fluid boundaries and automatic correction of topologic inaccuracies was performed, which we customized by setting the value for the lower threshold of the white matter to an appropriate value for our dataset.(Fischl, Liu and Dale 2001,

Ségonne, Pacheco and Fischl 2007) The process continued with surface deformation and inflation,(Dale, Fischl and Sereno 1999, Fischl, Sereno and Dale 1999) registration to a spherical atlas(Fischl et al. 1999), and automatic parcellation of the cortex surface based on gyral and sulcal organization.(Desikan et al. 2006, Fischl et al. 2004)

ROI analysis

In the ROI-based analyses, we used masks of the various grey and white matter structures of the visual pathways. *Figure 4.1* presents the ROIs: the pregeniculate structures, which contains the optic nerves, chiasm and optic tracts, the lateral geniculate bodies, the optic radiations, the calcarine region, the occipital pole, the inferior lateral occipital cortices, and the superior lateral occipital cortices. The masks for the pregeniculate structures were created manually, and adjusted to match the structures in each individual subject if needed. The masks for the lateral geniculate bodies and for the optic radiations were obtained from the Jülich histological atlas(Bürgel et al. 2006, Bürgel et al. 1999). The masks for the calcarine region, the occipital pole, the inferior lateral occipital cortices, and the superior lateral occipital cortices were obtained from the Harvard-Oxford cortical structural atlas.(Desikan et al. 2006) In all these ROIs, we analyzed the volume of the grey matter and white matter using VBM. In the calcarine region, the occipital pole, the inferior lateral occipital cortices, and the superior lateral occipital cortices, we also analyzed cortical thickness, gyrification, and surface area using SBM.

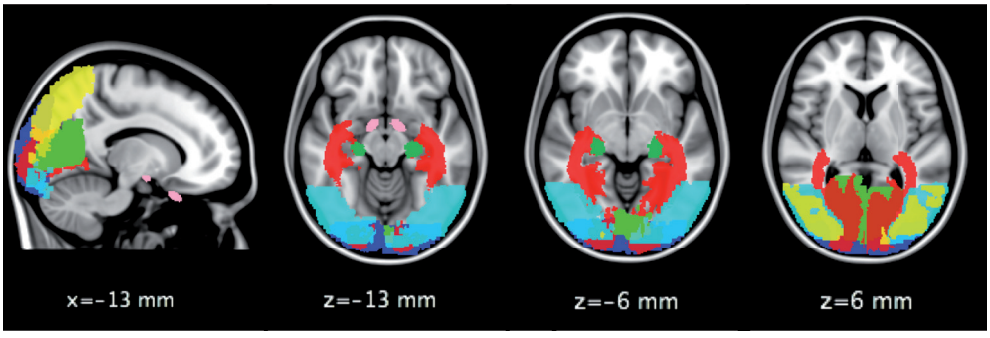

Figure 4.1. Regions of interest along the visual pathway.
Pink – pregeniculate structures; dark green – lateral geniculate bodies; red – optic radiations; lighter green – pericalcarine cortices; dark blue – occipital pole; lighter blue – inferior lateral occipital cortex; yellow – superior lateral occipital cortex.
The Talairach position of the slices is given by their "x", and "z" values.

Statistics

We examined differences between monocularly blind patients and healthy controls using multivariate analysis of covariance (MANCOVA) (IBM SPSS Statistics software

package, version 20). The white matter volume, grey matter volume, cortical thickness, gyrification pattern, and surface area for each ROI were included as dependent variables, and the subject groups were entered as a fixed factor. We added age as a covariate in the analysis. The threshold for significance in the ROI analyses was set to a *p*-value of 0.05 (uncorrected).

ROI-analysis of optic nerves

Since not all monocularly blind patients had their blind eye on the same side, we performed the ROI analyses in two stages. In the first analysis, we compared the volumes of the optic nerves between monocularly blind patients and healthy controls. This analysis was done separately for the monocularly blind patients with a blind right eye and for the monocularly blind patients with a blind left eye, in both cases comparing them to all the healthy controls.

ROI-analysis of post-chiasmal structures

The nerve fibers that carry the information from the homonymous hemifields of both eyes to the visual cortex are combined after the chiasm. Hence, no detectable volumetric differences in the post-chiasmal structures were expected between the monocularly blind patients with a blind right eye and those with a blind left eye. Therefore, in a second analysis, we compared the visual pathway structures onwards from the optic chiasm to the posterior parts of the visual pathways, this time for the entire group of monocularly blind patients and again comparing them to the healthy controls.

Exploratory whole-brain analysis

To determine the presence of unexpected differences in the neuroanatomy between monocularly blind patients and healthy controls, we performed additional exploratory whole-brain analyses using both VBM and SBM. With VBM, we compared grey and white matter volume, while with SBM, we compared the cortical thickness and mean curvature across the entire brain. In both cases, age was added as a covariate.

Comparisons were made after applying a family-wise error correction for multiple comparisons.

4.3 Results

In summary, in monocularly blind patients – compared to age-matched controls – we found a significantly smaller volume of the optic nerve on the side of the blind eye, of the optic chiasm, of the bilateral optic tracts, and of the bilateral superior lateral occipital cortices. We will describe these results in more detail below.

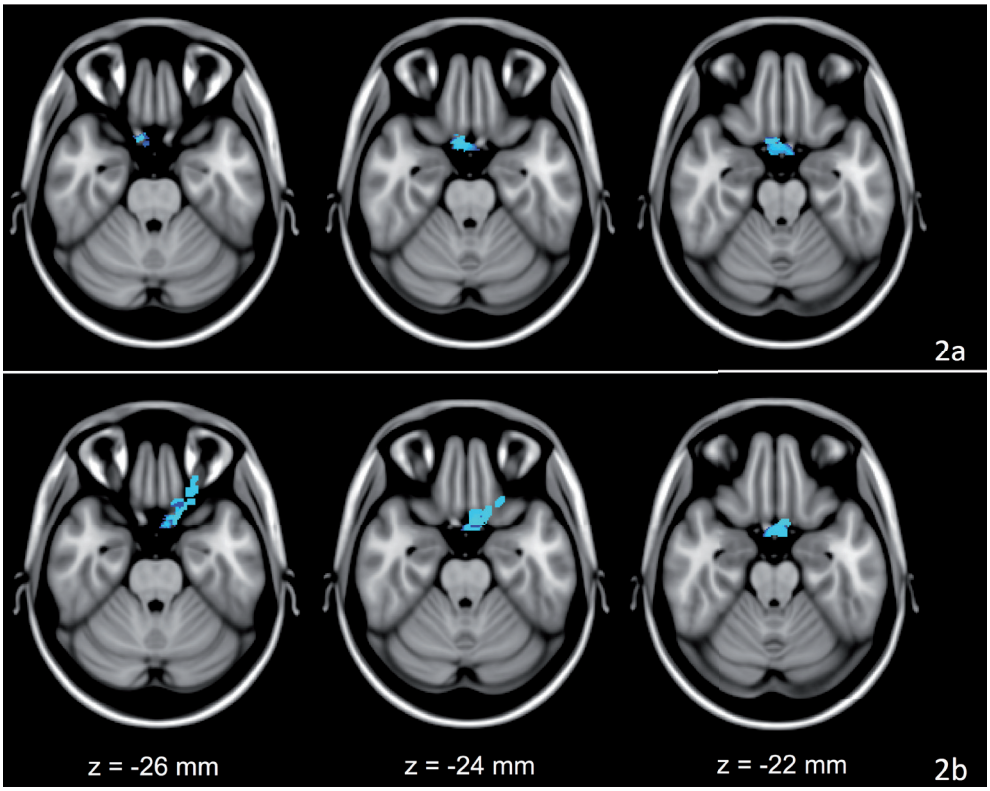

Figure 4.2. Volumetric differences in the optic nerve and the optic chiasm ROIs
a. The areas in blue highlight where the monocularly blind patients with a blind right eye show significantly lower volume in the ROI of the right optic nerve than the age-matched healthy controls. b. The areas in blue highlight where the monocular blind patients with a blind left eye show significantly lower volume in the ROI of the left optic nerve than the age-matched healthy controls. The Talairach position of the slices is given by their "z" values. ROIs are defined in figure 4.1.

4.3.1 ROI analyses

VBM ROI analysis of the optic nerves

To compare the white matter volume of the optic nerves of the monocularly blind patients to that of the healthy controls, we performed VBM analyses in two subgroups. *Table 4.1* lists the results of these analyses. On the one hand, in the patients with a blind right eye, the right optic nerve showed a significant decrease in volume, whereas the left optic nerve did not. On the other hand, in the patients with a blind left eye, the left optic nerve showed a significant decrease in volume, whereas the right optic nerve did not. *Figure 4.2* visualizes the location of these volumetric differences in the optic nerves for the patients with either a blind right eye (*Figure 4.2a*) or a blind left eye (*Figure 4.2b*).

ROI μ ± σμ			Right optic nerve	Left optic nerve
	Volume (mm3)	Monocular blind OD	27 ± 5	125 ± 6
		Monocular blind OS	144 ± 18	13 ± 4
		Healthy controls	141 ± 12	136 ± 12
	Monocular blind OD	f-value (df = 1,22)	31.890	0.335
		p-value	<0.001*	0.568
	Monocular blind OS	f-value (df = 1,23)	0.019	44.240
		p-value	0.892	<0.001*

Table 4.1. ROI morphometric values of the optic nerves
White matter volumes of the right and the left optic nerve for the subgroups of monocular blind patients with either a blind right eye or a blind left eye, and the healthy controls. ROI - region of interest; μ - mean; σμ - standard error of the mean; df – degrees of freedom; OD – oculus dexter (right eye); OS – oculus sinister (left eye).
* Significant difference between the patient group and the control group.

VBM ROI analysis of the visual pathways from the optic chiasm towards the visual cortex
This time including the entire group of monocularly blind patients, we performed ROI analyses of the optic chiasm, the optic tracts, the lateral geniculate bodies, the optic radiations, the calcarine region, the occipital pole, the inferior lateral occipital cortices, and the superior lateral occipital cortices. *Table 4.2* and the first row of *Table 4.3* show the results of these analyses, and highlight the ROIs for which we find significant reductions in white or grey matter volume: the optic chiasm, the bilateral optic tracts, and the bilateral superior lateral occipital cortices. We did not find any significant differences in grey matter volume in the pericalcarine region and the occipital pole. *Figure 4.3* visualizes the volumetric differences in the optic tracts (*Figure 4.3a*) and the visual cortex

ROI μ ± σμ			Chiasm	Optic tracts	Lateral geniculate bodies	Optic radiations
	Volume (mm3)	Monocular blind	119 ± 12	504 ± 17	1052 ± 38	128956 ± 554
		Healthy controls	247 ± 10	570 ± 13	1037 ± 34	128211 ± 525
		f-value (df = 1,30)	70.151	10.213	0.081	1.145
		p-value	<0.001*	0.003*	0.778	0.293

Table 4.2. ROI morphometric values of chiasm, optic tracts, lateral geniculate bodies, and optic radiations. ROI - region of interest; *μ* - mean; *σμ* - standard error of the mean; df – degrees of freedom.
* Significant difference between the patient group and control group.

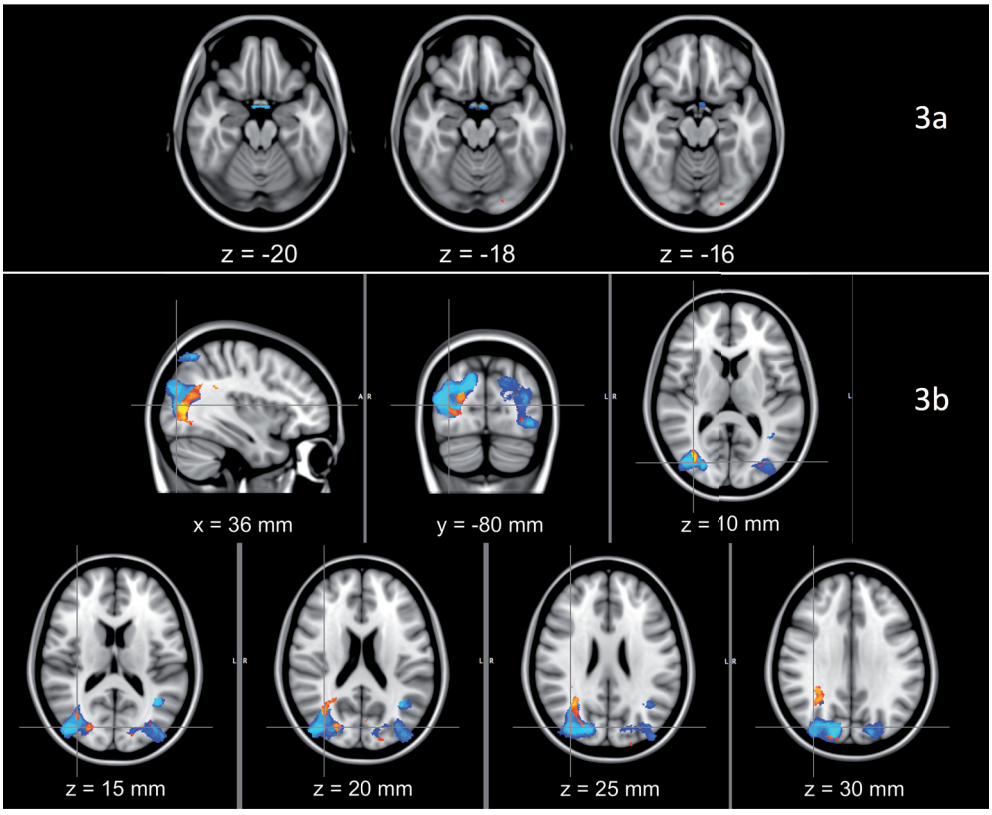

Figure 4.3. Volumetric differences in the optic chiasm, the optic tract, the optic radiation, and the visual cortex ROIs
a. The areas in blue highlight where the monocularly blind patients show significantly lower volume in the ROIs in the optic chiasm and the optic tracts (see figure 4.1) than the age-matched healthy controls. b. The areas in blue highlight where the monocular blind patients show significantly lower grey matter volume in the ROIs in the visual cortex than the age-matched healthy controls. The red-yellow areas highlight where the monocular blind patients show significantly higher white matter volume in the ROIs of the optic radiations than the age-matched healthy controls. Talairach position of the slices is given by their "x", "y" and "z" values. ROIs are defined in figure 4.1.

(*Figure 4.3b*). Grey matter volume was significantly reduced bilaterally in the superior lateral occipital cortices. We found no evidence for a reduced white matter volume of the optic radiations. However, within the optic radiations we did find –relatively small– sections of significantly increased white matter volume.

SBM ROI analysis of the visual cortex

We performed SBM analyses in the ROIs of the pericalcarine cortices, the occipital pole, the inferior lateral occipital cortices and the superior lateral occipital cortices. *Table 4.3* indicates that in none of these ROIs, cortical thickness, mean curvature or surface area (2nd, 3rd, and 4th row of *Table 4.3*, respectively) differed significantly between the

			Pericalcarine cortices	Occipital pole	Inferior lateral occipital cortices	Superior lateral occipital cortices
ROI μ ± σμ	**Volume (mm3)**	**Monocular blind**	15691 ± 408	31119 ± 831	30860 ± 955	62957 ± 1559
		Healthy controls	15669 ± 402	32288 ± 719	32634 ± 648	66604 ± 1354
		f-value (df = 1,30)	0.000	1.352	2.894	5.522
		p-value	0.985	0.254	0.099	0.026*
	Cortical thickness (mm)	**Monocular blind**	3.03 ± 0.03	2.99 ± 0.03	3.30 ± 0.04	3.12 ± 0.05
		Healthy controls	3.02 ± 0.05	2.98 ± 0.03	3.25 ± 0.04	3.08 ± 0.04
		f-value (df = 1,30)	0.015	0.017	0.865	0.669
		p-value	0.902	0.897	0.360	0.420
	Mean Curvature (mm-1)	**Monocular blind**	0.15 ± 0.002	0.16 ± 0.003	0.15 ± 0.002	0.14 ± 0.003
		Healthy controls	0.15 ± 0.003	0.16 ± 0.003	0.15 ± 0.003	0.14 ± 0.003
		f-value (df = 1,30)	0.062	1.090	0.240	0.316
		p-value	0.805	0.305	0.628	0.578
	Surface area (mm2)	**Monocular blind**	6838 ± 275	12387 ± 496	15093 ± 678	20666 ± 900
		Healthy controls	7112 ± 202	12510 ± 338	14737 ± 399	20148 ± 508
		f-value (df = 1,30)	0.651	0.045	0.213	0.268
		p-value	0.426	0.834	0.648	0.609

Table 4.3. ROI morphometric values of the pericalcarine cortices, occipital pole, and the inferior and superior lateral occipital cortices.
ROI - region of interest; μ - mean; σμ - standard error of the mean; df – degrees of freedom.
* Significant difference between the patient group and control group.

monocularly blind patients and the age-matched healthy controls.

4.3.2 Exploratory whole-brain analyses

Using whole-brain analyses, we examined whether unexpected neuroanatomical differences might be present beyond the previously examined visual pathways ROIs. However, we found no significant differences in either the grey or the white matter, or in cortical thickness or mean curvature.

4.4 Discussion

We find that binocular vision loss – as a result of acquired monocular blindness – is associated with a reduced volume of the superior lateral occipital cortices. Functionally, the location of this degeneration is consistent with the loss of binocular vision and stereopsis in the monocularly blind patients. Moreover, in the absence of accompanying volumetric reductions of the optic radiations and the early visual cortex, this implies that the cortical degeneration can only be explained by functional deprivation and not by propagated transsynaptic degeneration that originated at an earlier stage along the visual pathway.

4.4.1 Volumetric loss in the dorsal visual stream is consistent with functional deprivation due to loss of stereopsis

We found grey matter volumetric decreases in the bilateral superior lateral occipital cortices. The superior lateral occipital cortices are located in the dorsal visual stream, which processes information about the location of objects in space. Stereopsis is needed to perceive depth and to precisely localize objects in space. Several fMRI studies have shown that dorsal visual areas are involved in stereoscopic depth perception, specifically the dorsal V3.(Backus et al. 2001, Baecke et al. 2009, Ban et al. 2012, Brouwer, van Ee and Schwarzbach 2005, Goncalves et al. 2015, Ip et al. 2014, Minini, Parker and Bridge 2010, Neri, Bridge and Heeger 2004, Rutschmann and Greenlee 2004, Welchman et al. 2005) Furthermore, the area in which we found the grey matter volumetric decrease extends to the posterior part of the intraparietal sulcus, which has been implicated in visual attention and eye movements.(Culham and Kanwisher 2001) Since monocularly blind patients can only scan the outside world using one eye, they may have adjusted to a different pattern of eye movements. Therefore, the decrease in grey matter volume in the superior lateral occipital cortices in monocularly blind patients might be explained by both the loss of stereopsis as well as accompanying changes in oculomotor behavior. Irrespective, this volumetric decrease in the superior lateral occipital cortices is particularly significant, as we found no evidence for neuroanatomical changes in the early visual cortex. This implies that the observed differences in the dorsal stream are the exclusive result of functional deprivation rather than transsynaptic degeneration.

4.4.2. No anatomical differences in the postgeniculate pathways

If transsynaptic degeneration would play a significant role in causing anatomical changes, we would have expected to find degeneration of the postgeniculate pathways, in particular given the extensive pregeniculate degeneration. The absence of evidence for degeneration in the postgeniculate pathways suggests that transsynaptic degeneration played no role in causing anatomical changes higher up in the visual hierarchy.

4.4.3 Volumetric loss in pregeniculate structures is consistent with degeneration of the axons from the blind eye

We found a volumetric decrease of the optic nerve ipsilateral to the blind eye, the optic chiasm and the bilateral optic tracts. These volumetric losses are consistent with a degeneration of the axons from the removed blind eye. Such degeneration in the pregeniculate structures has been observed previously in a pathohistological study in a single patient that underwent enucleation of one eye 40 years prior to the study, in which evidence was found for axonal degeneration in the ipsilateral optic nerve relative to the blind eye, in both optic tracts, and in the neuronal laminae corresponding to the enucleated eye in both lateral geniculate nuclei.(Beatty et al. 1982) Our study shows that the results of *Beatty et al.* are common to monocularly blind patients. However, in contrast to *Beatty et al.* we did not find any differences in the lateral geniculate bodies. It could be that Beatty's finding was specific to their patient, or that the differences in the lateral geniculate bodies were too small or variable to be detected by MRI analysis.

4.4.4 Occipital white matter volumetric increase might reflect neural remodeling to compensate for the loss of stereopsis

We found a few small sections of increased white matter within the optic radiations, predominantly in the right optic radiation, located close to the region of grey matter volumetric reduction in the superior lateral occipital cortices. The areas of white matter volumetric increase were located within our masks of the optic radiation. However, since the configuration of the largest cluster of increased white matter is oriented vertically rather than horizontally, this cluster might also be part of the vertical occipital fasciculus, which connects the dorsolateral and ventrolateral visual cortices, as recently rediscovered by *Yeatman et al.*(Yeatman et al. 2014) Using diffusion tensor imaging (DTI), a number of studies showed that white matter fractional anisotropy increased in various brain areas after learning a specific skill.(Fields 2010, Schlegel, Rudelson and Tse 2012, Scholz et al. 2009) Therefore, the increase in white matter we found might indicate neural remodeling in monocularly blind patients due to their learning to rely on alternative cues for estimating depth, for example based on parallax or familiar size, or also adjusted eye-movement patterns.

4.4.5 Comparison with previous visual deprivation studies

Compared to our study, previous structural MRI studies in bilateral blind subjects found more widespread neuroanatomical changes.(Jiang et al. 2009, Leporé et al. 2010, Noppeney 2007, Noppeney et al. 2005, Pan et al. 2007, Park et al. 2007, Park et al. 2009, Ptito et al. 2008, Schoth et al. 2006, Shimony et al. 2006, Shu et al. 2009, Wang et al. 2013, Zhang et al. 2012) This is to be expected, as in bilateral blind subjects there is a complete lack of visual input, whereas in monocularly blind subjects visual input from the healthy eye sustains largely normal visual functioning. However, in bilateral blind cases, it is much harder to establish the selectivity of functional deprivation, whereas in our study we could. Moreover, previous studies in glaucoma and macular degeneration found neuroanatomical changes along the entire visual pathway, including the early visual cortex.(Boucard et al. 2009, Chen et al. 2013, Hernowo et al. 2011, Hernowo et al. 2014, Li et al. 2012, Plank et al. 2011, Williams et al. 2013) This is consistent with the fact that these studies examined patients with binocular visual field defects that overlapped thus causing complete functional deprivation of a region of visual cortex. Therefore, we can conclude that structural changes in the early visual cortex can be caused by functional deprivation but require a complete absence of signals due to either blindness or overlapping bilateral visual field defects.

4.4.6 Limitations

The reduced grey matter volume that we found in the lateral occipital cortex is consistent with a loss of stereopsis and binocular function. While we can be completely certain about the absence of these functions in the monocular blind patients, we could not verify their presence prior to the trauma or operation. However, there is no reason to assume that the (low) incidence of absence of stereopsis would have been higher in the – now monocular blind – patients than in the normal population.

Furthermore, the lateral occipital cortex is quite a large region in which – amongst depth perception – also other functions are represented. Functional studies have shown that depth perception specifically involves dorsal V3. (Baecke et al. 2009, Goncalves et al. 2015, Ip et al. 2014) Therefore, a more accurate linkage of the anatomical changes to the functional deprivation would require an analysis specifically of this area. This, in turn, would require exact localization of this area in individual observers using retinotopic mapping and localizer studies. However, these were not performed in the current observers.

The finding of decreased grey matter density in the superior lateral occipital cortices could also partly reflect the increased white matter volume in adjacent areas. If the nerve fibers extend from the white matter into the cortex, this might interfere with the grey matter analyses. In this case, the changes in grey matter in the superior lateral occipital cortices might not only represent a decrease in grey matter volume, but also a change in the ratio of grey and white matter in this specific area.

The abovementioned volumetric differences were obtained using VBM. With SBM, we found no differences in either the ROI or the whole-brain analysis. Such discrepancies between VBM and SBM results have been observed before. In accordance with our results, in most of these studies SBM showed no changes in cortical anatomical properties in areas where VBM found differences in grey matter volume.(Bridge et al. 2012, Hernowo et al. 2014, Lyoo et al. 2006, Palaniyappan and Liddle 2012, Prins et al. 2016, Voets et al. 2008, von Glehn et al. 2014, Whitwell et al. 2013) This suggests that VBM may be a more sensitive method to discover neuroanatomical differences than SBM.

4.4.7 Conclusion

In this study in monocularly blind patients, we established that the volumes of bilateral superior lateral occipital cortices are reduced, which is most likely caused by the loss of binocular vision, stereopsis and/or altered eye movement patterns. Importantly, we found no evidence for degeneration of the optic radiations and early visual cortex. This indicates that the volumetric reductions in the postgeniculate visual pathways are caused by a selective functional deprivation of the affected areas, rather than by transsynaptic degeneration originating from degenerated axons of the ganglion cells from the blind eye.

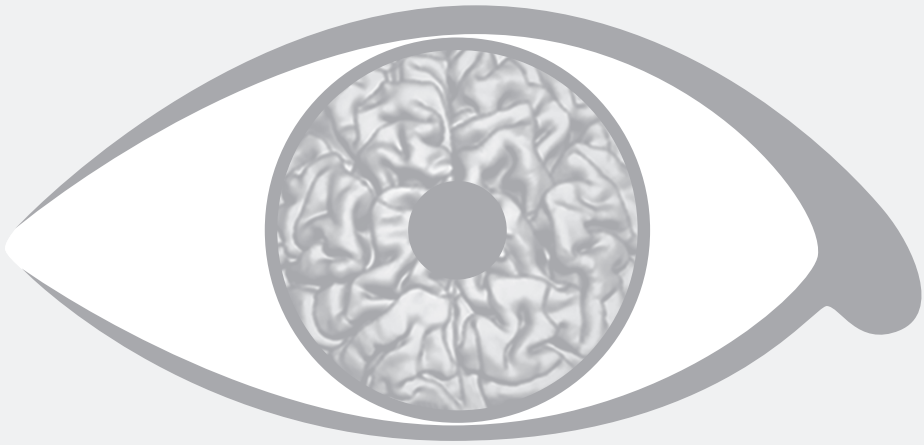

CHAPTER 5

Neuroanatomical changes of the visual pathways in patients with a monocular visual field defect due to primary open angle glaucoma

Doety Prins, Nomdo M. Jansonius, Frans W. Cornelissen

Submitted

Abstract

Introduction. Primary open-angle glaucoma (POAG) is associated with neuroanatomical changes in the brain. However, it is unclear whether this indicates that POAG is an eye disease that also causes neuroanatomical brain changes, due to functional deprivation or transsynaptic degeneration, or if this supports that POAG should be considered part of a more generalized neurodegenerative disease. Previous structural brain studies in POAG mainly focused on POAG patients with binocular visual field defects. However, a large fraction of the POAG patients has a monocular visual field defect. Here, we assess whether POAG with a monocular visual field defect is associated with neuroanatomical brain changes.

Methods. High-resolution T1-weighted magnetic resonance images in 19 POAG patients with a monocular visual field defect, 20 age-matched healthy controls, and 15 monocularly blind controls. Using voxel- and surface-based morphometry, we compared the volume of the grey and white matter, cortical thickness, mean curvature and surface area between the POAG patients and both control groups.

Results. We found extensive neuroanatomical changes in pregeniculate white matter volume and cortical thickness in the structures of the visual pathways in POAG patients with a monocular visual field defect, compared to both control groups.

Discussion. The neuroanatomical changes found in POAG patients are more widespread than the changes in monocularly blind patients. This is remarkable, given that all the POAG patients had monocular visual field loss only, that is, less extensive loss of visual input than the monocularly blind patients. Therefore, the widespread neuroanatomical changes throughout the visual pathways that we found in POAG patients cannot exclusively be explained by functional deprivation or transsynaptic degeneration. Hence, we conclude that POAG might be part of a more generalized neurodegenerative disorder that affects both the eye and the brain.

5.1 Introduction

Primary open angle glaucoma, an eye disease which is associated with visual field defects, is the second leading cause of blindness in the world.(Resnikoff et al. 2004) The visual field defects typically appear in the periphery of the visual field, and expand towards the center of the visual field if the disease progresses. An elevated intra-ocular pressure is an important risk factor. However, the pathophysiology of POAG is yet not fully understood. Previous research has shown that POAG is associated with neuroanatomical changes in the grey and white matter of the visual pathways. (Boucard et al. 2009, Chang et al. 2013, Chen et al. 2013, Chen et al. 2013, Dai et al. 2013, Doerfler et al. 2012, El-Rafei et al. 2013, Garaci et al. 2009, Hernowo et al. 2011, Li et al. 2012, Liu et al. 2012, Murai et al. 2013, Wang et al. 2013, Williams et al. 2013, Zhang et al. 2012) However, it is still not known whether POAG is primarily an eye disease that also causes neuroanatomical changes in the brain – due to transsynaptic degeneration or due to functional deprivation as a result of a decreased input – or if POAG should be considered part of a more generalized neurodegenerative disease that affects both the eye and the brain. The latter idea has been supported by the possible link between POAG and Alzheimer's disease.(Cumurcu et al. 2013, Ghiso et al. n.d., Inoue, Kawaji and Tanihara 2013, Janssen et al. 2013, Kessing et al. 2007, Kirby, Bandelow and Hogervorst 2010, Ou et al. 2012, Sivak 2013, Tamura et al. 2006, Wostyn, Audenaert and De Deyn 2010)

Previous structural brain MRI-studies in POAG mainly focused on POAG patients with binocular visual field defects. However, a monocular visual field defect commonly occurs in POAG patients. If we determine whether neuroanatomical changes also occur in POAG patients with a monocular visual field defect, then we would gain more insight in the pathophysiology of POAG. In POAG patients with a monocular visual field defect the visual input from the contralateral visual field is still intact. Therefore, finding neuroanatomical changes in POAG patients with a monocular visual field defect would suggest that such changes are not a direct consequence of the decreased input of visual information – i.e. functional deprivation – but might either be caused by transsynaptic degeneration or indicate that POAG is part of a more generalized neurodegenerative disease affecting both the eye and brain. Similarly, if neuroanatomical changes in the visual pathways would be absent in this group, then the previously reported changes in POAG patients with binocular visual field defects might exclusively be caused by functional deprivation.

In this study, we compared the following neuroanatomical properties between POAG patients with a monocular visual field defect and two different control groups: grey and white matter volume, cortical thickness, surface area, and mean curvature. The first control group consisted of age-matched healthy subjects (HC), in which there was no functional deprivation, no transsynaptic degeneration, and no generalized neurodegenerative disease. The second control group consisted of age-matched

subjects who were long-standing monocularly blind (MBC) due to a trauma or after surgery for a tumor, but otherwise healthy. In the latter control group there occurred functional deprivation, but no transsynaptic degeneration, and they do not have generalized neurodegenerative disease.

We addressed the following research questions. 1) Do the above-mentioned neuroanatomical properties differ between POAG patients with a monocular visual field defect and age-matched HC? 2) Do the above-mentioned neuroanatomical properties differ between POAG patients with a monocular visual field defect and age-matched MBC? The comparison of MBC to HC is addressed in a different paper. Using voxel-based morphometry (VBM) and surface-based (SBM) analyses, we specifically assessed the visual pathways, as this is where we expected the changes in the neuroanatomical properties to occur.

5.2 Methods

5.2.1 Ethics statement

The Medical Ethical committee of the University Medical Center Groningen approved this study. The study conformed to the tenets of the Declaration of Helsinki. All subjects gave written informed consent before participating in the study.

5.2.2 Subjects

The characteristics of the three subject groups are given in *Table 5.1*. *Figure 5.1* shows the mean location of the visual field defect of the POAG patients. This visual field is only shown for the left eye. For the patients with a visual field defect in their right eye, we mirrored the right visual field along the vertical meridian to match the left visual field. We included 54 subjects: 19 POAG patients with a monocular visual field defect (12 with left visual field defect, mean MD-value -22 dB; 7 with right visual field defect, mean MD-value -16 dB), 15 age-matched MBC (8 with blind left eye; 7 with a blind right eye) and 20 age-matched HC. The inclusion criteria for the POAG patients were that they suffered from a monocular visual field defect due to POAG, pseudo-exfoliation, or pigment dispersion syndrome. The contralateral eye had to have an intact visual field (Humphrey Field Analyzer (HFA; Carl Zeiss Meditec, Jena, Germany) 30-2 SITA with glaucoma hemifield test "within normal limits") and a good visual acuity (Snellen visual acuity at least 0.8 (0.1 logMAR or less). Moreover, they had to be free of any other ocular disease. MBC had to be light-perception negative in one eye for at least five years, due to a trauma (n = 11, in 11 subjects eye removed) or after surgery for a tumor (n = 4, in 3 subjects eye removed). The contralateral eye had to have an intact visual field and a good visual acuity. HC had to have an intact visual field and a good visual acuity in both eyes. All controls, MBC as well as HC, were free of any degenerative ocular disease. None of the subjects was previously diagnosed with neurological or psychiatric disorders.

Figure 5.1. Mean visual field defect
The average values of each point in the visual field of the POAG patients with a visual field defect in the left eye are given on the left. The average values of each point in the visual field of the POAG patients with a visual field defect in the right eye are given on the right. Measurements were done by Humphrey Field Analyzer (HFA).

	POAG patients		HC	MBC	
Number of subjects	19		20	15	
Age, median (inter-quartile range), years	59 (56 – 72)		64 (58 – 67)	62 (58 – 67)	
Male, %	47%		61%	47%	
	Better eye	Worse eye			
BCVA, median (interquartile range), logMAR	0 (0 to -0.1)	0.2 (0.25 to 0)		0 (0 to -0.1)	-0.1 (0 to -0.1)
NFI, median (inter-quartile range)	24 (19 – 31)	86 (63 – 98)		21 (15 – 26)	15 (7 – 28)
Visual field defect, median (interquartile range), MD, dB	-1.5 (-0.7 to -2.3)	-15.5 (-11.7 to -27.5)			

Table 5.1. Subject characteristics
Number of subjects, median age, gender proportion, median BCVA and median NFI-number are given for all groups. BCVA and NFI-number were split up for the POAG group in median values for the better eye and median values for the worse eye. Mean visual field defect was only given for the POAG group, split up in median values for the better eye and median values for the worse eye.
BCVA – best corrected visual acuity; logMAR – logarithm of minimum angle of resolution; NFI – nerve fiber indicator; HFA – Humphrey field analyzer; MD – mean deviation.

5.2.3 Data acquisition

MR-images of all subjects were obtained on a 3.0 Tesla MRI scanner (Philips Intera, Eindhoven The Netherlands) at the Neuroimaging Center of the University Medical Center Groningen. We acquired whole brain T1-weighted images with a voxel dimension of 1 mm x 1 mm x 1 mm using a sequence of T1W/3D/FFE, 30° flip angle, repetition time 25 ms, matrix size 256 x 256, field of view 256 x 160 x 204, yielding 160 slices.

The visual acuity was measured with a Snellen chart with optimal correction for the viewing distance (6 m). The Nerve Fiber Indicator (NFI) was measured by the Glaucoma Diagnostic instrument (GDx; Carl Zeiss Meditec, Jena, Germany). In the POAG patients,

the visual field was measured by using the HFA (see above). In the control groups, we used Frequency Doubling Technology (FDT; Carl Zeiss Meditec, Jena, Germany) in C20-1 screening mode to verify that they had an intact visual field. For a normal visual field, all test locations had to be intact (P≥1%)

5.2.4 Data analysis

Voxel-based morphometric (VBM) analysis

We compared the volumes of the grey and white matter between patients and controls using VBM. We used the FMRIB Software Library analysis tools (FSL, version 5.0.6, available at: http://www.fmrib.ox.ac.uk/fsl).(Jenkinson et al. 2012, Woolrich et al. 2009) First, we applied nonlinear noise reduction using Smallest Univalue Segment Assimilating Nucleus (SUSAN). Second, we segmented the brain from non-brain tissue, using the Brain Extraction Tool (BET).(Smith 2002) Subsequently, we performed bias field correction and segmented the brain into grey matter, white matter and cerebrospinal fluid with FMRIB's Automated Segmentation Tool (FAST).(Zhang, Brady and Smith 2001) We registered all the images to the template of the Montreal Neurological Institute (MNI template) with FMRIB's Linear Image Registration Tool (FLIRT) and FMRIB's Non-linear Image Registration Tool (FNIRT), and applied the registration to the grey and white matter segments.(Jenkinson et al. 2002, Jenkinson and Smith 2001)

Surface-based morphometric (SBM) analysis

We compared the cortical thickness, mean curvature and surface area between patients and controls using the surface-based approach of Freesurfer (version 5.3.0, available at: http://surfer.nmr.mgh.harvard.edu/). We removed the non-brain tissue,(Ségonne et al. 2004) performed automated Talairach transformation and intensity normalization. (Sled, Zijdenbos and Evans 1998) Subsequently, tessellation of the grey/white and grey/cerebrospinal fluid boundaries and automatic correction of topologic inaccuracies was performed, which we customized by setting the value for the lower threshold of the white matter to an appropriate value for our dataset.(Fischl, Liu and Dale 2001, Ségonne, Pacheco and Fischl 2007) The process continued with surface deformation and inflation,(Dale, Fischl and Sereno 1999, Fischl, Sereno and Dale 1999) registration to a spherical atlas (Fischl et al. 1999) and automatic parcellation of the cortical surface based on gyral and sulcal organization.(Desikan et al. 2006, Fischl et al. 2004)

Region-of-interest (ROI) analysis

In the ROI-based analyses, we used masks of the various grey and white matter structures of the visual pathways. Figure 5.2 depicts the ROIs: the pregeniculate structures, which contains the optic nerves (ON), the optic chiasm (OC) and optic tracts (OT); the lateral geniculate bodies (LGB); the optic radiations (OR); the supracalcarine cortex (SCC); the

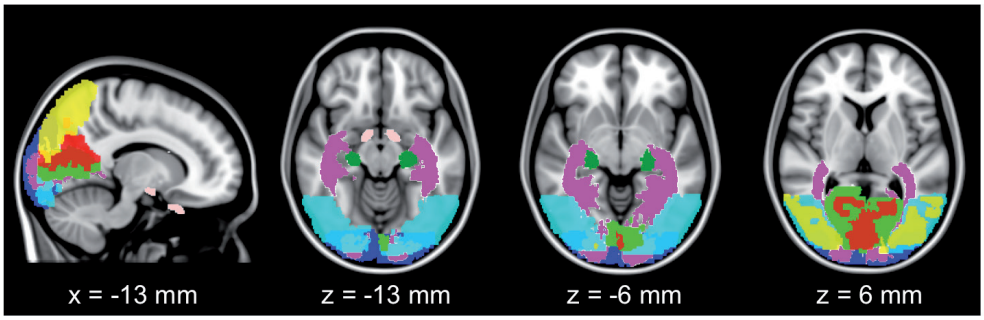

Figure 5.2. Regions of interest along the visual pathway.
Pink – pregeniculate structures; dark green – LGB; magenta – OR; lighter green – ICC; red – SCC; dark blue – OP; lighter blue – iLOC; yellow – sLOC.
Talairach position of the slices is given by their "x", "y" and "z" values.

intracalcarine cortex (ICC); the occipital pole (OP); the inferior lateral occipital cortices (iLOC) and the superior lateral occipital cortices (sLOC). The masks for the pregeniculate structures were created manually, and were adjusted to the individual subject if needed. The masks for the LGB and for the OR were obtained from the Jülich histological atlas(Bürgel et al. 2006, Bürgel et al. 1999). The masks for the SCC, the ICC, the OP, the iLOC and the sLOC were obtained from the Harvard-Oxford cortical structural atlas. (Desikan et al. 2006) In all these ROIs, we analyzed the volume of the grey or white matter using VBM. In the SCC, the ICC, the OP, the iLOC and the sLOC we also analyzed the cortical thickness, gyrification pattern and surface area using SBM.

Statistics

We examined differences between POAG patients and both the MBC and HC applying MANCOVA, using the IBM SPSS Statistics software package, version 20. The white matter volume, grey matter volume, cortical thickness, gyrification pattern, and surface area for each hemisphere and ROI were included as dependent variables, and the subject groups were entered as a fixed factor. We added age as a covariate in the analysis. We performed a Tukey post-hoc test to determine whether significant differences occurred between subject groups. The threshold for significance was set to a p-value <0.05.

Correction for visual field defect asymmetry

Not all POAG patients had their visual field defect in the same eye. Therefore, we performed the ROI analysis in two stages. In the first analysis, we compared the volumes of the optic nerves between POAG patients and both control groups. This analysis was divided in two parts: first, we compared POAG patients with their visual field defect in the right eye to the HC and to the MBC with a blind right eye; second, we compared POAG patients with their visual field defect in the left eye to the HC and to the MBC with a blind left eye. In the second analysis, we analyzed the visual pathway structures

onwards from the optic chiasm to the posterior parts of the visual pathways in the entire group of POAG patients, compared to both control groups. Once they have passed the optic chiasm, the nerve fibers that carry the information from the homonymous hemifields of both eyes travel together to the visual cortex. For this reason, after this stage we expected no detectable volumetric differences between the POAG patients with their visual field defect in either the right or the left eye. This justified a combined analysis.

Exploratory whole-brain analysis
We performed additional exploratory whole-brain analyses using both VBM and SBM. With VBM, we assessed whole-brain grey matter and white matter volume, whereas with SBM we assessed the cortical thickness, area, and mean curvature across the entire brain. In both analyses, age was added as a covariate.

5.3 Results

In summary, in POAG patients with a monocular visual field defect – compared to both control groups – we found neuroanatomical changes in pregeniculate white matter volume and cortical thickness in the structures of the visual pathways. We will describe these results in more detail below.

Table 5.2a

ROI	Hemi	Para-meter	POAG		HC	MBC		POAG vs. HC		POAG vs. MBC	
			VFD OS	VFD OD		Blind OS	Blind OD	VFD OS p-value	VFD OD p-value	VFD OS p-value	VFD OD p-value
ON	Left	Volume	80 ± 12	142 ± 10	139 ± 11	13 ± 4	125 ± 6	0.001*	0,98	0.003*	0.70
	Right	Volume	158 ± 11	139 ± 10	144 ± 11	144 ± 18	27 ± 5	0.73	0.96	0.81	<0.001*

Table 5.2. ROI morphometric values
a. White matter volumes of the left and right ON in the separate subgroups of POAG patients with a visual field defect in the left eye and POAG patients with a visual field defect in the right eye; each group was compared to the HC and to the MBC with a blind eye on the same side as the POAG patients had the visual field defect. **b.** Parameters in OC, OT, LGB, OR, OP, ICC, SCC, iLOC, and sLOC were compared between POAG patients and HC and between POAG patients and MBC.
ROI - region of interest; Hemi - hemisphere; Parameter: Surface area in mm2, average cortical thickness in mm, mean curvature in mm-1 and volume in mm3; VFD – visual field defect; OS – oculus sinister; OD – oculus dexter; values indicate mean ± standard error of the mean. F-values, degrees of freedom (df) and p-values are given.
* Indicates a significant difference between the patients group and both age-matched control groups ($p \leq 0.05$ after Tukey post-hoc).

Table 5.2b

ROI	Parameter	POAG	HC	MBC	POAG vs. HC	POAG vs. MBC
					p-value	p-value
OC	Volume	171 ± 18	246 ± 11	119 ± 12	0.001*	0.043*
OT	Volume	532 ± 16	573 ± 13	504 ± 16	0.11	0.42
LGB	Volume	1034 ± 37	1043 ± 32	1052 ± 38	0.98	0.94
OR	Volume	127180 ± 735	128014 ± 490	128956 ± 554	0.58	0.13
OP	Surface area	12334 ± 329	12419 ± 340	12387 ± 495	0.99	1.00
	Average thickness	2.86 ± 0.02	2.98 ± 0.03	2.99 ± 0.03	0.006*	0.008*
	Mean curvature	0.150 ± 0.003	0.155 ± 0.003	0.160 ± 0.003	0.43	0.06
	Volume	33380 ± 1009	32425 ± 660	31119 ± 831	0.69	0.17
ICC	Surface area	5921 ± 171	5990 ± 176	5738 ± 221	0.96	0.78
	Average thickness	2.84 ± 0.02	2.91 ± 0.05	2.91 ± 0.04	0.37	0.36
	Mean curvature	0.149 ± 0.003	0.153 ± 0.003	0.153 ± 0.003	0.57	0.60
	Volume	12668 ± 390	11905 ± 339	11881 ± 337	0.27	0.31
SCC	Surface area	3856 ± 102	3742 ± 104	3693 ± 169	0.77	0.64
	Average thickness	3.02 ± 0.03	3.14 ± 0.04	3.19 ± 0.04	0.06	0.006*
	Mean curvature	0.143 ± 0.003	0.146 ± 0.002	0.148 ± 0.003	0.74	0.51
	Volume	12511 ± 376	11917 ± 309	11577 ± 299	0.40	0.15
iLOC	Surface area	15290 ± 490	14590 ± 393	15093 ± 678	0.57	0.96
	Average thickness	3.17 ± 0.02	3.25 ± 0.03	3.30 ± 0.04	0.15	0.017*
	Mean curvature	0.141 ± 0.003	0.146 ± 0.002	0.148 ± 0.002	0.36	0.14
	Volume	32681 ± 1126	32770 ± 589	30860 ± 955	1.00	0.37
sLOC	Surface area	20733 ± 537	20088 ± 494	20666 ± 900	0.73	1.00
	Average thickness	2.95 ± 0.02	3.06 ± 0.03	3.12 ± 0.05	0.047*	0.004*
	Mean curvature	0.135 ± 0.003	0.139 ± 0.002	0.142 ± 0.003	0.56	0.20
	Volume	66434 ± 1806	66714 ± 1231	62957 ± 1559	0.99	0.29

Table 5.2 lists the results of the ROI analyses in the ONs, the OC, the OT, the LGB, the OR, the SCC, the ICC, the OP, the iLOC, and the sLOC. We found a lower volume of the left ON in the POAG with a visual field defect in the left eye compared to the HC. We found a higher volume of the ON on the affected side in the POAG compared to the MBC. A MANCOVA analysis including all ROIs showed the presence of differences between groups ($p<0.001$). After performing Tukey's post-hoc test, we found a significantly lower volume of the OC in the POAG patients compared to the HC and MBC. Additionally, we

found a thinner cortex in the POAG in the OP and sLOC compared to both HC and MBC. We also found a thinner cortex in the SCC and iLOC in the POAG patients compared to the MBC.

Using whole-brain analyses, we found no further unexpected neuroanatomical differences beyond the previously examined visual pathways ROIs.

5.4 Discussion

Neuroanatomical changes in POAG patients with a monocular visual field defect occur in the ON, the OC and in various areas of the visual cortex. We did not find any changes at the level of the OT, the LGB, and OR.

As in these patients the visual input from the contralateral visual field is still intact, we expected no or only very limited influence of functional deprivation. Not finding changes in the OT, LGB, and OR indicates that the changes in the visual cortex are not due tot transsynaptic degeneration. Therefore, this implies that the neuroanatomical changes in the visual cortex in the POAG patients are a consequence of POAG being part of a neurodegenerative disease that also directly affects the brain. This is also supported by the finding that monocular POAG affects the brain more than monocular blindness. Below, we will discuss the results and these conclusions in more detail.

5.4.1 ROI analysis

Grey and white matter volume

We found volumetric differences between POAG patients and both control groups in the pregeniculate structures. We found lower volumes compared to the HC, and higher volumes compared to the MBC. Compared to the HC, we found a lower volume of the left ON in POAG that had their visual field defect in the left eye, and we found a lower volume of the OC. We expected to find degeneration in the ON on the side of the affected eye, as a consequence of direct degeneration of the ON in POAG. However, we did not find a lower volume of the right ON in the POAG with the visual field defect in the right eye. This might be due to the fact that the POAG with the visual field defect in the right eye had a smaller visual field defect (MD value -16 dB) than the POAG with the visual field defect in the left eye (MD value -22 dB). Although this difference seems modest, with disease progress the central part of the visual field becomes more involved, and a central visual field defect causes more loss of nerve fibers than a peripheral visual field defect.

We found higher volumes of the ONs in the affected eye compared to the MBC. This was expected, as substantial volumetric decrease of these structured occurred in the MBC due to direct degeneration.

We found no differences in the volume of the OT, LGB, OR, or any of the structures of the visual cortex. The absence of volumetric differences in the OT, LGB, and OR suggests that transsynaptic degeneration might not play a role in the neuroanatomical changes in POAG.

Cortical thickness

Compared to HC and MBC, we found a thinner cortex in the OP and the sLOC in the POAG patients. We also found a thinner cortex in the SCC and the iLOC in the POAG compared to the MBC. Cortical thinning in the visual cortex could be explained by functional deprivation due to the visual field defect. However, in our previous study in which we compare the MBC to the HC, we found volumetric decrease in the sLOC, but no differences in cortical thickness. Since the MBC have complete loss of their visual field in one eye, while the POAG only have a visual field defect in one eye, one would expect to find less neuroanatomical changes in the POAG than in the MBC, if these changes were a consequence of functional deprivation. Therefore, we think that a more feasible hypothesis is that the cortical thinning is the result of a more generalized neurodegenerative process.

5.4.2 Comparison with previous structural brain MRI-studies

In contrast to the current study in POAG patients with a monocular visual field defect, previous research on neuroanatomical changes in POAG focused mainly on POAG patients with binocular visual field defects. In POAG patients with binocular visual field defects, *Boucard et al.* found a lower grey matter density in POAG patients in the anterior region of the calcarine sulcus.(Boucard et al. 2009) *Hernowo et al.* found volumetric decreases in both grey and white matter throughout the entire visual pathway in POAG.(Hernowo et al. 2011) Others studies found decreases as well as increases of grey matter volume in POAG patients in various areas of the brain, also outside of the visual pathways.(Chen et al. 2013, Li et al. 2012, Williams et al. 2013) The abovementioned studies analyzed neuroanatomical changes in POAG patients with binocular visual field defects, whereas in the present study we included only POAG patients with a monocular visual field defect. This indicates that the extent of the visual field defect does not play an important role in the development of neuroanatomical changes in POAG.

5.4.3 Underlying mechanism of the association between POAG and neuroanatomical changes

Overall, we conclude that the extensive neuroanatomical changes in the visual cortex that we found here in POAG patients with a monocular visual field defect are unlikely to be explained exclusively based on functional deprivation or transsynaptic degeneration. Therefore, we hypothesize that these changes might reflect the presence of more generalized neurodegenerative processes. Hence, POAG might be part of

a more generalized neurodegenerative disorder, which affects the brain and the eye simultaneously. This latter theory has been supported by a suggested link between POAG and Alzheimer's disease, although the reports on this topic show conflicting results.(Cumurcu et al. 2013, Ghiso et al. 2013 Inoue, Kawaji and Tanihara 2013, Janssen et al. 2013, Kessing et al. 2007, Kirby, Bandelow and Hogervorst 2010, Ou et al. 2012, Sivak 2013, Tamura et al. 2006, Wostyn, Audenaert and De Deyn 2010)

5.4.4 Limitations

In this study, we included POAG patients with a monocular visual field defect. Since not all patients had their visual field defect on the same side, we decided to perform the ROI analysis in two stages. We analyzed the ONs separately for the POAG patients that had their visual field defect in the left eye, which we compared to the MBC with a blind left eye and to the HC. For the POAG patients that had their visual field defect in the right eye, we performed the same procedure. In the OC, the nerve fibers from the nasal parts of the retinas of both eyes decussate. Therefore, we reasoned that the structures from the OC to the visual cortex could be analyzed in all POAG patients together.

We used both VBM and SBM to assess various neuroanatomical properties. These methods pre-process the data in different ways and assess different aspects of brain anatomy. As a consequence, their results may not always be congruent, as we also observed. For example, we found no volumetric changes in areas where the cortex was thinner.

5.4.5 Future research

By determining that neuroanatomical changes occur in POAG patients with a monocular visual field defect, we contributed to the knowledge on the etiology of neuroanatomical changes in POAG patients. However, it is still not fully clear in which stage of the disease such neuroanatomical changes occur and if the changes are reversible when applying for example neuroprotective agents. Therefore, future research should focus on longitudinal data from POAG patients; such research should reveal how the exact development of neuroanatomical changes takes place. Furthermore, in an intervention study with neuroprotective agents, it would be possible to determine whether neuroanatomical changes are stoppable or even reversible.

5.4.6 Conclusion

Extensive neuroanatomical changes in pregeniculate white matter volume and cortical thickness occur in the visual pathways in both hemispheres in POAG patients with a monocular visual field defect. Remarkably, these changes are more widespread than neuroanatomical changes that were found in the brains of monocularly blind patients. Therefore, we conclude that the possible effect of the loss of visual input – through functional deprivation or transsynaptic degeneration – on the neuroanatomical properties in POAG patients can not explain all of the changes in the brain that we found here. Hence, our findings support the notion that POAG might be part of a more generalized neurodegenerative disorder that affects both the eye and the brain.

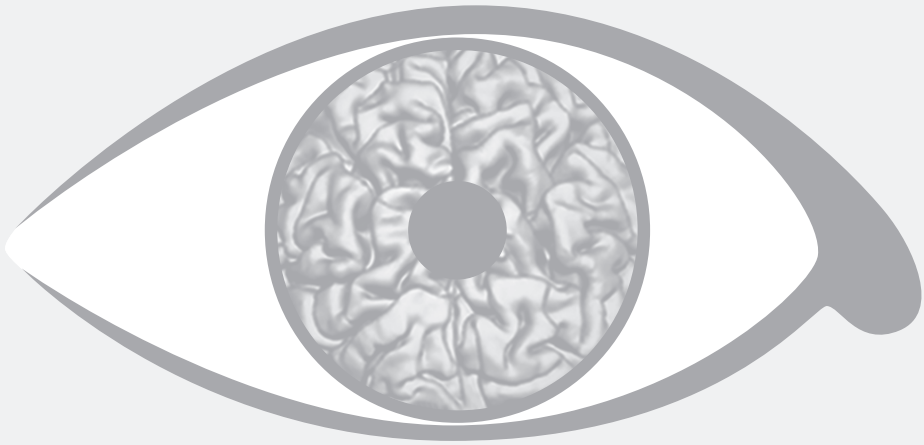

CHAPTER 6

General discussion of the topic

Based on: Doety Prins, Sandra Hanekamp & Frans W. Cornelissen. Structural brain MRI studies in eye diseases: are they clinically relevant? A review of current findings.

Acta Ophthalmologica 2016; 94(2): 113-21.

In chapter 1 of this thesis, I described the current state of knowledge of structural MRI studies in various eye diseases. Within it, I did not aim to resolve all outstanding issues nor to cover in depth the physiological mechanisms that can explain how eye diseases might cause brain damage, such as retinal remodelling or transsynaptic degeneration. I summarized the current findings, the relevance of these findings for understanding the aetiology of eye diseases and its current and future clinical relevance. Below, I answer our main questions and give directions for future research.

6.1 What have studies on structural brain changes in ocular diseases revealed thus far?

Regarding the current research findings, in all eye diseases described in the introduction – glaucoma, hereditary retinal dystrophies, AMD, albinism, and amblyopia – MRI studies have shown the presence of structural changes in the visual pathways. Changes in the post-geniculate pathways are observed in glaucoma, hereditary retinal dystrophies, macular degeneration, albinism, and amblyopia, whereas geniculate changes were seen in glaucoma and amblyopia, and pregeniculate changes were shown in glaucoma and albinism.

Furthermore, the studies described in chapter 4 and 5 of this thesis show that pregeniculate as well as cortical changes also occur in monocularly blind patients and glaucoma patients with a monocular visual field defect.

6.2 What is the potential clinical relevance of the findings?

Clinical focus

The brain changes in the eye diseases that I reviewed here have several implications for clinical practice. Presently, the clinical focus is on the ocular treatment of these diseases. The primary goal of the current treatment is to maintain existing visual function and to prevent a further decline. However, our finding of brain involvement in all eye diseases suggests that the current clinical focus on treating the eye might have to be expanded to treating the brain as well. Involvement of the brain could also explain why some treatment strategies, such as restoring of visual function in AMD, have poor outcome results.

Treatments focused on restoring visual function

In retinitis pigmentosa, retinal implants are being used experimentally in patients who are blind to restore their visual function (da Cruz et al. 2013, Zrenner 2002). The results

of these implanted devices are encouraging, but rather variable. Since the central visual system needs to process the signals from these implants, it is questionable whether patients can benefit optimally from such a retinal implant if the eye disease has caused changes to the brain. Therefore, the timing of the insertion of a retinal implant in the disease process might have a substantial impact on the result of the retinal implant. A retinal implant might be more effective on the long term when implanting it at a stage in the disease in which degeneration of the visual pathways has not yet occurred. If in the future retinal implants become a broadly used therapy for retinitis pigmentosa, MRI-based group studies studies might help to determine the appropriate timing for the implanting of a retinal device and thus for the improvement of such treatment.

Treatments focused on protecting the brain

Neurodegeneration can be considered as therapeutic target in eye diseases. Neuroprotective agents may be beneficial in treating eye diseases due to its ability to protect neurons from degeneration or aptosis (Shahsuvaryan 2012). The target neurons should be in the visual pathways, in particular the RCGs for glaucoma and photoreceptors and retinal pigment epithelial cells for retinitis pigmentosa (Cottet & Schorderet 2009, Doonan & Cotter 2004). In glaucoma for example, neuroprotective medication could be prescribed to prevent degeneration of visual pathway structures, in addition to the standard treatment that is aimed at reducing intra-ocular pressure (Chang & Goldberg 2012, Gupta & Yücel 2007, Nucci, Strouthidis & Khaw 2013, Osborne 2009, Pascale, Drago & Govoni 2012). With such combination therapies, it could even be possible to prevent brain damage.

MRI as a diagnostic tool

Some studies suggest that DTI examination can be helpful in the early diagnosis of glaucoma in individual patients (Li et al. 2014). However, statistical evidence for this is lacking. Current MRI findings are obtained in-group studies and as of yet, no study has demonstrated that individual patient diagnosis can become more accurate when adding MRI information to the ophthalmological examination. In addition, the use of MRI examination in individuals requires a sufficient specificity and selectivity and cost effectiveness. On the assumption that MRI could be used as a diagnostic tool in the future, it could contribute to the monitoring of the effect of neuroprotective medication. MRI research can reveal whether the visual pathways have been prevented from further degeneration or perhaps reversed degeneration during the use of neuroprotective medication in a group of glaucoma patients.

Reversibility

Given these findings, an important question on the topic remains: to what extent is structural brain damage in eye diseases reversible? To our knowledge, only one structural

neuroimaging study has been performed so far to address the issue of reversibility of brain changes. A study of Rosengarth et al. (2013) showed an increase in grey and white matter in the posterior cerebellum in AMD patients after 6 months of oculomotor training, compared to AMD patients that were given sham training. Although this is the most relevant study performed so far on the role of reversibility of structural changes, it does not directly indicate that reversibility is possible. The increased grey and white matter in the cerebellum might reflect a general effect of learning to control eye movements rather than reversibility of degeneration of the visual pathways. Additional studies on the role of reversibility results from two functional MRI studies. In a functional MRI study, an AMD patient who underwent treatment with intravitreal antiangiogenic injections with ranibizumab, and whose visual acuity improved after the treatment, showed an increased activation area in the visual cortex after the first treatment Baseler et al. 2011). A study by Lou et al. (2013) examined changes in grey matter volume after cataract surgery in patients with unilateral cataract. Compared to two days after surgery, six weeks after surgery grey matter volume was increased in the V2 area contralateral to the operated eye. These studies provide some limited support for the notion that improving visual function – and therefore increasing the activity in the visual pathways – may induce neural regeneration in the visual cortex. However, this may not necessarily be true for all eye diseases for which changes in the brain have been reported.

Aetiology

With specific relevance to understanding aetiology, the presence of cortical structural changes raises the causality question. Did the manifestation of the eye disease subsequently cause changes in the visual pathways and visual cortex, or did the disease start with brain changes and subsequently – or simultaneously – affect the eye?

In all eye diseases described in this review, a decrease in visual acuity or a visual field defect occurs. Both of these symptoms cause sensory deprivation in the visual pathways. Since these eye diseases are of diverse origin, I believe that the most parsimonious explanation is that eye diseases cause changes in the brain; this explanation requires the fewest disease-specific assumptions. Two mechanisms could support this hypothesis. First, visual deprivation can induce brain changes due to decreased activity along the visual pathways. This sensory deprivation can eventually lead to retinotopic-specific neuronal degeneration. Second, brain changes in eye diseases may be caused by anterograde transsynaptic degeneration, in which a breakdown of axons at the primary injury site spreads to connected neurons, resulting in axonal damage along the visual pathways towards the visual cortex. In support, this process has also been observed to occur in the opposite direction. In retrograde transsynaptic degeneration, breakdown of an axon from the point of damage spreads back towards the cell body. In other words, damage that occurs at the visual cortex will spread towards the eye resulting in

retinal atrophy. It has been suggested that this mechanisms contributes to axon damage in a number of neurodegenerative disorders in which atrophy of the retinal layers was observed after a long-standing disease, such as multiple sclerosis, Parkinson's disease and Alzheimer's disease, and after stroke (Balk et al. 2014, Gabilondo et al. 2014, Jindahra et al. 2010, Kirbas et al. 2013, Klistorner et al. 2014, Tanito & Ohira 2013).

Besides that neurodegeneration can be caused by a decreased visual input, for glaucoma and AMD there is additional evidence for a primary neuronal degeneration process that could also explain the brain changes in these eye diseases. In chapter 5 of this thesis I described neuroanatomical changes in glaucoma patients with a monocular visual field, which could not be explained by functional deprivation or transsynaptic degeneration. Furthermore, recent studies found possible links between Alzheimer's disease and the two eye diseases described here that occur later in life: glaucoma (Cumurcu et al. 2013, Inoue, Kawaji & Tanihara 2013, Tamura et al. 2006) and AMD (Ikram et al. 2012, Klaver et al. 1999, Woo et al. 2012). Moreover, an association between fluctuations in intracranial pressure and glaucoma has been found (Wostyn et al. 2013, Zhang et al. 2013, Zhang et al. 2014). These findings contribute to the notion that in glaucoma and AMD, the changes to the visual pathways and the brain might – at least partially – be interpreted also as the primary manifestation of a neurological or neurodegenerative disease. The finding of volumetric reduction of frontal white matter in AMD patients also supports this theory (Hernowo et al. 2013).

6.3 Recommendations for future research

Future studies on treatment of the aforementioned eye diseases should consider shifting their focus to research on therapies that can combine eye treatment with treatment of the neurodegeneration. Furthermore, the association between eye diseases and brain changes should be studied, particularly on the issue whether the eye disease causes the brain changes, or if the specific eye disease should be considered as part of a neurodegenerative disease. A longitudinal study could be performed in which patients with one of the aforementioned eye diseases undergo periodic structural brain scans. Ideally, patients would be included even before the disease is diagnosed, thus in a cohort study. In such a study, the development of structural brain changes can be monitored. This could help answer the question of whether brain alterations occur due to the specific eye disease, or if the supposed eye disease is only a symptom of a more general neurodegenerative disease.

Furthermore, future research is needed on the issue of regeneration of brain changes in eye diseases. More specifically, it could address the question to what extend structural damage can be reversed following restoration of input by a retinal implant. It would be interesting to perform a study in which patients with retinitis pigmentosa that received

a retinal implant would undergo a structural brain scan before treatment and several times after. In such a study it would be possible to determine if the retinal implant influences the brain, and if implanting such a device can reverse anatomical brain changes. Together with measurements of visual function in these patients this would provide valuable information about the influence of the retinal implant on the brain, and would help to determine whether a retinal implant is more effective if implanted early in the disease process.

Moreover, future MRI-studies are needed to determine whether MRI examination on an individual basis can be helpful in the diagnosis and monitoring of treatment in eye diseases. For instance, in retinitis pigmentosa MRI would be helpful to determine the optimal timing of implanting a retinal device. For glaucoma, MRI can be a useful tool for monitoring the use of neuroprotective medication.

6.4 Main messages

In summary, structural brain MRI studies in eye disease have shown us the following:

- Glaucoma, hereditary retinal dystrophies, AMD, albinism and amblyopia are associated with structural changes in the visual pathways;
- The most parsimonious explanation for the association between eye diseases and structural changes in the visual pathways is that eye diseases cause changes in the brain;
- In addition, for glaucoma and AMD, there are indications that these eye diseases might be part of a more general neurological or neurodegenerative disorder;
- Treatment should perhaps be expanded to treatment of both the eye and the brain;
- Future structural brain MRI studies are needed to:
- Establish whether specific eye diseases (such as AMD and glaucoma) should be considered part of a more general neurodegenerative disease;
- Investigate the degree to which degeneration of the brain in eye diseases is reversible, relevant for effectively restoring vision following retinal restoration;
- Evaluate and monitor the effect of neuroprotective medication in ocular disease (e.g. in glaucoma);
- Determine the optimal timing for the insertion of a retinal implant, if in the future such treatment would become more common (e.g. in retinitis pigmentosa or MD);
- Assess whether MRI examination can be a useful diagnostic tool in certain eye diseases (i.e. has sufficient specificity and selectivity and cost effectiveness for such a purpose).

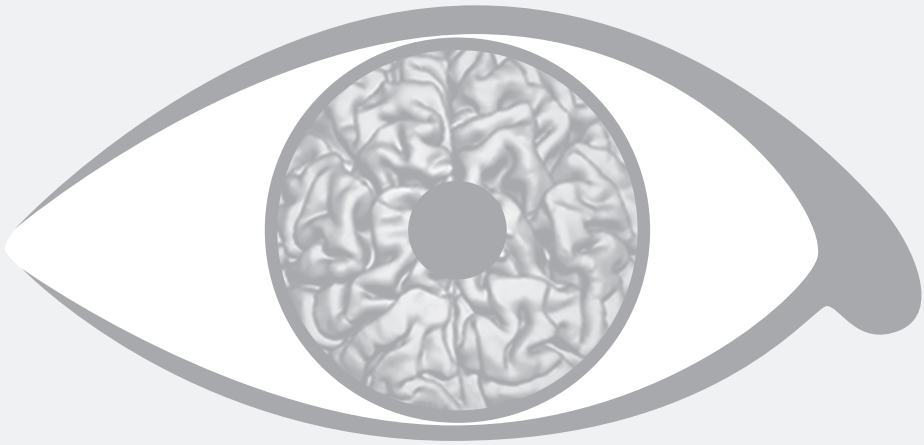

Conclusions

My thesis described research on the association between ocular pathology and anatomical changes in the brain. My aim was to discover which mechanisms underlie this association. To do so, I studied brain changes in a variety of patient groups: AMD, JMD, monocular blindness, and POAG with a monocular field defect, using structural magnetic resonance imaging (MRI) of the brain. My assumption was that by assessing and comparing the results over these different groups, we could determine the contributions of functional deprivation, anterograde transsynaptic degeneration, and general neurodegenerative mechanisms to the association between ocular pathology and neuroanatomical changes.

In **Chapter 2**, I found grey and white matter volumetric reductions throughout the visual pathways in AMD and JMD patients, compared to age-matched healthy controls. Additionally, AMD patients also showed decreased white matter volume outside of the visual pathways, specifically in the frontal lobe. I suggested the latter finding to be the possible neural correlate that reflects a previously described association between AMD and mild cognitive impairment and Alzheimer's disease. In **Chapter 3**, I found marked differences in the cortical thickness, surface area and grey matter volume of the areas V1 and V2 in JMD patients, compared to their age-matched healthy controls. Specifically, the posterior parts of V1 and V2 were more extensively affected than the anterior parts. This reflects retinotopic-specific neuronal degeneration of the visual cortex. In AMD patients, I only found a thinner cortex in V2, whereas V1 did not show any differences. This implies that the volumetric differences found with VBM (chapter 5) in the visual cortex of AMD patients are less apparent than those in JMD patients.

The anatomical changes found in both AMD and JMD in chapter 2 and 3 are generally consistent with both functional deprivation and transsynaptic degeneration. The binocular overlapping central visual field defects lead to decreased activity in the visual pathways. Due to the retinotopic organisation of the visual cortex, a part of the visual pathways will have been deprived of visual input for a long period of time, which may lead to neuroanatomical changes. Finding degeneration in all structures along the entire pathway also suggests that transsynaptic degeneration could explain the degeneration. Given the wide-spread frontal white matter volumetric reductions observed in AMD, also a more general neurodegenerative process may have contributed to the neuroanatomical changes in AMD.

In **Chapter 4**, I found a loss of white matter volume in monocularly blind patients in the optic nerve on the side of the blind eye, in the chiasm and in the bilateral optic tracts, compared to age-matched healthy controls. This white matter volumetric loss in the pregeniculate structures is most consistent with a direct degeneration of the axons that originate from the blind eye. I did not find any anatomical changes in the early visual cortex, which suggests that anterograde transsynaptic degeneration did not play any major role. Furthermore, I found grey matter volumetric loss in the bilateral superior lateral occipital cortices. The superior lateral occipital cortices are located in

the dorsal visual cortex, which is involved in the perception of stereoscopic depth. Therefore, the grey matter volumetric loss in the superior lateral occipital cortices of monocularly blind patients is consistent with functional deprivation caused by their loss of stereopsis. Generalizing from these findings, I deduce that functional deprivation causes anatomical changes, and that transsynaptic degeneration plays no or only a minor role.

In **Chapter 5**, I found neuroanatomical changes in volume and cortical thickness throughout the visual pathway in POAG patients with a monocular visual field defect compared to age-matched healthy controls and age-matched monocularly blind controls. Considering that the visual field defect only existed monocularly, visual function is still supported by the other eye, and stereopsis is mostly preserved. Therefore, these changes can neither be fully explained by functional deprivation nor by transsynaptic degeneration. Furthermore, the brain was more affected in POAG with a monocular visual field defect than in monocular blindness. Hence, this suggests that in POAG also a more general neurodegenerative disorder may contribute to the visual pathway changes.

To conclude, I studied neuroanatomical changes in various ocular diseases that cause visual deprivation. I found evidence for a role of functional deprivation in monocular blind patients. Generalizing, this mechanism presumably plays an important role in all cases in which loss of visual function is associated with neuroanatomical changes. In monocular blindness, I found no indication that transsynaptic degeneration plays any major role, suggesting that this process plays no important role in causing neuroanatomical changes in ocular pathology in general. Furthermore, in both AMD and POAG, I found neuroanatomical changes that could not be explained by functional deprivation. This suggests that in both AMD and POAG more general neurodegenerative processes contribute to the neuroanatomical changes.

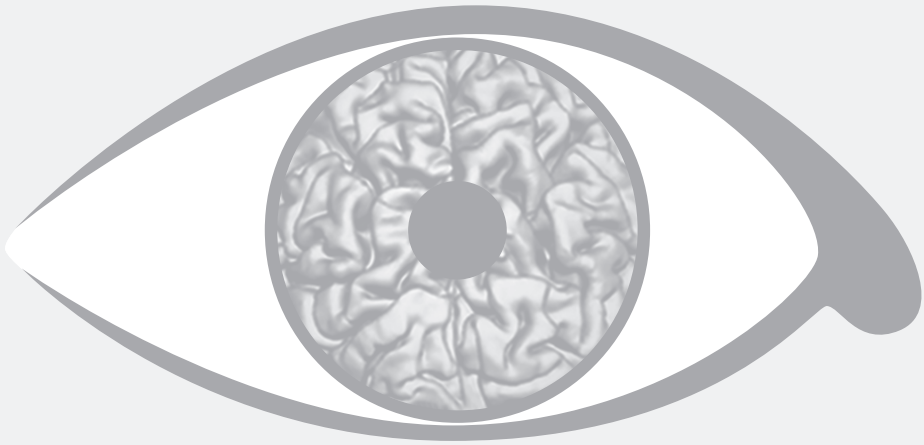

References

Alcauter S, Barrio FA, Diaz R, and Fernandez-Ruiz J. Gray and white matter alterations in spinocerebellar ataxia type 7: an in vivo DTI and VBM study. *Neuroimage* 2011*;* 55 (1):1-7.

Alexander AL, Lee JE, Lazar M, Field AS. Diffusion Tensor Imaging of the brain. *Neurotherapeutics* 2007; 4:316-329.

Arden GB. Age-related macular degeneration. *Journal of the British Menopause Society* 2006; 12 (2):64-70.

Ashburner J and Friston KJ. Voxel-based morphometry--the methods. *Neuroimage* 2000; 11 (6 Pt 1):805-821.

Ashburner J and Friston KJ. Why voxel-based morphometry should be used. *Neuroimage* 2001; 14:1238-1243.

Ashburner J. A fast diffeomorphic image registration algorithm. *Neuroimage* 2007; 38 (1):95-113.

Augood CA, Vingerling JR, De Jong PT, Chakravarthy U, Seland J, Soubrane G, et al. Prevalence of age-related maculopathy in older Europeans: the European Eye Study (EUREYE). *Archives of Ophthalmology 2006;* 124 (4):529-535.

Backus BT, Fleet DJ, Parker AJ, Heeger DJ. Human cortical activity correlates with stereoscopic depth perception. *Journal of Neurophysiology* 2001; *86*(4):2054–2068.

Baecke S, Lützkendorf R, Tempelmann C, Müller C, Adolf D, Scholz M, and Bernarding J. Event-related functional magnetic resonance imaging (efMRI) of depth-by-disparity perception: additional evidence for right-hemispheric lateralization. *Experimental Brain Research* 2009; *196*(3):453–458.

Baker CI, Peli E, Knouf N, and Kanwisher N. Reorganization of visual processing in macular degeneration. *Journal of Neuroscience* 2005; 25 (3):614-618.

Baker CI, Dilks DD, Peli E, and Kanwisher N. Reorganization of visual processing in macular degeneration: replication and clues about the role of foveal loss. *Vision Research* 2008; 48:1910-1919.

Baker CI, Dilks DD, Peli E, and Kanwisher N. Reorganization of visual processing in macular degeneration: replication and clues about the role of foveal loss. *Vision Research* 2008; 48 (18):1910-1919.

Balk LJ, Twisk JWR, Steenwijk MD, Daams M, Tewarie P, Killestein J, et al. A dam for retrograde axonal degeneration in multiple sclerosis? *Journal of Neurology, Neurosurgery & Psychiatry* 2014; 85: 782–9.

Ban H, Preston TJ, Meeson A, and Welchman AE. The integration of motion and disparity cues to depth in dorsal visual cortex. *Nature Neuroscience* 2012; *15*(4):636–643.

Barnes GR, Li X, Thompson B, Singh KD, Dumoulin SO, Hess RF. Decreased gray matter concentration in the lateral geniculate nuclei in human amblyopes. *Investigative Ophthalmology & Visual Science* 2010; 51:1432-1438.

Baseler HA, Gouws A, Crossland MD, Leung C, Tufail A, Rubin GS, et al. Objective visual assessment of antiangiogenic treatment for wet age-related macular degeneration. *Optometry & Vision Science* 2011; 88: 1255–61.

Baseler HA, Gouws A, Haak KV, Racey C, Crossland MD, Tufail A, et al. Large-scale remapping of visual cortex is absent in adult humans with macular degeneration. *Nature Neuroscience* 2011; 14 (5):649-655.

Basser PJ, Pajevic S, Pierpaoli C, Duda J, Aldroubi A. In vivo fiber tractography using DT-MRI data. *Magnetic Resonance in Medicine* 2000; 44(4):625-632.

Bayer AU, Ferrari F, Erb C. High occurrence rate of glaucoma among patients with Alzheimer's disease. *European Journal of Neurology* 2002; 47(3):165-168.

Beatty RM, Sadun AA, Smith L, Vonsattel JP, and Richardson EP. Direct demonstration of transsynaptic degeneration in the human visual system: a comparison of retrograde and anterograde changes. *Journal of Neurology, Neurosurgery, and Psychiatry*. 1982; *45*(2):143–146.

Biarnés M, Monés J, Alonso J, and Arias L. Update on geographic atrophy in age-related macular degeneration. *Optometry & Vision Science* 2011; 88 (7):881-889.

Bookstein F. "Voxel-based morphometry" should not be used with imperfectly registered images. *Neuroimage* 2001; 14:1454-1462.

Boucard CC, Hernowo AT, Maguire RP, Jansonius NM, Roerdink JB, Hooymans JM, and Cornelissen FW. Changes in cortical grey matter density associated with long-standing retinal visual field defects. *Brain* 2009; 132 (Pt 7):1898-1906.

Bridge H, von dem Hagen E, Davies G, Chambers C, Gouws A, Hoffmann M, et al. Changes in brain morphology in albinism reflect reduced visual acuity. *Cortex* 2012; 56:64-72.

Briggs F and Usrey WM. Corticogeniculate feedback and visual processing in the primate. *Journal of Physiology* 2011*;* 589 (pt1):33-40.

Brouwer GJ, van Ee R, and Schwarzbach J. Activation in visual cortex correlates with the awareness of stereoscopic depth. *The Journal of Neuroscience* 2005; *25*(45):10403–10413.

Bürgel U, Amunts K, Hoemke L, Mohlberg H, Gilsbach JM, and Zilles K White matter fiber tracts of the human brain: three-dimensional mapping at microscopic resolution, topography and intersubject variability. *NeuroImage* 2006; 29(4):1092–1105.

Bürgel U, Schormann T, Schleicher A, and Zilles K. Mapping of histologically identified long fiber tracts in human cerebral hemispheres to the MRI volume of a reference brain: position and spatial variability of the optic radiation. *Neuroimage* 1999; 10 (5):489-499.

Bürgel U, Amunts K, Hoemke L, Mohlberg H, Gilsbach J, and Coenen VA. White matter fiber tracts of the human brain: three-dimensional mapping at microscopic resolution, topography and intersubject variability. *Neuroimage* 2006; 29 (4):1092-1105.

Chang EE, Goldberg JL. Glaucoma 2.0: Neuroprotection, neuroregeneration, neuroenhancement. *Ophthalmology* 2012; 119:979-986.

Chang ST, Xu J, Trinkaus K, Pekmezci M, Arthur SN, Song S-K, et al. Optic nerve Diffusion Tensor Imaging parameters and their correlation with optic disc topography and disease severity in adult glaucoma patients and controls. *Journal of Glaucoma* 2014; 23(8):513-520.

Chen WW, Wang N, Cai S, Fang Z, Yu M, Wu Q, et al. Structural brain abnormalities in patients with primary open-angle glaucoma: a study with 3T MR imaging. *Investigative Opthalmology & Visual Science* 2013; 54: 545-54.

Chen Z, Lin F, Wang J, Li Z, Dai H, Mu K, et al. Diffusion tensor magnetic resonance imaging reveals visual pathway damage that correlates with clinical severity in glaucoma. *Clinical & Experimental Ophthalmology* 2013; 41:43-49.

Cheung CM, Tai ES, Kawasaki R, Tay WT, Lee JL,Hamzah H, and Wongh TY. Prevalence of and Risk Factors for Age-Related Macular Degeneration in a Multiethnic Asian Cohort. *Archives of Ophthalmology* 2012; 130(4):480-486.

Clarke S. Modular organization of human extrastriate visual cortex: evidence from cytochrome oxidase pattern in normal and macular degeneration cases. *European Journal of Neuroscience* 1994; 6 (5):725-736.

Congdon N, O'Colmain B, Klaver CCW, Klein R, Muñoz B, et al. Causes and prevalence of visual impairment among adults in the United States. *Archives of Ophthalmology* 2004; 122:477-485.

Culham JC, and Kanwisher NG. Neuroimaging of cognitive functions in human parietal cortex. *Current Opinion in Neurobiology* 2001; 11(2):157–163.

Cumurcu T, Dorak F, Cumurcu BE, Erbay LG, Ozsoy E. Is there any relation between pseudoexfoliation syndrome and Alzheimer's type dementia? *Seminars in Ophthalmology* 2013; 28:224-229.

Da Cruz L, Coley BF, Dorn J, Merlini F, Filley E, Christopher P, et al. The Argus II epiretinal prosthesis system allows letter and word reading and long-term function in patients with profound vision loss. *The British Journal of Ophthalmology* 2013; *97*(5):632–636.

Dai H, Yin D, Hu C, Morelli JN, Hu S, Yan X, et al. Whole-brain voxel-based analysis of diffusion tensor MRI parameters in patients with primary open angle glaucoma and correlation with clinical glaucoma stage. *Neurology* 2013; 55(2):233-243.

Dale AM, Fisch B, Sereno MI. Cortical surface-based analysis. I. Segmentation and surface reconstruction. *Neuroimage* 1999; 9:179-194.

Desikan RS, Ségonne F, Fischl B, Quinn BT, Dickerson BC, Blacker D, et al. An automated labeling system for subdividing the human cerebral cortex on MRI scans into gyral based regions of interest. *Neuroimage* 2006; 31 (3):968-980.

Dilks DD, Baker CI, Peli E, and Kanwisher N. Reorganization of visual processing in macular degeneration is not specific to the "preferred retinal locus". *Journal of Neuroscience* 2009; 29 (9):2768-2773.

Doerfler A, Waerntges S, Michelson G, Otto M, Struffert T, El-Rafei et al. Changes of radial diffusivity and fractional anisotopy in the optic nerve and optic radiation of glaucoma patients. *The Scientific World Journal* 2012; 2012:1-5.

Eckhardt C, Eckhardt U. Macular translocation in nonexsudative age-related macular degeneration. *Retina* 2002; 22:786-794.

El-Rafei A, Engelhorn T, Wärntges S, Dörfler A, Hornegger J, Michelson G. Glaucoma classification based on visual pathway analysis using diffusion tensor imaging. *Magnetic Resonance Imaging* 2013; 31:1081-1091.

Fechtner RD, Weinreb RN. Mechanisms of optic nerve damage in primary open angle glaucoma. *Survey of Ophthalmology* 1994; 39:23-42.

Fields RD. Neuroscience. Change in the brain's white matter. *Science* 2010; *330*(6005):768–769.

Finger RP, Fimmers R, Holz FG, and Scholl HP. Prevalence and causes of registered blindness in the largest federal state of Germany. *British Journal of Ophthalmology* 2011; 95 (8):1061-1067.

Fischl B, van der Kouwe A, Destrieux C, Halgren E, Ségonne F, et al. Automatically parcellating the human cerebral cortex. *Cerebral Cortex* 2004; 14:11-22.

Fischl B, Liu A, Dale AM. Automated manifold surgery: constructing geometrically accurate and topologically correct models of the human cerebral cortex. *IEEE Transactions on Medical Imaging* 2001; 20:70-80.

Fischl B, Sereno MI, Dale AM. Cortical surface-based analysis. II: Inflation, flattening, and a surface-based coordinate system. *Neuroimage* 1999a; 9:195-207.

Fischl B, Sereno MI, Tootell RB, Dale AM. High-resolution intersubject averaging and a coordinate system for the cortical surface. *Human Brain Mapping* 1999b; 8:272-284.

Forrester JV, Xu H, Kuffová L, Dick AD, and McMenamin PG. Dendritic cell physiology and function in the eye. *Immunological Reviews* 2010; 234 (1):282-304.

Frazier JA, Chiu S, Breeze JL, Makris N, Lange N, Kennedy DN, et al. Structural brain magnetic resonance imaging of limbic and thalamic volumes in pediatric bipolar disorder. *American Journal of Psychiatry* 2005; 162 (7):1256-1265.

Gabilondo I, Martínez-Lapiscina EH, Martínez-Heras E, Fraga-Pumar E, Llufriu S, Ortiz S, et al. Trans-synaptic axonal degeneration in the visual pathway in multiple sclerosis. *Annals of Neurology* 2014; 75: 98–107.

Garaci FG, Bolacchi F, Cerulli A, Melis M, Spanò A, Cedrone C, et al. Optic nerve and optic radiation neurodegeneration in patients with glacuoma: in vivo analysis with 3-T diffusion-tensor MR imaging. *Radiology* 2009; 252:496-501.

Gehrs KM, Anderson DH, Johnson LV, and Hageman GS. Age-related macular degeneration--emerging pathogenetic and therapeutic concepts. *Annals of Medicine* 2006; 38 (7):450-471.

Ghiso JA, Doudevski I, Ritch R, Rostagno AA. Alzheimer's disease and glaucoma: mechanistic similarities and differences. *Journal of Glaucoma* 2013; 22 suppl 5:S36-38.

Von Glehn F, Jarius S, Cavalcanti Lira RP, Alves Ferreira MC, Von Glehn FHR, et al. Structural brain abnormalities are related to retinal nerve fiber layer thinning and disease duration in neuromyelitis optica spectrum disorders. *Multiple Sclerosis Journal* 2014; 20(9):1189-1197.

Göbel AP, Fleckenstein M, Schmitz-Valckenberg S, Brinkmann CK, and Holz FG. Imaging Geographic Atrophy in Age-Related Macular Degeneration. *Ophthalmologica* 2011; 226 (4):182-190.

Goldstein JM, Seidman LJ, Makris N, Ahern T, O'Brien LM, Caviness VS Jr, et al. Hypothalamic abnormalities in schizophrenia: sex effects and genetic vulnerability. *Biological Psychiatry* 2007; 61 (8):935-945.

Good C, Johnsrude I, Ashburner J, Henson RN, Friston KJ, Frackowiak RS. A voxel-based morphometric study of ageing in 465 normal adult human brains. *Neuroimage* 2001; 14:21-36.

Goncalves NR, Ban H, Sánchez-Panchuelo RM, Francis ST, Schluppeck D, and Welchman AE. 7 tesla FMRI reveals systematic functional organization for binocular disparity in dorsal visual cortex. *The Journal of Neuroscience* 2015; *35*(7):3056–3072.

Guillery RW, Okoro AN, Witkop CJ. Abnormal visual pathways in the brain of a human albino. *Brain Research* 1975; 96:373-377.

Gupta N, Ang L-C, Noël de Tilly L, Bidaisee L, Yücel YH. Human glaucoma and neural degeneration in intracranial optic nerve, lateral geniculate nucleus, and visual cortex. *British Journal of Ophthalmology* 2006; 90:674-678.

Gupta N, Greenberg G, de Tilly LN, Gray B, Polemidiotis M, Yücel YH. Atrophy of the lateral geniculate nucleus in human glaucoma detected by magnetic resonance imaging. *British Journal of Ophthalmology* 2009; 93:56-60.

Gupta N, Yücel YH. What changes can we expect in the brain of glaucoma patients? *Survey of Opthalmology* 2007; 52 suppl 2:S122-126.

Haak KV, Langers DRM, Renken R, van Dijk P, Borgstein J, Cornelissen FW. Abnormal visual field maps in human cortex: A mini-review and a case report. *Cortex* 2014; 56:14-25.

Von dem Hagen EAH, Houston GC, Hoffmann MB, Jeffery G, Morland AB. Retinal abnormalities in human albinism translate into a reduction of grey matter in the occipital cortex. *European Journal of Neuroscience* 2005; 22:2475-2480.

Hernowo AT, Boucard CC, Jansonius NM, Hooymans JM, and Cornelissen FW. Automated Morphometry of The Visual Pathway in Primary Open-Angle Glaucoma. *Investigative Ophthalmology & Visual Science* 2011; *52 (5):2758-2766*.

Hernowo AT, Prins D, Baseler HA, Plank T, Gouws AD, Hooymans JMM, et al. Morphometric analyses of the visual pathways in macular degeneration. *Cortex* 2014; 56:99-110.

Holz FG, Pauleikhoff D, Klein R, and Bird AC. Pathogenesis of lesions in late age-related macular disease. *American Journal of Ophthalmology* 2004; 137 (3):504-510.

Hutton C, Draganski B, Ashburner J, Weiskopf N. A comparison between voxel-based cortical thickness and voxel-based morphometry in normal aging. *Neuroimage* 2009; 48:371-380.

Ikram MK, Cheung CY, Wong TY, Chen CPLH. Retinal pathology as biomarker for cognitive impairment and Alzheimer's disease. *Journal of Neurology, Neurosurgery & Psychiatry* 2012; 83:917-922.

Inoue T, Kawaji T, Tanihara H. Elevated levels of multiple biomarkers of Alzheimer's disease in the aqueous humor of eyes with open-angle glaucoma. *Investigative Ophtahlmology & Visual Science* 2013; 54:5353-5358.

Ip IB, Minini L, Dow J, Parker AJ, and Bridge H Responses to interocular disparity correlation in the human cerebral cortex. *Ophthalmic & Physiological Optics* 2014; *34*(2):186–198.

Iwata F, Patronas NJ, Caruso RC, Podgor MJ, Remaley NA, Kupfer C, et al. Association of visual field, cup-disc ratio, and magnetic resonance imaging of optic chiasm. *Archives of Opthalmology* 1997:729-732.

Jack CR Jr, Bernstein MA, Fox NC, Thompson P, Alexander G, Hervey D, et al. The Alzheimer's Disease Neuroimaging Initiative (ADNI): MRI methods. *Journal of Magnetic Resonance Imaging* 2008; 27 (4):685-691.

Janssen SF, Gorgels TGMF, Ramdas WD, Klaver CCW, van Duijn CM, Jansonius NM, et al. The vast complexity of primary open angle glaucoma: disease genes, risks, molecular mechanisms and pathobiology. *Progress in Retinal and Eye Research* 2013; 37:31-67.

Jenchitr W, Ruamviboonsuk P, Sanmee A, and Pokawattana N. Prevalence of age-related macular degeneration in Thailand. *Ophthalmic Epidemiology* 2011; 18 (1):48-52.

Jenkinson M, Bannister P, Brady M, and Smith S. Improved optimization for the robust and accurate linear registration and motion correction of brain images. *NeuroImage* 2002; *17*(2):825–841.

Jenkinson M, Beckmann CF, Behrens TEJ, Woolrich MW, and Smith SM. FSL. *NeuroImage* 2002; *62*(2):782–790.

Jenkinson M, and Smith S. A global optimisation method for robust affine registration of brain images. *Medical Image Analysis* 2001; *5*(2):143–156.

Jones DK, Horsfield MA, Simmons A. Optimal strategies for measuring diffusion in anisotropic systems by magnetic resonance imaging. *Magnetic Resonance in Medicine* 1999a; 42(3):515-525.

Jones DK, Simmons A, Williams SC, Horsfield MA. Non-invasive assessment of axonal fiber connectivity in the human brain via diffusion tensor MRI. *Magnetic Resonance in Medicine* 1999b; 42(1):37-41

Jiang J, Zhu W, Shi F, Liu Y, Li J, Qin W, et al. Thick visual cortex in the early blind. *The Journal of Neuroscience* 2009; *29*(7):2205–2011.

Jindahra P, Hedges TR, Mendoza-Santiesteban CE, Plant GT. Optical coherence tomography of the retina: applications in neurology. *Current Opinion in Neurology* 2010; 23: 16–23.

Johansson BB. Brain plasticity in health and disease. *Keio Journal of Medicine* 2004; 53 (4):231-246.

Jonas JB, Wang NL, Wang YX, You QS, Xie XB, Yang DY, et al. Estimated trans-lamina cribrosa pressure difference versus intraocular pressure as biomarker for open-angle glaucoma. The Beijing Eye Study 2011. *Acta Ophthalmologica* 2015; 93(1):e7-e13.

Jonasson F, Arnarsson A, Eiríksdottir G, Harris TB, Launer LJ, Meuer SM, et al. Prevalence of age-related macular degeneration in old persons: Age, Gene/environment Susceptibility Reykjavik Study. *Ophthalmology* 2011; 118 (5):825-830.

Kashiwagi K, Okubo T, Tsukahara S. Association of magnetic resonance imaging of anterior optic pathway with glaucomatous visual field damage and optic disc cupping. *Journal of Glaucoma* 2004; 13:189-195.

Keane PA and Sadda SR. Imaging chorioretinal vascular disease. *Eye* 2010; 24 (3):422-427.

Keenan TD, Goldacre R, and Goldacre MJ. Associations between age-related macular degeneration, Alzheimer disease, and dementia: record linkage study of hospital admissions. *JAMA Ophthalmology* 2014; 132(1):63-68.

Kessing LV, Lopez AG, Andersen PK, Kessing SV. No increased risk of developing Alzheimer disease in patients with glaucoma. *Journal of Glaucoma* 2007; 16:47-51.

Kim SY, Sadda S, Humayun MS, de Juan E Jr, Melia BM, and Green WR. Morphometric analysis of the macula in eyes with geographic atrophy due to age-related macular degeneration. *Retina* 2002; 22 (4):464-470.

Kinnear PE, Jay B, Witkop CJ. Albinism. *Survey of Ophthalmology* 1988; 30:75-101.

Kirbas S, Turkyilmaz K, Tufekci A, Durmus M. Retinal nerve fiber layer thickness in Parkinson disease. *Journal of Neuroophthalmology* 2013; 33: 62–5.

Kirby E, Bandelow S, Hogervorst E. Visual impairment in Alzheimer's disease: a critical review. *Journa of Alzheimer's disease* 2010; 21:15-34.

Kitajima M, Korogi Y, Hirai T, Hamatake S, Ikushima I, Sugahara T, et al. MR changes in the calcarine area resulting from retinal degeneration. *American Journal of Neuroradiology* 1997; 18 (7):1291-1295.

Klaver CCW, Ott A, Hofman A, Assink JJM, Breteler MMB and De Jong PTVM. Is age-related maculopathy associated with Alzheimer's disease? *American Journal of Epidemiology* 1999; 150:963-8.

Klaver CC, Wolfs RC, Vingerling JR, Hofman A, De Jong PT. Age-specific prevalence and causes of blindness and visual impairment in an older population: the Rotterdam Study. *Archives of Ophthalmology* 1998; 116:653-658.

Klein A, Andersson J, Ardekani BA, Ashburner J, Avants B, Chiang MC, et al. Evaluation of 14 nonlinear deformation algorithms applied to human brain MRI registration. *Neuroimage* 2009; 46 (3):786-802.

Klein R, Chou CF, Klein BE, Zhang X, Meuer SM, and Saaddine JB. Prevalence of age-related macular degeneration in the US population. *Archives of Ophthalmology* 2011, 129 (1):75-80.

Klistorner A, Sriram P, Vootakuru N, Wang C, Barnett MH, Garrick R, et al. Axonal loss of retinal neurons in multiple sclerosis associated with optic radiation lesions. *Neurology* 2014; 82: 2165–72.

Kocur I and Resnikoff S. Visual impairment and blindness in Europe and their prevention. *British Journal of Ophthalmology* 2002; 86 (7):716-722.

Leporé N, Voss P, Lepore F, Chou Y-Y, Fortin M, Gougoux F, et al. Brain structure changes visualized in early- and late-onset blind subjects. *NeuroImage* 2010; *49*(1):134–140.

Levin N, Dumoulin SO, Winawer J, Dougherty RF, and Wandell BA. Cortical maps and white matter tracts following long period of visual deprivation and retinal image restoration. *Neuron* 2010 ; *65*(1):21–31.

Li C, Cai P, Shi L, Lin Y, Zhang J, Liu S, et al. Voxel-based morphometry of the visual-related cortex in primary open angle glaucoma. *Current Eye Research* 2012; 37:794-802.

Li J, Liu Y, Qin W, Jiang J, Qiu Z, Xu J, et al. Age of onset of blindness affects brain anatomical networks constructed using diffusion tensor tractography. *Cerebral Cortex* 2013b; *23*(3):542–551.

Li K, Lu C, Huang Y, Yuan L, Zeng D, Wu K. Alteration of fractional anisotropy and mean diffusivity in glaucoma: novel results of a meta-analysis of diffusion tensor imaging studies. *PLoS One* 2014; 9:e97445

Li Q, Jiang Q, Guo M, Li Q, Cai C, Yin X. Grey and white matter changes in children with monocular amblyopia: voxel-based morphometry and diffusion tensor imaging study. *British Journal of Ophthalmology* 2013a; 97:524-529.

Liepert J, Bauder H, Wolfgang HR, Miltner WH, Taub E, and Weiller C. Treatment-induced cortical reorganization after stroke in humans. *Stroke* 2000; 31(6):1210-1216.

Liu T, Cheung SH, Schuchard RA, Glielmi CB, Hu X, He S, and Legge GE. Incomplete cortical reorganization in macular degeneration. *Investigative Ophthalmology & Visual Science* 2010; 51 (12):6826-6834.

Liu T, Shi L, Wang J, Li C, Du H, Lu P, et al. Reduced white matter integrity in primary open-angle glaucoma: A DTI study using tract-based spatial statistics. *Journal of Neuroradiology* 2012; 40:89-93.

Lou AR, Madsen KH, Julian HO, Toft PB, Kjaer TW, Paulson OB, et al. Postoperative increase in grey matter volume in visual cortex after unilateral cataract surgery. *Acta Ophthalmologica* 2013; 91: 58–65.

Lv B, He H, Li X, Zhang Z, Huang W, Li M, et al. Structural and functional deficits in human amblyopia. *Neuroscience Letters* 2008; 437:5-9.

Lyoo IK, Sung YH, Dager SR, Friedman SD, Lee J-Y, et al. Regional cerebral cortical thinning in bipolar disorder. *Bipolar disorders* 2006; 8:65-74.

MacLaren RE, Groppe M, Barnard AR, Cottriall CL, Tolmachova T, Seymour L, et al. Retinal gene therapy in patients with choroideremia: initial findings from a phase 1/2 clinical trial. *Lancet* 2014; *383*(9923):1129–1137.

Makris N, Goldstein JM, Kennedy D, Hodge SM, Caviness VS, Faraone SV, et al. Decreased volume of left and total anterior insular lobule in schizophrenia. *Schizophrenia Research* 2006; 83 (2-3):155-171.

Margalit E and Sadda SR. Retinal and optic nerve diseases. *Artificial Organs* 2003; 27 (11):963-974.

Masuda Y, Dumoulin SO, Nakadomari S, and Wandell BA. V1 projection zone signals in human macular degeneration depend on task, not stimulus. *Cerebral Cortex* 2008; 18 (11):2483-2493.

Medeiros NE and Curcio CA. Preservation of ganglion cell layer neurons in age-related macular degeneration. *Investigative Ophthalmology & Visual Science* 2001; 42 (3):795-803.

Mendola JD, Conner IP, Roy A, Chan S-T, Schwartz TL, Odom JV, et al. Voxel-based analysis of MRI detects abnormal visual cortex in children and adults with amblyopia. *Human Brain Mapping* 2005; 25:222-236.

Menke MN, Dabov S, Knecht P, and Sturm V. Reproducibility of retinal thickness measurements in patients with age-related macular degeneration using 3D Fourier-domain optical coherence tomography (OCT) (Topcon 3D-OCT 1000). *Acta Ophthalmologica* 2011; 89 (4):346-351.

Merzenich MM, Nelson RJ, Stryker MP, Cynader MS, Schoppmann A, and Zook JM. Somatosensory cortical map changes following digit amputation in adult monkeys. *Journal of Comparative Neurology* 1984; 224 (4):591-605.

Michelson G, Engelhorn T, Wärntges S, El Rafei A, Hornegger J, Doerfler A. DTI parameters of axonal integrity and demyelination of the optic radiation correlate with glaucoma indices. *Graefe's Archives for Clinical and Experimental Ophthalmology* 2013; 251:243-253.

Minini L, Parker AJ, and Bridge H. Neural modulation by binocular disparity greatest in human dorsal visual stream. *Journal of Neurophysiology* 2010; *104*(1):169–178.

Muñoz B, West SK, Rubin GS, Schein OD, Quigley HA, et al. Causes of blindness and visual impairment in a population of older Americans: The Salisbury Eyee Evaluation Study. *Archives of Ophthalmology* 118:819-825.

Murai H, Suzuki Y, Kiyosawa M, Tokumaru AM, Ishii K, Mochizuki M. Positive correlation between the degree of visual field defect and optic radiation damage in glaucoma patients. *Japanese Journal of Ophthalmology* 2013; 57:257-262.

Nangia V, Jonas JB, Kulkarni M, and Matin A. Prevalence of age-related macular degeneration in rural central India: the Central India Eye and Medical Study. *Retina* 2011; 31 (6):1179-1185.

Neri P, Bridge H, and Heeger DJ. Stereoscopic processing of absolute and relative disparity in human visual cortex. *Journal of Neurophysiology* 2004; *92*(3):1880–1891.

Neveu MM, von dem Hagen E, Morland AB, Jeffery G. The fovea regulates symmetrical development of the visual cortex. *Journal of Comparative Neurology* 2008; 506:791-800.

Ngai LY, Stocks N, Sparrow JM, Patel R, Rumley A, Lowe G, et al. The prevalence and analysis of risk factors for age-related macular degeneration: 18-year follow-up data from the Speedwell eye study, United Kingdom. *Eye* 2011; 25 (6):784-793.

Nguyen TH, Stievenart JL, Saucet JC, Le Gargasson JF, Cohen YS, Pelegrini-Issac M, et al. [Cortical response to age-related macular degeneration (Part II). Functional MRI study]. *Journal Français d'Ophtalmologie* 2004; 27 (9 Pt 2):3S72-3S86.

Nickells RW. Retinal ganglion cell death in glaucoma: the how, the why, and the maybe. *Journal of Glaucoma* 1996; 5:345-356.

Noppeney U. The effects of visual deprivation on functional and structural organization of the human brain. *Neuroscience and Biobehavioral Reviews* 2007; *31*(8):1169–1180.

Noppeney U, Friston KJ, Ashburner J, Frackowiak R, and Price CJ. Early visual deprivation induces structural plasticity in gray and white matter. *Current Biology* 2005; *15*(13):R488–490.

Nucci C, Strouthidis NG, Khaw PT. Neuroprotection and other novel therapies for glaucoma. *Current Opinion in Pharmacology* 2013; 13:1-4.

Ohno-Matsui K. Parallel findings in age-related macular degeneration and Alzheimer's disease. *Progress in Retinal and Eye Research* 2011; 30:217-238.

Osborne NN. Recent clinical findings with memantine should not mean that the idea of neuroprotection in glaucoma is abandoned. *Acta Ophthalmology* 2009; 87:450-454.

Ou Y, Grossman DS, Lee PP, Sloan FA. Glaucoma, Alzheimer disease and other dementia: a longitudinal analysis. *Ophthalmic Epidemiology* 2012; 19:285-292.

Palaniyappan L, Liddle PF. Differential effects of surface area, gyrification and cortical thickness on voxel-based morphometric deficits in schizophrenia. *Neuroimage* 2008; 43:665-675.

Pan W-J, Wu G, Li C-X, Lin F, Sun J, and Lei H. Progressive atrophy in the optic pathway and visual cortex of early blind Chinese adults: A voxel-based morphometry magnetic resonance imaging study. *NeuroImage* 2007; *37*(1):212–220.

Park H-J, Jeong S-O, Kim EY, Kim J Il, Park H, Oh M-K, et al. Reorganization of neural circuits in the blind on diffusion direction analysis. *Neuroreport* 2007; *18*(17), 1757–1760.

Park H-J, Lee JD, Kim EY, Park B, Oh M-K, Lee S, and Kim J-J. Morphological alterations in the congenital blind based on the analysis of cortical thickness and surface area. *NeuroImage* 2009; *47*(1):98–106.

Pascale A, Drago F, Govoni S. Protecting the retinal neurons from glaucoma: Lowering ocular pressure is not enough. *Pharmacological Research* 2012; 66:19-32.

Pascual-Leone A, Amedi A, Fregni F, Merabet LB. The plastic human brain cortex. *Annual Review of Neuroscience* 2005; 28:377-401

Pham TQ, Kifley A, Mitchell P and Wang JJ. Relation of age-related macular degeneration and cognitive impairment in an older population. *Gerontology* 2006; 52:353-358.

Pi LH, Chen L, Liu Q, Ke N, Fang J, Zhang S, et al. Prevalence of eye diseases and causes of visual impairment in school-aged children in Western China. *Journal of Epidemiology* 2012; 22 (1):37-44.

Plank T, Frolo J, Brandl-Rühle S, Renner AB, Hufendiek K, Helbig H, and Greenlee MW. Gray matter alterations in visual cortex of patients with loss of central vision due to hereditary retinal dystrophies. *Neuroimage* 2011; 56 (3):1556-1565.

Prins D, Hanekamp S, and Cornelissen FW. Structural brain MRI studies in eye diseases: are they clinically relevant? A review of current findings. *Acta Ophthalmologica* 2016; *94*(2):113–121.

Prins D, Plank T, Baseler HA, Gouws AD, Beer A, Morland AB, et al. Surface-Based Analyses of Anatomical Properties of the Visual Cortex in Macular Degeneration. *PloS One* 2016; *11*(1): e0146684.

Proitsi P, Lupton MK, Dudbridge F, Tsolaki M, Hamilton G, Daniilidou M, et al. Alzheimer's disease and age-related macular degeneration have different genetic models for complement gene variation. *Neurobiology of Aging* 2012; 33(8):1843.e9-17.

Przedborski S, Vila M, Jackson-Lewis V. Neurodegeneration: What is it and where are we? *Journal of Clinical Investigation* 2003; 111:3-10.

Ptito M, Schneider FCG, Paulson OB, and Kupers R. Alterations of the visual pathways in congenital blindness. *Experimental Brain Research* 2008; 187(1):41–49.

Pu M, Xu L, Zhang H. Visual response properties of retinal ganglion cells in the Royal College of Surfeons dystrophic rat. *Investigative Ophthalmology & Visual Science* 2006; 47:3579.

Rahmani B, Tielsch JM, Katz J, Gottsch J, Quigley H, et al. The cause-specific prevalence of visual impairment in an urban population. The Baltimore Eye Survey. *Ophthalmology* 1996; 103:1721-1726.

Raz N, Lindenberger U, Rodrigue KM, Kennedy KM, Head D, Williamson A, et al. Regional brain changes in aging healthy adults: general trends, individual differences and modifiers. *Cerebral Cortex* 2005; 15 (11):1676-1689.

Resnikoff S, Pascolini D, Etya'ale D, Kocur I, Pararajasegaram R, Pokharel GP, and Mariotti SP. Global data on visual impairment in the year 2002. *Bulletin of the World Health Organization* 2004; 82 (11):844-851.

Rosengarth K, Keck I, Brandl-Rühle S, Frolo J, Hufendiek K, Greenlee MW, et al. Functional and structural brain modifications induced by oculomotor training in patients with age-related macular degeneration. *Frontiers in Psychology* 2013; 4: 428.

Rutschmann RM, and Greenlee MW. BOLD response in dorsal areas varies with relative disparity level. *Neuroreport* 2004; *15*(4):615–619.

Schlegel AA, Rudelson JJ, and Tse PU. White matter structure changes as adults learn a second language. *Journal of Cognitive Neuroscience* 2012; *24*(8):1664–1670.

Schmitz B, Schaefer T, Krick CM, Reith W, Backens M, Käsmann-Kellner B. Configuration of the optic chiasm in humans with albinism as revealed by magnetic resonance imaging. *Investigative Ophthalmology & Visual Science* 2003; 44:16-21.

Scholz J, Klein MC, Behrens TEJ, and Johansen-Berg H. Training induces changes in white-matter architecture. *Nature Neuroscience* 2009; *12*(11):1370–1371.

Schoth F, Burgel U, Dorsch R, Reinges MHT, and Krings T. Diffusion tensor imaging in acquired blind humans. *Neuroscience Letters* 2006; *398*(3):178–182.

Schotz F, Burgel U, Dorsch R, Reinges MHT, Krings T. Diffusion tensor imaging in acquired blind humans. *Neuroscience Letters* 2006; 398:178-182.

Schumacher EH, Jacko JA, Primo SA, Main KL, Molomey KP, Kinzel EN, and Ginn J. Reorganization of visual processing is related to eccentric viewing in patients with macular degeneration. *Restorative Neurology and Neuroscience* 2008; 26 (4-5):391-402.

Ségonne F, Dale AM, Busa E, Glessner M, Salat D, et al. A hybrid approach to the skull stripping problem in MRI. *Neuroimage* 2004; 22:1060-1075.

Ségonne F, Pacheco J, Fischl B. Geometrically accurate topology-correction of cortical surfaces using nonseparating loops. *IEEE Transactions on Medical Imaging* 2007; 26:518-529.

Shimony JS, Burton H, Epstein AA, McLaren DG, Sun SW, and Snyder AZ. Diffusion tensor imaging reveals white matter reorganization in early blind humans. *Cerebral Cortex* 2006; *16*(11):1653–1661.

Shu N, Li J, Li K, Yu C, and Jiang T. Abnormal diffusion of cerebral white matter in early blindness. *Human Brain Mapping* 2009; *30*(1):220–227.

Sivak JM. The aging eye: common degenerative mechanisms between the Alzheimer's brain and retinal disease. *Investigative Ophthalmology & Visual Science* 2013; 54:871-880.

Sled JG, Zijdenbos AP, Evans AC. A nonparametric method for automatic correction of intensity nonuniformity in MRI data. *IEEE Transactions on Medical Imaging* 1998; 17:87-97.

Smirnakis SM, Brewer AA, Schmid MC, Tolias AS, Schüz A, Augath M, et al. Lack of long-term cortical reorganization after macaque retinal lesions. *Nature* 2005; 435 (7040):300-307.

Smith SM. Fast robust automated brain extraction. *Human Brain Mapping* 2002; *17*(3):143–155.

Smith SM and Brady JM. SUSAN - a new approach to low level image processing. *International Journal of Computer Vision* 1997; 23 (1):45-78.

Smith SM and Nichols TE. Threshold-free cluster enhancement: addressing problems of smoothing, threshold dependence and localization in cluster inference. *Neuroimage* 2009; 44 (1):83-98.

Spanish Eyes Epidemiological (SEE) study group. Prevalence of age-related macular degeneration in Spain. *British Journal of Ophthalmology* 2011; 95 (7):931-936.

Stasheff SF. Emergence of sustained spontaneous hyperactivity and temporary preservation of OFF responses in ganglion cells of the retinal degeneration (rd1) mouse. *Journal of Neurophysiology* 2008; 99:1408-1421.

Steeves JKE, González EG, and Steinbach MJ. Vision with one eye: a review of visual function following unilateral enucleation. *Spatial Vision* 2008; *21*(6):509–529.

Stein JD, Vanderbeek BL, Talwar N, Nan B, Musch DC, and Zachs DN. Rates of nonexudative and exudative age-related macular degeneration among Asian American ethnic groups. *Investigative Ophthalmology & Visual Science* 2011; 52 (9):6842-6848.

Stingl K, Greppmaier U, Wilhelm B, Zrenner E. Subretinal visual implants. *Klinische Monatsblätter für Augenheilkunde* 2010; 227:940-945.

Sunness JS, Liu T, and Yantis S. Retinotopic mapping of the visual cortex using functional magnetic resonance imaging in a patient with central scotomas from atrophic macular degeneration. *Ophthalmology* 2004; 111 (8):1595-1598.

Szlyk JP, Little DM. An fMRI study of word-level recognition and processing in patients with age-related macular degeneration. *Investigative Ophthalmology & Visual Science* 2009; 50:4487-4495.

Tamura H, Kawakami H, Kanamoto T, Kato T, Yokoyama T, Sasaki K, et al. High frequency of open-angle glaucoma in Japanese patients with Alzheimer's disease. *Journal of the Neurological Sciences* 2006; 246:79-83.

Tanito M, Ohira A. Hemianopic inner retinal thinning after stroke. *Acta Ophthalmologica* 2013; 91: e237–8.

VanNewkirk MR, Weih L, McCarty CA, Taylor HR. Cause-specific prevalence of bilateral visual impairment in Victoria, Australia: the Visual impairment project. *Ophthalmology* 2001; 108:960-967.

Voets NL, Hough MG, Douaud G, Matthews PM, James A, et al. Evidence for abnormalities of cortical development in adolescent-onset schizophrenia. *Neuroiamge* 2008; 43:665-675.

Wandell BA, Smirnakis SM. Plasticity and stability of visual field maps in adult primary visual cortex. *Nature Reviews Neuroscience* 2009; 10:873-884.

Wang D, Qin W, Liu Y, Zhang Y, Jiang T, and Yu C. Altered white matter integrity in the congenital and late blind people. *Neural Plasticity* 2013; 128236.

Wang M-Y, Wu K, Xu J-M, Dai J, Qin W, Liu J, et al. Quantitative 3-T diffusion tensor imaging in detecting optic nerve degeneration in patients with glaucoma: association with retinal nerve fiber layer thickness and clinical severity. *Neuroradiology* 2013; *55*, 493–498.

Wang YX, Xu L, Lu W, Liu FJ, Qu YZ, Wang J, et al. Parapapillary atrophy in patients with intracranial tumours. *Acta Ophthalmology* 2013; 91:521-525.

Welchman AE, Deubelius A, Conrad V, Bülthoff HH, and Kourtzi Z. 3D shape perception from combined depth cues in human visual cortex. *Nature Neuroscience* 2005; *8*(6):820–827.

Whitwell JL, Tosakulwong N, Weigand SD, Senjem ML, Lowe VJ, et al. Does amyloid deposition produce a specific atrophic signature in cognitively normal subjects? *Neuroimage Clinical* 2013; 2:249-257.

Williams AL, Lackey J, Wizov SS, Chia TMT, Gatla S, Moster ML, et al. Evidence for widespread structural brain changes in glaucoma: a preliminary voxel-based MRI study. *Investigative Ophthalmology & Visual Science* 2013; 54:5880-5887.

Winkler AM, Ridgway GR, Webster MA, Smith SM, and Nichols TE. Permutation inference for the general linear model. *NeuroImage* 2014 *92*:381–397.

Woo SJ, Park KH, Ahn J, Choe JY, Jeong H, Han JW, et al. Cognitive impairment in age-related macular degeneration and geographic atrophy. *Ophthalmology* 2012*;* 119 (10):2094-2101.

Woolrich MW, Jbabdi S, Patenaude B, Chappell M, Makni S, Behrens T, et al. Bayesian analysis of neuroimaging data in FSL. *NeuroImage* 2009; *45*(1 Suppl):S173–186.

Wostyn P, Audenaert K, De Deyn PP. Alzheimer's disease: cerebral glaucoma? *Medical Hypotheses* 2010; 74:973-977.

Wostyn P, De Groot V, Van Dam D, Audenaert K, De Deyn PP. Intracranial pressure fluctuations: a potential risk factor for glaucoma? *Acta Ophthalmologica* 2015; 93(1):e83-84.

Xiao JX, Xie S, Ye JT, Liu HH, Gan XL, Gong GL, et al. Detection of abnormal visual cortex in children with amblyopia by voxel-based morphometry. *American Journal of Ophthalmology* 2007; 143(3):489-493.

Xie S, Gong GL, Xiao JXI Ye JT, Liu HH, Gan XL, et al. Underdevelopment of optic radiation in children with amblyopia: a tractography study. *American Journal of Ophthalmology* 2007; 143(4):642-646.

Ye JH, Goo YS. The slow wave component of retinal activity in rd/rd mice recorded with a multi-electrode array. *Physiological Measurement* 2007; 28:1079-1088.

Yeatman JD, Weiner KS, Pestilli F, Rokem A, Mezer A, and Wandell BA. The vertical occipital fasciculus: A century of controversy resolved by in vivo measurements. *Proceedings of the National Academy of Sciences of the United States of America* 2014; 111(48):e5214-5223.

Yoon KC, Mun GH, Kim SD, Kim SH, Kim CY, Park KH, et al. Prevalence of eye diseases in South Korea: data from the Korea National Health and Nutrition Examination Survey 2008-2009. *Korean Journal of Ophthalmology* 2011; 25 (6):421-33.

Zarbin MA. Current concepts in the pathogenesis of age-related macular degeneration. *Archives of Ophthalmology* 2004; 122 (4):598-614.

Van Zeeburg EJT, Maaijwee KJM, Missotten TOAR, Heimann H, Van Meurs JC. A free retinal pigment epitheliumchoroid graft in patients with exsudative age-related macular degeneration: Results up to 7 years. *American Journal of Ophthalmology* 2012; 153(1):120-127.

Zhang Y, Brady M, and Smith S. Segmentation of brain MR images through a hidden Markov random field model and the expectation-maximization algorithm. *IEEE Transactions on Medical Imaging* 2001; *20*(1):45–57.

Zhang YQ, Li J, Xu L, Zhang L, Wang ZC, Yang H, et al. Anterior visual pathway assessment by magnetic resonance imaging in normal-pressure glaucoma. *Acta Ophthalmologica* 2012a; 90:e295-302.

Zhang Y, Wan S, Ge J, and Zhang X. Diffusion tensor imaging reveals normal geniculocalcarine-tract integrity in acquired blindness. *Brain Research* 2012b; *1458*:34–39.

Zhang Z, Wang X, Jonas JB, Wang H, Zhang X, Peng X, et al. Intracranial pressure fluctuations: a potential risk factor for glaucoma? *Acta Ophthalmologica* 2015; 93(1):e84-85.

Zhang Z, Wang X, Jonas JB, Wang H, Zhang X, Peng X, et al. Valsalva manoeuver, intra-ocular pressure, cerebrospinal fluid pressure, optic disc topography: Beijing intracranial and intra-ocular pressure study. *Acta Ophthalmologica* 2014; 92:e475;480.

Zikou AK, Kitsos G, Tzarouchi LC, Astrakas L, Alexiou GA, Argyropoulou MI. Voxel-based morphometry and diffusion tensor imaging of the optic pathway in primary open-angle glaucoma: a preliminary study. *American Journal of Neuroradiology* 2012; 33:128-134.

Zrenner E. Will retinal implants restore vision? *Science* 2002; 295 (5557):1022-1025.

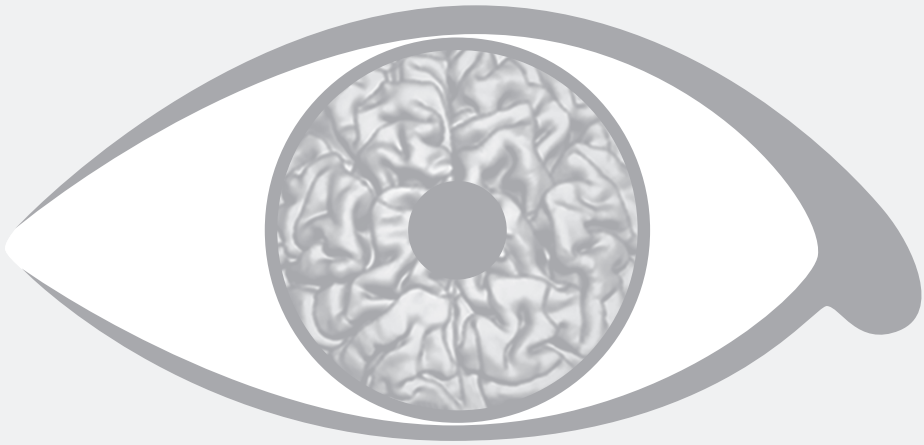

Summary

Ocular pathology that causes loss of visual function is associated with neuroanatomical changes of the visual pathways. However, the underlying mechanism of this association is still unclear. Research into the association between ocular pathology and neuroanatomical changes is important, since the remaining capacity of the central visual system to guide the input from the eye towards the visual cortex is believed to be a crucial factor that can affect the success of future vision restoration treatments. Moreover, such research can provide information for a better understanding of the pathophysiology of the investigated eye disease. This, in turn, can give directions to future research on the treatment of the eye disease, which might have to expand its focus from treatment of the eye alone towards treatment of both the eye and brain.

There are several mechanisms that have been postulated to explain the association between ocular pathology and neuroanatomical changes:

- Functional deprivation: the ocular pathology may reduce the activity in the visual pathways which may lead to neuroanatomical changes;
- Anterograde transsynaptic degeneration. This process might cause neuroanatomical changes by "passing on" the pregeniculate degeneration of axons from the eye towards postgeniculate neurons and even to the visual cortex;
- Ocular pathology, such as glaucoma and macular degeneration, could be part of a more generalized neurodegenerative disorder that affects the brain as well as the eye.

In this thesis, I studied neuroanatomical changes in various ocular diseases that cause visual deprivation. Functional deprivation plays an important role in all of the cases. I found no indications that anterograde transsynaptic degeneration plays a role in monocular blindness, suggesting this process plays no important role in causing the neuroanatomical changes in macular degeneration and glaucoma either, Furthermore, POAG should probably be considered part of a more general neurodegenerative disorder. Moreover, such more general neurodegenerative processes may also play a role in AMD.

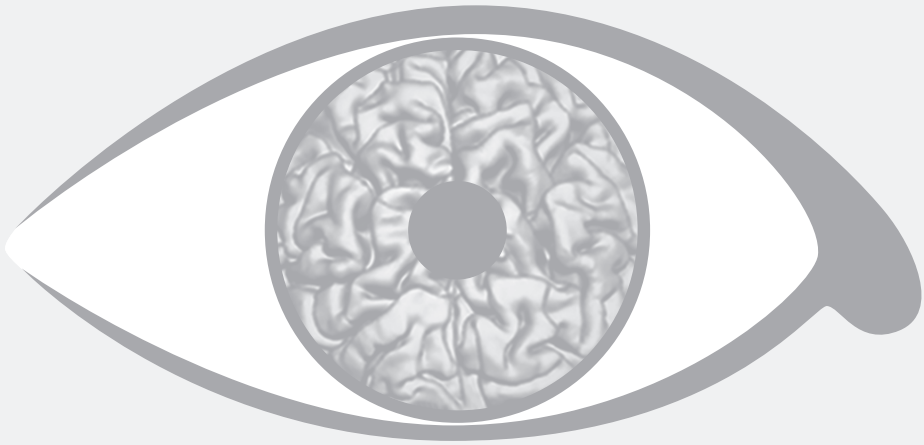

Samenvatting

Oogaandoeningen die leiden tot gezichtsveldverlies zijn geassocieerd met neuro-anatomische veranderingen van de visuele banen. De onderliggende oorzaak van deze associatie is onbekend. Onderzoek naar deze associatie kan belangrijke informatie opleveren voor toekomstige behandelingen om het gezichtsveld te herstellen. Een cruciale factor die het succes van deze behandelingen kan beïnvloeden is namelijk het vermogen van het centrale visuele systeem om informatie van het oog naar de visuele cortex te geleiden en vervolgens te verwerken. Bovendien kan dergelijk onderzoek waardevolle informatie verschaffen over de etiologie van de onderzochte oogziekte. Deze informatie kan richting geven aan toekomstig onderzoek naar de behandeling van de oogziekte. Het kan zijn dat de behandeling zich meer zou moeten richten op behandeling van het oog en het brein tezamen, dan alleen op behandeling van het oog.

Er zijn verschillende mechanismen aangedragen om de associatie tussen oogaandoeningen en neuro-anatomische veranderingen te kunnen verklaren:

- Functionele deprivatie: de oogaandoening veroorzaakt een afname van de activiteit in de visuele banen; dit kan leiden tot neuro-anatomische veranderingen;
- Anterograde transsynaptische degeneratie: neuro-anatomische veranderingen worden veroorzaakt doordat degeneratie van de anterieure structuren van de visuele banen wordt doorgegeven naar de meer posterieure structuren, zelfs tot aan de visuele cortex;
- Oogaandoeningen zoals glaucoom en maculadegeneratie zouden onderdeel kunnen zijn van een meer algemene neurodegeneratieve aandoening, die zowel het oog als het brein aantast.

Het doel van mijn onderzoek was te achterhalen welke mechanismen het verband tussen gezichtsveldverlies en neuro-anatomische veranderingen kunnen verklaren. Om dit te onderzoeken, heb ik meerdere studies verricht.

Ik vond een afname van het volume van de grijze en witte stof in de gehele visuele banen in maculadegeneratie patiënten, vergeleken met gezonde controle proefpersonen. Verder vond ik verschillen in de dikte van de cortex, het oppervlak van de cortex en het volume van de grijze stof in de visuele gebieden V1 en V2 in jonge maculadegeneratie patiënten, en een dunnere cortex in V2 in oudere degeneratie patiënten. Daarnaast vond ik in maculadegeneratie patiënten ook een afname van het volume van de witte stof buiten de visuele banen, met name in de frontaal kwab. Ik veronderstel dat deze laatste bevinding mogelijk het neuraal correlaat kan zijn van het eerder beschreven verband tussen maculadegeneratie en milde cognitieve achteruitgang en de ziekte van Alzheimer.

In eenzijdig blinde patiënten vond ik een afname van het volume van de grijze stof in de superior laterale occipitale cortex. De superior laterale occipitale cortex is gelegen in de

dorsale visuele cortex, en is betrokken bij het stereoscopisch diepte zien. Opmerkelijk is dat ik geen anatomische veranderingen vond in de primaire visuele cortex. Dit geeft aan dat anterograde transsynaptische degeneratie geen rol van betekenis speelt in deze patiënten. Het verlies van het volume van de grijze stof in de superior laterale occipitale cortex kan dus verklaard worden door functionele deprivatie, veroorzaakt door het verdwijnen van stereoscopie.

In glaucoom patiënten met een eenzijdig gezichtsvelddefect vond ik neuro-anatomische veranderingen in meerdere structuren van de visuele banen, vergeleken met zowel gezonde proefpersonen als met eenzijdig blinde proefpersonen. Rekening houdend met het feit dat het gezichtsvelddefect eenzijdig was, kan ik deze anatomische veranderingen niet alleen verklaren door functionele deprivatie of transsynaptische degeneratie. Daarom denk ik dat glaucoom gezien zou kunnen worden als een onderdeel van een meer algemene neurodegeneratieve aandoening.

Samengevat onderzocht ik neuro-anatomische veranderingen in verschillende oogziekten die gezichtsveldverlies veroorzaken. Verandering van de neuro-anatomie lijkt in alle gevallen voor een belangrijk deel verklaard te kunnen worden door functionele deprivatie. Ik vond geen aanwijzingen dat anterograde transsynaptische degeneratie een rol speelt bij het ontstaan van neuro-anatomische veranderingen in eenzijdige blindheid. Dit suggereert dat dit proces waarschijnlijk ook geen belangrijke rol speelt in het ontstaan van neuro-anatomische veranderingen in andere oogaandoeningen. Verder lijkt glaucoom onderdeel van een meer algemene neurodegeneratieve aandoening. Zulke algemene neurodegeneratieve processen lijken ook een rol te spelen in maculadegeneratie.

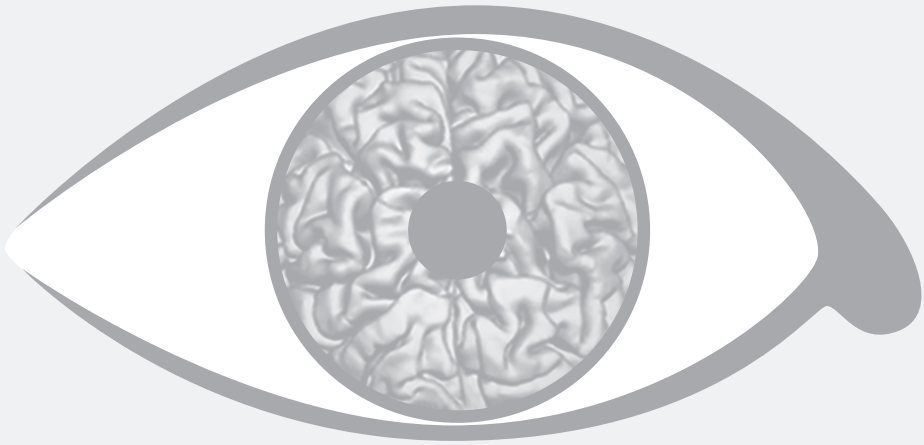

Dankwoord

Dit proefschrift had ik natuurlijk nooit alleen kunnen schrijven. Graag wil ik iedereen bedanken die op wat voor manier dan ook heeft bijgedragen aan de totstandkoming van dit proefschrift. Een aantal mensen wil ik hierbij in het bijzonder bedanken.

Als eerste mijn promotoren. Professor Cornelissen, beste Frans, jij hebt mij de kans gegeven dit promotieonderzoek te doen. Bedankt voor al je steun, enthousiasme, en de vrijheid die jij me gaf om mijn onderzoek te doen. Ik heb veel van je geleerd. Professor Hooymans, beste Anneke, bedankt voor je interesse in mijn onderzoek, en het in mij gestelde vertrouwen. Door de voortgangsgesprekken met jou wist ik weer dat ik op het goede spoor zat, ook al liep de planning anders dan gedacht. Professor Jansonius, beste Nomdo, jij raakte betrokken bij mijn onderzoek door de studie in glaucoompatiënten, wat resulteerde in hoofdstuk 4 en 5. Bedankt voor alle tijd en moeite, en je scherpe blik, die de betreffende hoofdstukken naar een hoger niveau hebben getild.

De beoordelingscommissie, prof. dr. A.V. van den Berg, prof. dr. P. van Dijk en prof. dr. T. van Laar, wil ik bedanken voor het lezen en beoordelen van mijn proefschrift.

For the macular degeneration study we collaborated with colleagues from York and Regensburg. I would like to thank Tina Plank, Mark Greenlee, Anton Beer, Heidi Baseler, André Gouws and Tony Morland for the collaboration and their useful comments on my manuscripts.

Graag wil ik de Junior Scientific Masterclass bedanken voor de mogelijkheid dit MD/PhD traject te doen.

Zonder proefpersonen geen onderzoek, en dus ook geen proefschrift. Alle proefpersonen die hebben deelgenomen aan mijn onderzoek wil ik bij deze hartelijk bedanken.

Ondersteuning is onmisbaar, ook bij dit onderzoek. Judith en Anita, bedankt voor het maken van de MRI scans. Jan Bernard en Remco bedankt voor de ondersteuning en het meedenken bij de data-analyse. Hedwig, Evelyn en Diana, bedankt voor de administratieve ondersteuning. Ella, Stella, Fenna, Luuk en Wim, bedankt voor al jullie hulp en ondersteuning tijdens mijn promotieonderzoek.

Mijn collega's op het neuro-imaging centre maakten het dagelijkse werk veel leuker. Iedereen op het NIC bedankt voor de gezelligheid, de interessante gesprekken en het delen van grote en kleine onderzoeksmijlpalen. In het bijzonder dank aan mijn naaste collega's: Adit, Barbara, Funda, Nicolas, Sandra, Mirjan, Charlotte en Elouise.

Ik kwam ook altijd erg graag op het LEO, uiteraard om te werken, maar zeker ook vanwege de fijne sfeer. Bart, Bernadette, Christiaan, Esther, Francisco, Lisanne, Lisette, Nancy, Ronald, Tim en Wietse: bedankt voor de leuke tijd!

Mijn collega's, de AIOS, oogartsen en andere medewerkers van de afdeling oogheelkunde, bedank ik voor de interesse in mijn onderzoek en jullie begrip dat ik hier de laatste tijd erg druk mee was naast de klinische werkzaamheden. Ook ben ik dank verschuldigd aan mijn opleider, dr. Pott. Beste Jan Willem, bedankt dat je mij de ruimte gaf om mijn proefschrift af te ronden naast de opleiding.

Mijn familie, schoonfamilie en vrienden wil ik bedanken voor de interesse die jullie altijd toonden in mijn onderzoek, jullie steun, maar bovenal natuurlijk voor alle mooie momenten die ik samen met jullie beleef die helemaal niets met onderzoek te maken hebben. Mijn paranimfen, Riemke en Margriet, jullie in het bijzonder bedankt voor jullie ondersteuning op deze belangrijke dag voor mij.

Lieve Wout, jou noem ik laatste omdat jij de belangrijkste persoon bent in mijn leven. Bedankt dat je er altijd voor me bent.

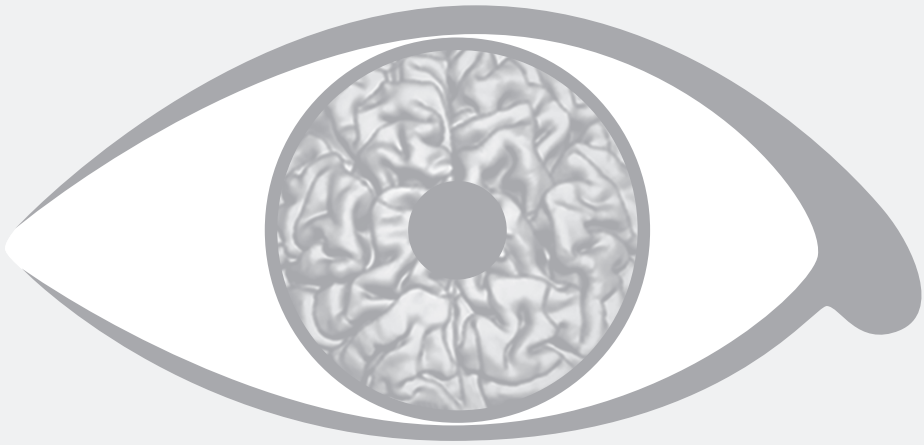

Curriculum Vitae

Doety Prins was born on the the 24th of October 1986 in Sneek, The Netherlands. In 2004 she finished secondary school at Dockinga college in Dokkum. Subsequently, she started studying medicine at the University of Groningen. Clinical internships were followed in the University Medical Center Groningen, Antonius Ziekenhuis in Sneek, and Magunga hospital in Korogwe, Tanzania. The last year of her master was dedicated to research and internship at the department of ophthalmology at the University Medical Center Groningen. During the research internship, under supervision of prof. dr. F.W. Cornelissen, she studied neuroanatomical changes in patients with macular degeneration. In 2011 she was awarded an MD/PhD trajectory by the Junior Scientific Masterclass, which allowed her to continue the research in this field. During the MD/PhD trajectory, Doety presented her scientific work at national and international conferences on ophthalmology and visual perception. In 2012, she obtained her medical degree. Currently, Doety is working as a resident at the department of ophthalmology at the University Medical Center Groningen.